DISPERSION MODELLING OF JET PROPELLANT 8 SPILL IN THE AEROSPACE INDUSTRY

A THESIS SUBMITTED TO
THE GRADUATE SCHOOL OF NATURAL AND APPLIED SCIENCES
OF
MIDDLE EAST TECHNICAL UNIVERSITY

BY

OLGUN ÇELİK

IN PARTIAL FULFILLMENT OF THE REQUIREMENTS
FOR
THE DEGREE OF MASTER OF SCIENCE
IN
OCCUPATIONAL HEALTH AND SAFETY

JANUARY 2020

Approval of the thesis:

DISPERSION MODELLING OF JET PROPELLANT 8 SPILL IN THE AEROSPACE INDUSTRY

submitted by **OLGUN ÇELİK** in partial fulfillment of the requirements for the degree of **Master of Science in Occupational Health and Safety Department, Middle East Technical University** by,

Prof. Dr. Halil Kalıpçılar
Dean, Graduate School of **Natural and Applied Sciences** _____

Prof. Dr. Mahmut Parlaktuna
Head of Department, **Occupational Health and Safety** _____

Assoc. Prof. Dr. Çağlar Sınayuç
Supervisor, **Occupational Health and Safety, METU** _____

Examining Committee Members:

Prof. Dr. Yavuz Yaman
Aerospace Engineering, METU _____

Assoc. Prof. Dr. Çağlar Sınayuç
Petroleum and Natural Gas Engineering, METU _____

Prof. Dr. Mahmut Parlaktuna
Petroleum and Natural Gas Engineering, METU _____

Prof. Dr. Ülkü Mehmetoğlu
Chemical Engineering, Ankara University _____

Assist. Prof. Dr. İsmail Durgut
Petroleum and Natural Gas Engineering, METU _____

Date: 29.01.2020

I hereby declare that all information in this document has been obtained and presented in accordance with academic rules and ethical conduct. I also declare that, as required by these rules and conduct, I have fully cited and referenced all material and results that are not original to this work.

Name, Surname: Olgun Çelik

Signature:

ABSTRACT

DISPERSION MODELLING OF JET PROPELLANT 8 SPILL IN THE AEROSPACE INDUSTRY

Çelik, Olgun
Master of Science, Occupational Health and Safety
Supervisor: Assoc. Prof. Dr. Çağlar Sınayuç

December 2019, 143 pages

The purpose of this study is to identify hazards, evaluate risks and suggest safety measures in order to prevent fire and explosions due to the uncontrolled charging and the ignition of jet propellant 8, shortly JP-8, at the fueling stations in the aerospace industry. There are many different surveys on the ignition and the explosion of the fuels in the literature. However, not enough researches have been made in order to model the dispersion of the JP-8 spill in aviation. JP-8 is a petroleum product which has wide usage in aviation as a jet engine propellant. JP-8 is a flammable hydrocarbon mixture and its vapors can be ignited very quickly. JP-8 vapors can start a fire and explode in open air or in the confined spaces in case of exposure to flame, spark, heat, static electricity discharge and different types of ignition sources. A case scenario of JP-8 spill during the fueling operations in the aviation sector is investigated to model evaporation of JP-8 spill and dispersion of its vapors. Different evaporation and dispersion models are discussed and compared for deciding the most suitable model for the JP-8 spill. According to the assessment results, the area affected by the JP-8 spill and evacuation zones are defined. This research provides the required information to design safe fueling stations and to increase the safety during fueling operations for the aerospace industry.

Keywords: Dispersion modelling, Evaporation modelling, Oil spill, Aerospace

ÖZ

HAVACILIK SANAYİNDE JET YAKITI 8 DÖKÜNTÜSÜNÜN DAĞILIM MODELLEMESİ

Çelik, Olgun
Yüksek Lisans, İş Sağlığı ve Güvenliği
Tez Danışmanı: Doç. Dr. Çağlar Sınayuç

Aralık 2019, 143 sayfa

Bu çalışmanın amacı havacılık sanayindeki yakıt istasyonlarında jet yakıtı 8'in, kısaca JP-8, kontrol edilemeyen tutuşma ve ateşleme yüzünden patlamasını önlemek için tehlikeleri belirlemek, riskleri değerlendirmek ve güvenlik önlemleri önermektir. Literatürde yakıtların parlaması ve patlaması ile ilgili birçok farklı araştırma mevcuttur. Fakat havacılıkta sektöründe JP-8 döküntüsünün havada dağılımını değerlendiren yeterli miktarda araştırma henüz yapılmamıştır. JP-8 yanıcı bir hidrokarbon karışımıdır ve buharı çok çabuk alevlenebilir. JP-8 buharları açık veya kapalı ortamda alev, kıvılcım, ısı, statik elektrik ve diğer ateşleme kaynaklarına maruz kalması durumunda patlayabilir. Havacılık sektöründeki yakıt işlemleri esnasında JP-8 dökülmesi durum senaryosuna göre buharlaşma ve havada dağılım modellemesi yapılmıştır. JP-8 döküntüsüne en uygun buharlaşma ve havada dağılım modelini belirlemek için farklı buharlaşma ve havada dağılım modelleri araştırılmış ve karşılaştırılmıştır. Araştırma sonuçlarına göre, JP-8 döküntüsünden etkilenen alanlar ve tahliye bölgeleri belirlenmiştir. Bu araştırma, havacılık sanayinde güvenli yakıt istasyonlarının tasarımı ve güvenliği artıracak yakıt işlemi kurallarının belirlenmesi için gerekli bilgiyi sağlamaktadır.

Anahtar Kelimeler: Dağılım modellemesi, Buharlaşma modellemesi, Petrol döküntüsü, Havacılık

To my beloved family...

ACKNOWLEDGMENTS

First of all, I would like to express my deepest appreciation to Assoc.Prof. Çağlar Sınayuç. It was a great chance for me to work with him. His positive attitude, encouragement and involvement kept me working harder. Without his supervision and guidance, the whole thesis process would become much more challenging for me.

Besides my advisor, I would like to thank to all my Professors in the program for sharing their wisdom and knowledge.

I would also like to thank all of my friends and colleagues for their contribution and for sharing their experience throughout the thesis process.

Above all, I would like to express my gratefulness to my family for showing their infinite love and endless support no matter what. I feel very lucky to have my mom, Nazlı Çelik who feeds me with all her delicious and nutritious foods giving me the energy that I need during my thesis marathon. I want to thank my dad, Ali Çelik who advise me to have the patience that I require when I struggled. I want to show my gratefulness to my sister, Duygu Gleissner for giving me motivation and being my mentor every time I need. I love you all so much!

TABLE OF CONTENTS

LIST OF TABLES

TABLES

LIST OF FIGURES

FIGURES

LIST OF ABBREVIATIONS

ABBREVIATIONS

AIT	: Autoignition temperature
JP-8	: Jet propellant 8
LFL	: Lower flammability limit
UFL	: Upper flammable limit
VCE	: Vapor cloud explosion
ISO	: International Organization for Standardization
NFPA	: National Fire Protection Agency
MIE	: Minimum ignition energy
SPR	: Single point refuel
FSSZ	: Fuel servicing safety zone
ASMB	: Alberta Sweet Mixed Blend
PBL	: Planetary boundary layer
TLV	: Threshold limit value
TWA	: Time weighted average
LEL	: Lower explosion limit
UEL	: Upper explosion limit
DDT	: Deflagration to detonation transition

NOMENCLATURE

Roman Symbols:

a	Experimental constant in Briggs (1973) formula
A	Area of oil layer
b	Experimental coefficient in Briggs (1973) formula
c	Experimental coefficient in Briggs (1973) formula
C	Concentration
c_0	Equilibrium concentration of vapor at the top layer of the oil
C_s	Evaporating liquid concentration
d	Experimental coefficient in Briggs (1973) formula
d_a	Pool area
d_1	Pool length
D	Oil spill diameter
Di	Diffusivity
e	Experimental coefficient in Briggs (1973) formula
E	Evaporation rate
E_i	Evaporation rate of oil compound I or total evaporation
f	Experimental coefficient in Briggs (1973) formula
F_v	Volume of the evaporated compound
h	Effective height
H	Henry's law constant
k	Experimental rate
k_m	Constant which involves all factors related to K
k_v	Von Karman coefficient
K	Mass transfer constant
K_{ma}	Constant which includes all factors concerning oil evaporation after the surface film formed

K_{mb}	Constant which includes all factors concerning oil evaporation before the surface film formed
K_{ev}	Atmospheric stability coefficient
M	Molecular weight
n	Power law dimensionless parameter
N	Carbon number of oil product
P	Vapor pressure
P_i	Vapor pressure of oil compound, i, on the boundary
$P_{i\infty}$	Vapor pressure of oil compound, i, at infinite altitude
P_{oi}	Vapor pressure of the oil compound i
P_s	Vapor pressure at boiling point
P_v	Saturated vapor pressure
R	Universal gas constant
q	Experimental constant in Yang and Wang (1977) equation.
Q	Emission rate
S	Saturation factor
S_n	Sink term
Sc	Schmidt number
T	Time
T	Temperature
T_s	Boiling point temperature
T_u	Relative intensity factor of turbulence
U	Velocity of wind
u^*	Friction velocity
v	Molar volume of the liquid
V_0	Volume of the spillage at the beginning
x	Amount of specific oil product at time t
x_o	Amount of specific oil product at time t equals zero

X	Pool diameter
z_1	Height above the surface
z_0	Roughness length
%D	Percentage distilled by weight

Greek Symbols:

α	Meteorological coefficient
α_1	Coefficient which is the combination of wind speed and all factor
β	Meteorological coefficient
$\Delta_{vap}H^0$	Heat of evaporation
Δh	Drop in thickness of layer
γ	Experimental constant in Yang and Wang (1977) equation.
σ_y	Horizontal dispersion parameter
σ_z	Vertical dispersion parameter
θ	Evaporative exposure

Superscripts:

r	Experimental value in Brighton model

CHAPTER 1

INTRODUCTION

The aviation sector is growing very rapidly for decades in Turkey. Accordingly, the number of accidents in the aviation sector is increasing. Accidents resulting from fueling operations are major concerns of safety in aviation. Many explosions and fire accidents occur during the fueling process of aircrafts. One of the main causes of fires and explosions is ignition of fuel vapors, mists and sprays due to uncontrolled ignition source during the fueling operations. Additionally, fuel has a toxic effect on humans who are exposed to its vapors by inhalation.

The fuel vapors can arise from various liquid fuel sources such as fuel storage tanks, fuel tanks of aircraft or fuel spills on the flight line. In the case of a fuel spill, liquid fuel evaporates continuously and fuel vapors are emitted from the spill to the air. Fuel vapors disperse in the air and are carried away from the source by the effect of wind. According to the emission rate of fuel vapors from the source, vapor concentration can rise up to flammability range and toxic level. Thus, the consequences of fuel spill are needed to be forecasted in order to identify possible risks and maintain safety in fueling operations. In order to estimate the possible consequences of the JP-8 spill, the dispersion mechanism of fuel vapors is needed to be understood.

Crowl & Louvar (2011) states that fuel, oxidizer and ignition source are the main elements of fire. Fire is an exothermic oxidation reaction of ignited fuel. Fuel, oxidizer and an ignition source should be present in the adequate amount to start a fire process. If not, the burning of fuel does not occur. To prevent fire and explosion, ignition sources should be kept under control and flammable atmospheric condition should be eliminated.

Jet fuel is a petroleum product and has different types of usage in aircraft engines. JP-8 is kerosene typed fuel which is used in aviation. According to the U.S. Department of Defense (2015), JP-8 has wide usage because of its safely handling characteristics and benefits in usage such as low icing point. Ghassemi et al. (2006) says that kerosene and dodecane, $C_{12}H_{26,}$ have very similar properties. Kerosene is more volatile than diesel oil but not more volatile than gasoline (Speight & El-Gendy, 2018).

Dispersion modelling of the JP-8 spill requires determination of emission rate of fuel vapors which is equal to the evaporation rate of the JP-8 spill. There are several evaporation models for calculation of the evaporation rate of kerosene. Five main approaches are used and compared in evaporation modelling. Most evaporation models regard the evaporation rate as constant during the evaporation process. However, approaches like the empirical equation model have a logarithmic rate of evaporation. Thus, each model has advantages and drawbacks. The most important point in modeling is to select the most suitable model regarding the simulated case scenario.

Mass transfer constant is also required for evaporation rate calculation. Various models are present for mass transfer constant determination. Mainly, mass transfer constant formulas are empirical and obtained by laboratory experiments. Some of the mass transfer constant formulas are complex and require several information about the spill. On the contrary, some models are simple and easy to apply. Three widely used model is applied for evaporation modeling and results are assessed.

Numerous dispersion models are available for approximation of chemical vapors concentration emitted from pollutant sources. In order to decide the most suitable dispersion model, emission rate, emission duration and type of source should be known. In this thesis, five main dispersion models are discussed. Gaussian dispersion model is used for determining vapor concentrations arising from JP-8 spill in downwind distances. In the Gaussian dispersion model, it is assumed that the vapor concentration of JP-8 has Gaussian distribution over the lateral and vertical axis.

Variation of concentration in axis is correspondent to atmospheric stability class and downwind distance from the spill.

In this current work, the scenario of JP-8 spill from the fueling system to the flight line due to misconduct in fueling operation is evaluated. According to the spill accident scenario, JP-8 is stored next to fueling hangars and fueling operations of aircraft are conducted in this area. Spillage of JP-8 evaporates immediately and the JP-8 vapor will disperse into the air by the wind. Possible safety and health concerns such as fire, explosion and exposure to chemical vapors are discussed. As an outcome of this study, required safety measures to maintain safe fueling operations are advised.

CHAPTER 2

LITERATURE SURVEY

2.1. Fire and Explosions

Chemicals can cause important fire and explosion hazards. According to Crowl & Louvar (2011), in United States, chemical and hydrocarbon plants were estimated to have $300 million worth of property losses in addition to life losses and production stoppage in 1997 as a result of fire and explosions.

Crowl & Louvar (2011) say that the prevention of fires and explosion can only be provided by knowing fire and explosion characteristics of chemicals, by understanding the process of fire and explosion and recognizing the ways of reducing fire and explosion probability.

2.1.1. The Fire Triangle

According to Crowl & Louvar (2011), the important components of the fire process are fuel, oxidizer and ignition source. Figure 2.1. provides an understanding of fire process and its components.

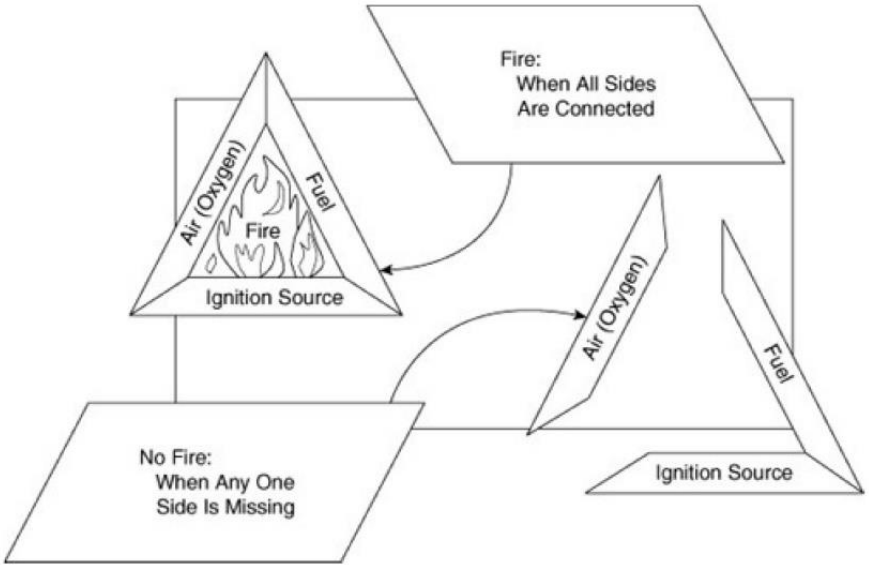

Figure 2.1. Fire Triangle (Crowl & Louvar, 2011)

According to Crowl & Louvar (2011), fire can be described as a fast exothermic oxidation reaction of ignited fuel. The fuel can be in many different forms such as solid, liquid or vapor however vapors of liquid fuels are easier to be ignited. Before the combustion process, liquids are volatized and solids are decomposed into the gaseous phase, accordingly, the process of combustion is always conducted in the vapor phase.

In order to fire process to occur, fuel, oxidizer and an ignition source should be available in a sufficient amount. Therefore, burning will not take place in case of absence or insufficiency of fuel or oxidizer and if ignition source does not have sufficient energy to start the fire.

In the past decades, the main methodology for fire and explosion control was to eliminate or reduce the source of ignition. However, it was realized that eliminating or reducing sources of ignition is not adequate for fire and explosion prevention since the required energy for ignition of flammable chemicals is very low and there are various sources of ignition. Therefore, it was found to be more effective in fire and

explosion control to eliminate sources of ignition while avoiding flammable atmospheric conditions to occur.

Many different types of fuels, oxidizers and ignition sources can be found in the aviation industry. Fuels and oxidizers can be in the form of solid, liquid or gas. Additionally, ignition sources can be found as sparks, flames static electricity and heat.

2.1.2. Distinction between Fires and Explosions

Crowl & Louvar (2011) states that the main difference between fire and explosion is the energy output rate. In burning process, the energy output rate is slower than the explosion energy release rate which is in degrees of microseconds. Fires can be initiated by explosions and also explosions can be caused by fires.

2.1.3. Definitions

Fire or combustion can be defined as a chemical process in which a material reacts with an oxidizing agent and outputs some energy.

Ignition can be initiated by interaction of ignition source with the required energy and flammable gas in high temperatures which is sufficient for flammable gas to auto-ignite (Crowl & Louvar, 2011).

Autoignition temperature (AIT) is the minimum required temperature for the ignition of a combustible gas by its own heat in the absence of a glow or flame. An increase in chain length of straight-chain hydrocarbons causes AIT to decrease (Nolan, 2014).

Flash point is the minimum temperature at which combustible vapors can be ignited by an ignition source (Hattwig & Steen, 2004). One of the main characteristics to specify fire and explosion hazard of liquids is the flash point temperature.

Fire point is the minimum temperature for a flammable gas to maintain burning after ignition (Crowl & Louvar, 2011).

Lower Flammability Limit (LFL) is the lowest concentration of a flammable gas in air below which ignition cannot take place (Moosemiller, 2014). Flammable limits and explosive limits are the technical terms which can be used interchangeably (Nolan, 2014).

Explosion can be described as a sudden discharge of energy resulting in a blast (Baker et al., 2010).

Blast is a temporary alteration in the density gas mixture, pressure and speed of air flow at the surrounding of an explosion source (Baker et al., 2010).

Confined explosion occurs inside an enclosed volume such as tank, container or structure. Confined explosion is the most destructive type of explosion causing injury and demolition of buildings.

An unconfined explosion occurs in the open atmosphere. Unconfined explosions are mostly caused by flammable chemical spillage. As a result of a spill, flammable vapors disperse in the air and can form an explosive mixture with air until it is ignited by an ignition source. Unconfined explosions are not common since explosive vapors are diluted by wind below the LFL. On the other hand, unconfined explosion can also be very damaging since a huge amount of flammable vapor is involved (Crowl & Louvar, 2011).

Deflagration is caused by an explosion where the propagation of the reaction front occurs at a speed slower than the speed of sound in front of the pressure front (Vinnem, 2014).

Detonation is the dispersion of energy resulting from a very fast chemical reaction in which reaction front moves outward from explosion source at higher than the speed of sound (Woodward, 1998).

Shock wave is a sudden pressure wave causing strong wind. The combination of shock wave and wind is known as blast wave. Shock wave has a very fast pressure rise which is a mostly adiabatic process (Crowl & Louvar, 2011).

Overpressure is negative or positive pressure which is formed as a result of an explosion (Nolan, 2014).

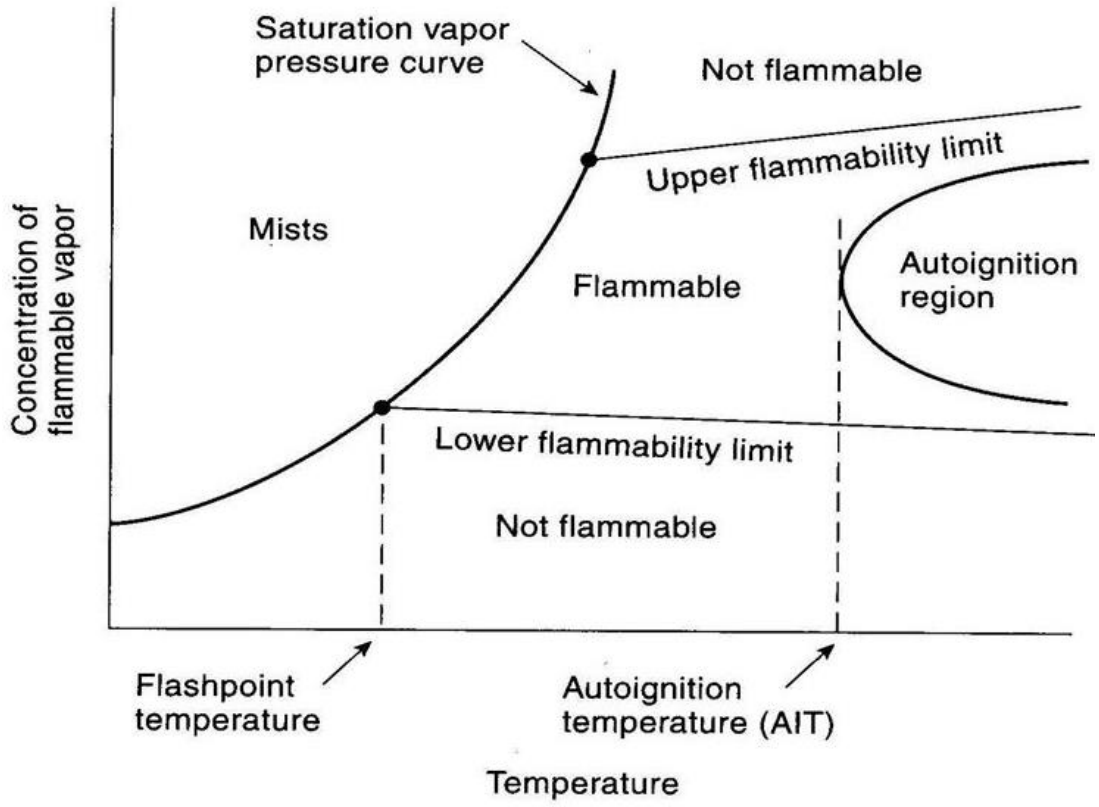

Figure 2.2. Relationships Between Various Flammability Properties (Crowl & Louvar, 2011).

In figure 2.2, it can be seen the graph of concentration of flammable vapor versus temperature and the relationship of the above definitions. The exponential curvature signifies the saturation vapor pressure curve of the liquid substance. As usual, upper flammable limit (UFL) becomes higher and lower flammable limit (LFL) becomes

lower with an increase in temperature. In theory, the intersection point of LFL and the saturation vapor pressure curve of the liquid represents flash point however sometimes empirical data does not validate this idea. The lowest temperature of the autoignition curve gives the autoignition temperature. The flash point and flammability limits are not the main characteristics of a liquid and can only be identified by special laboratory equipment.

2.1.4. Explosions

There are lots of factors that determine the explosion process. The most important factors that affect the explosion are given in the table below.

Table 2.1. *Main Factors That Affect Explosion Process (Crowl & Louvar, 2011)*

Ambient temperature
Ambient pressure
Composition of explosive material
Physical properties of explosive material
Nature of ignition source: type, energy and duration
Geometry of surrounding: confined or unconfined
Amount of combustible material
Turbulence of combustible material
Time before ignition
Rate at which combustible material is released

Explosion is a very complex process to estimate. Theoretical, experimental and semi-empirical methodologies have been carried out for modelling explosions. However, the explosion process cannot be completely figured out. Hence, engineers should take

into consideration all probable outcomes carefully in order to guarantee safety in designing.

Explosions are caused by a very fast release of energy. The discharge of energy must be very quick to provide energy to accumulate at the blast source. After that, the energy is dispersed by pressure wave, projectiles, thermal radiation, and acoustic energy. The disposed energy causes the explosion damage.

If a gas explosion occurs, immediately gas starts to disperse very fast to the environment causing a pressure wave that pushes nearby gases backward from the site of the explosion. The energy contained in the pressure wave causes surroundings to be damaged. For chemical explosions, the main factor that causes damage is the pressure wave. Therefore, the dynamics of the pressure wave should be understood to predict explosion damage.

The pressure wave dispersing outward from the explosion is also known as the blast wave since a strong wind occurs after the explosion. A shock wave or shock front is caused in case of sudden pressure change. Very explosive chemicals can cause a shock wave to occur. The maximum pressure reached after an explosion is known as the peak overpressure.

2.1.4.1. Detonation and Deflagration

According to Crowl & Louvar (2011), the damage of the explosion is mainly dependent on whether the explosion is a result of detonation or deflagration. The distinction relies upon whether the reaction front disperses above or below the speed of sound in the ambient atmosphere. The speed of sound is 344 m/s regarding ideal gases at 20 °C and it only varies with temperature.

In detonation, the reaction front is transferred by a very high-pressure wave that pressurizes the ambient air in front of the reaction front above its autoignition temperature. This sudden pressure change causes a shock front to occur in front of the

reaction front. So, the front wave and the shock wave disperse at the speed of sound into the surrounding atmosphere.

In deflagration, explosion energy disperses into ambient air by heat conduction and molecular diffusion. Since these transfer processes are slower than the speed of sound, the reaction front disperses slower than sonic speed.

In figure 2.3, the gas dynamics of detonation and deflagration in the open air are compared. In detonation, the movement speed of the reaction front is greater than sonic velocity. A shock front is present in front of the reaction front. For the shock front to move at the speed of sound, the required energy is provided by the reaction front. Both fronts move at the same velocity. In deflagration, movement speed of reaction front is lower than sonic velocity while pressure front disperses at the speed of sound and moves away from the reaction front. Therefore, it can be thought that the deflagration reaction front produces a series of separate pressure fronts continuously. Resulting pressure fronts added to each other and collected in the main pressure front. The main pressure front grows continuously as additional energy is accumulated.

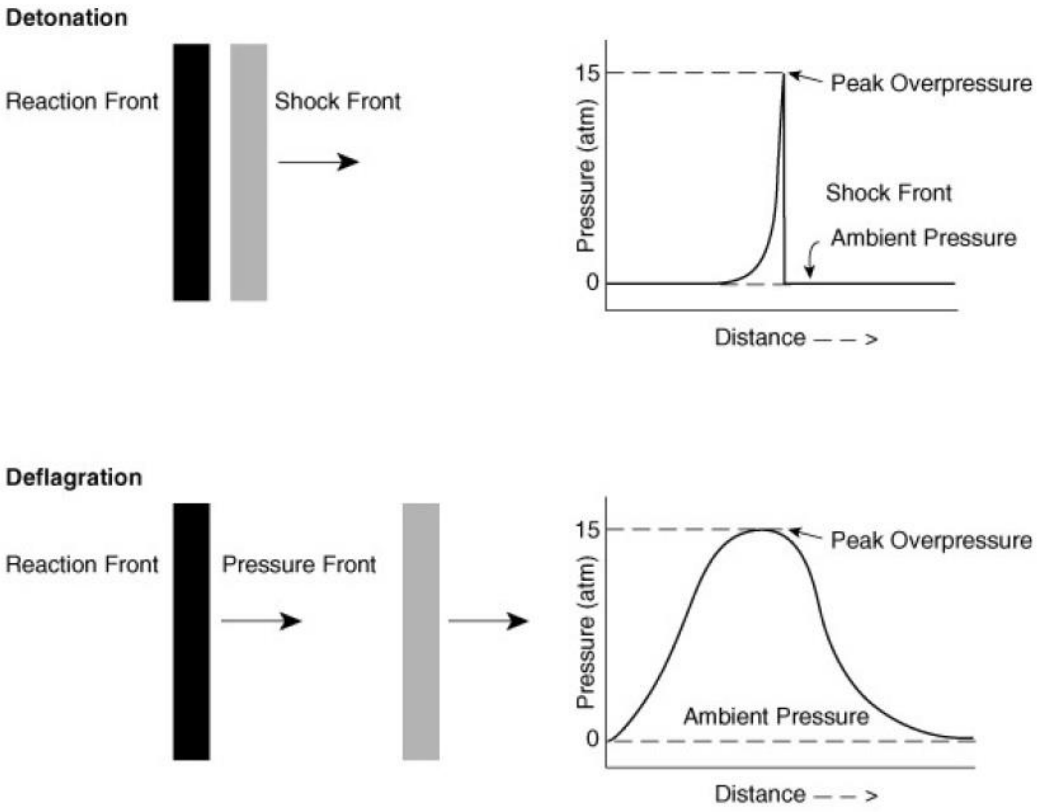

Figure 2.3. Comparison of Physical Differences between Detonation and Deflagration (Crowl & Louvar, 2011)

Detonation and deflagration produce pressure fronts which are obviously different from each other. In detonation, a shock front is formed with sudden pressure change of about 10 atm for a duration of 1 millisecond. In deflagration, a shock front is not formed and the pressure front lasts for many milliseconds and has lower pressure characteristically 1 or 2 atm.

Reaction fronts and pressure fronts can differ because of the enclosing environment of the explosion source. Altered behaviors of fronts can be observed if the explosion occurs in a confined volume like a vessel or a pipeline.

According to Crowl & Louvar (2011), the transformation of a deflagration to detonation can be observed in some cases. This transformation is known as deflagration to detonation transition (DDT). DDT can occur in pipelines however, it is not likely to occur in vessels and open air. In pipelines, deflagration energy provides additional pressure to the main pressure wave causing pressure increase which can result in detonation.

2.1.4.2. Blast Damage Resulting from Overpressure

After the explosion of a gas, whether detonation or deflagration, the reaction front is occurred dispersing from explosion source and it is followed by a shock wave or pressure wave. After the combustion reaction is complete, the reaction front disappears but the pressure front carries on to its movement. A blast wave consists of a pressure front and resulting wind. Most of the damage is caused by the blast wave.

Figure 2.4 provides an understanding of chance in blast pressure over time for a characteristic shock wave at a certain point away from the explosion source. In figure 2.4, t_0 represents time of explosion, t_1 signifies the arrival time of blast pressure to damaged location from explosion source. At t_1, shock front causes maximum overpressure to occur and followed by subsequent wind at a fixed location. The blast pressure reduces rapidly to the ambient pressure at t_2 but the wind continues to move forward for a period of time. The time interval between t_1 and t_2 is known as shock duration. The shock duration has the most destructive effect on surrounding structures during an explosion thus, it is important to know its value to assess the damage. Since the pressure continues to decrease below the ambient pressure, at t_3, the maximum underpressure is reached. For the time period between t_2 and t_4, the explosion wind moves in the opposite direction towards the explosion source. There can be some damage caused by underpressure, however, the damage is limited compared to overpressure damage. From t_3 to t_4, the pressure increases and reaches ambient pressure at t_4. At t_4, the explosion wind and destruction effect is over.

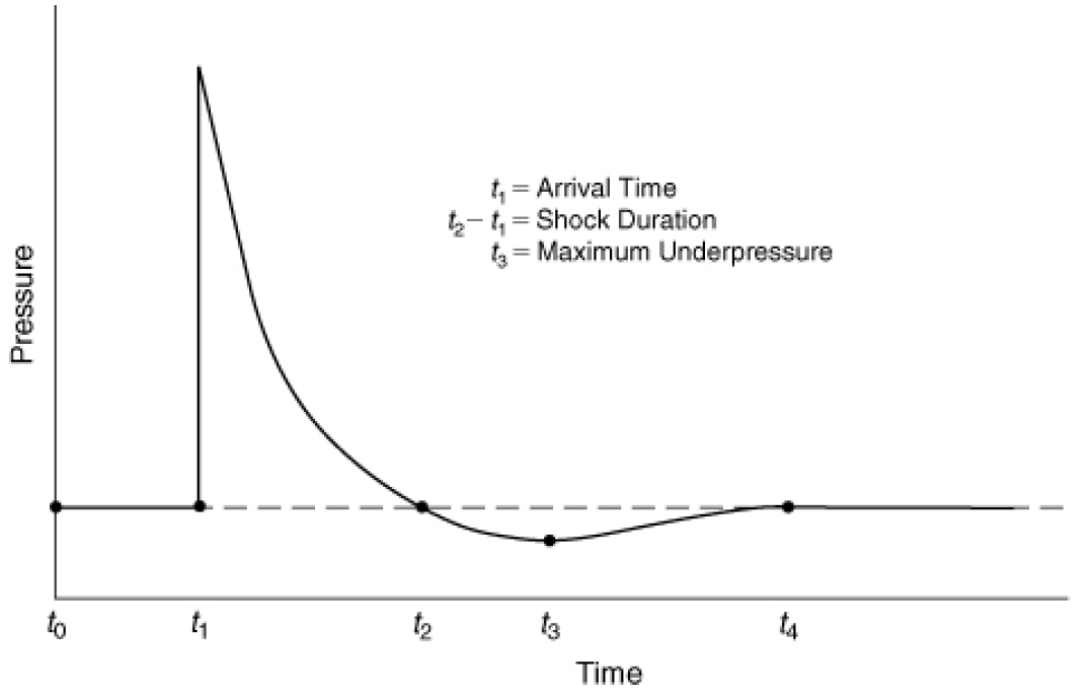

Figure 2.4. Blast Pressure Change at a Certain Point versus Time (Crowl & Louvar, 2011).

The blast damage can be determined by peak overpressure that is caused by the pressure wave of the explosion. Generally, the blast damage depends on the pressure increase rate and time period of the blast wave. Accurate estimation of blast damage can be estimated by just using the peak overpressure (Crowl & Louvar, 2011).

2.1.4.3. Vapor Cloud Explosions

According to Crowl & Louvar (2011), vapor cloud explosions (VCEs) causes the most damaging effect in chemical operations. VCEs has three occurrence steps:

1. Immediate discharge of huge amount of flammable vapor (such as vessel brust)
2. Dispersal of flammable vapors through the operation area
3. Ignition of flammable vapors

The occurrence rate of VCEs is increasing in process plants since the number of flammable chemicals is also increasing and operations are conducted in harder conditions. It is very hard to classify an event as a VCEs since there are lots of parameters that are needed to describe an event. VCEs happen under uncontrolled conditions and real incident data are not reliable for comparison.

The most important factors that affect VCE are amount of flammable vapor discharge, concentration of flammable vapor in the air, ignition probability of flammable gas vapor, dispersion distance of vapor cloud, duration before ignition of flammable gas, possibility of explosion, presence of threshold amount of gas, effectiveness of explosion and position of the ignition source.

Crowl & Louvar (2011) says that ignition possibility of flammable vapor cloud increases if the volume of cloud increases, VCEs are much unlikely to happen compared to vapor cloud fires, effectiveness of explosion is low (around 2% of the combustion energy is transformed to blast wave), the effects of explosion increases with the effective flammable gas and air mixture and ignition of vapor cloud at a far distance from the source.

Regarding safety, the most effective way of explosion prevention is to avoid flammable material discharge. It is very hard to control a huge volume of vapor cloud to be ignited even all safety measures are in place.

The ways of VCEs prevention are reducing amount and number of flammable materials, process control providing that probability of vapor cloud ignition is at minimum, detection systems for chemical leakage, installation of automatic blockage valves for shutting the system down to prevent leakage.

2.2. Source of Ignition

Ignition can be described as immediate change to a self-sustained, high-temperature oxidation reaction. According to Moosemiller (2014), International Organization for

Standardization (ISO) describes ignition as the beginning of combustion while the National Fire Protection Agency (NFPA) describes ignition as an oxidation process which occurs at a quick rate for forming heat and typically in the form of a glow or a flame.

Chemical vapor ignition can be started by different means like contact with open flame, electric spark, or a hot surface (Baker et al., 2010). In some cases, ignition can also be initiated by auto-ignition and forced ignition. Additionally, average temperature sources, electrical sources like powered equipment, electrostatic accumulation, lightning and chemical sources can cause immediate ignition (Moosemiller, 2014). Other important sources of ignition are some motorized vehicles, mechanical sparks arising from the friction between moving parts of machinery (Baker et al., 2010). In the British Standard of Explosive Atmospheres – Explosion prevention and protection – Part 1 Basic concepts and methodology (BS EN 1127-1:2007) ignition sources are grouped as hot surfaces, flames and hot gases, mechanical sparks, electrical equipment, electric current, static electricity, lightning, high frequency electromagnetic waves, radio frequency electromagnetic waves, ionizing radiation, ultrasonics, adiabatic compression and exothermic reactions (BSI, 2008).

For each situation, there is the lowest contact time and the lowest energy transfer required to develop self-combusting volume (Baker et al., 2010). It is quite important to compare the ignition capacity of the ignition source regarding flammability characteristics of the combustible material such as MIE and ignition temperature (BSI, 2008). Minimum energy required for electrical spark to initiate the ignition of flammable chemical vapor under certain conditions is described as Minimum Ignition Energy (MIE) (Baker et al., 2010). Ignition temperature of an explosive atmosphere is the lowest required temperature for the ignition of air-gas mixture depending on pressure and type of ignition source (Hattwig & Steen, 2004).

2.2.1. Mechanical Ignition

Combustible vapors can be ignited by sparks resulting from rotating cutting machinery, friction in equipment or by impact and falling of sparking objects (Moosemiller, 2014). Friction and impact of materials cause hot spots on the surface which behaves as an ignition source. According to the formation process of the sparks, the surface temperature of the particles can rise to 2000 °C (Roth et al., 2014). The increase of the temperature is in correlation with kinetic energy which can cause ignition (Mannan, 2014). Mechanical sparks cause temperature increase by conduction and heat radiation while flying through combustible vapor clouds. Since spark particles have a high surface volume ratio, the energy transfer is very fast for the ignition of flammable mixtures which have a self-ignition temperature under 1000 °C (Roth et al., 2014). Beside temperature rise as a result of friction, materials with increased temperature such as aluminum, magnesium or titanium, can start a chemical reaction with ambient oxygen causing energy release and further temperature rise (Groh, 2004).

2.2.2. Electrical Ignition

One of the most significant ignition source is electrical ignition sources in explosion protection. Electrical ignition can be caused by short circuits or by shorting to earth in deformed electrical machinery (Hattwig & Steen, 2004). Additionally, switches, brushes and alike electrical equipment can generate electric sparks and arcs during the daily process (BP, 2006).

Simply, electrical ignition can be seen as electrical discharges in numerous kinds in the explosive atmosphere. According to the type of electrical discharge, the capability to ignite an explosive atmosphere changes (Hattwig & Steen, 2004).

2.2.3. Open Flame

Open flames can be considered as highly efficient ignition source because of their high temperature (Woodward, 1998). Existing flames from some equipment in the plant such as fired heaters can cause combustible vapors to ignite (Moosemiller, 2014). Elimination of such flames is not possible hence, necessary precautions should be taken in place (Mannan, 2014). In order to ignite flammable gas-air mixture, higher temperature than the flash point is required. Table 2.2 shows flash points of some flammable chemical vapors are shown (Groh, 2004).

Table 2.2. *Flash Points of Flammable Chemical Vapors*

Substance	*Chemical formula*	*FP*	
		°C	°F
Acetaldehyde	CH_3CHO	-38...-27	-36...-17
Acetic acid	CH_3COOH	+40	+104
Acetone	CH_3COCH_3	-20	-4
Benzene	C_6H_6	-11	+ 12
Benzene chloride	C_6H_5Cl	+28... + 30	+82...+86
Carbon disulphide	CS_2	-30	-22
Castor oil	-	+229	+444
Ethanol	C_2H_5OH	+ 11...+13	+52...+55
Formic acid	HCOOH	+42	+108
Lanoline	-	+240	+464
Methanol	CH_3OH	+ 11	+52
Naphthalene	$C_{10}H_8$	+80	+ 176
Nitrobenzene	$C_6H_5NO_2$	+88	+ 190
Nitrotoluene	$CH_3C_6H_4NO_2$	+ 106	+223
Olive oil	-	+225	+437
Phenol	C_6H_5OH	+82	+ 180
Phthalic acid	$C_6H_4(COOH)_2$	+ 168	+334
Phthalic anhydride	$C_6H_4(C0)_20$	+ 152	+306
Propyl alcohol	C_3H_7OH	+ 15	+59
Sulphur	S	+207	+405
Toluene	$C_6H_5CH_3$	+6	+43
Vinyl chloride	CH_2CHCl	-43	-45
Crude oil products			
Benzine	-	+21	+70
Petrol	-	<+81	<+178
Kerosene	-	<-20...+60	<-4... +140
Diesel fuel	-	>+55	>+131
Fuel oil (light)	-	>+55	>+131
Fuel oil	-	>+65	>+149
Motor oil	-	>+ 185	>+365
Transformer oil	-	>+ 145	>+293

2.2.4. Hot Surfaces

Exposure of flammable vapors to hot surfaces can cause ignition (Nolan, 2014). Hot surfaces can occur in routine processes such as heating, dryers or electrical equipment in the plants. Any malfunction of equipment can cause a flammable gas-air atmosphere to ignite (Hattwig & Steen, 2004). Hot surfaces required to be isolated, cooled or repositioned in order to prevent the ignition of flammable vapors when there is a possibility of spillage or leakage (Nolan, 2014).

Since there is a steady dispersion of flammable gas vapor close to hot surfaces in the open air because of the wind, the contact time of flammable gas to the hot surface is very short. As a result of the short contact time, the required surface temperature to start ignition is relatively high compared to AITs. Table 2.3 shows the minimum surface temperature for ignition of kerosene in open air according to different wind velocities (API, 2003).

Table 2.3. *Effect of Wind Velocity in AITs Using Kerosene (API, 2003)*

Wind Velocity Over the Hot Surface meters/sec.	Surface Temperature Required for Ignition °C
0.3	405
1.5	660
3.0	775

2.2.5. Static Electricity

In some cases, the ignition of a flammable mixture can occur in the absence of energy addition or operation failure such as electrostatic charging. Generally, static electricity is thought to be the reason for explosions in which any ignition cause was observed since electrostatic discharge leaves no evidence (Hattwig & Steen, 2004). Electrostatic ignition should be analyzed to understand how the charging process can take place

and to find out the location of the accumulation of static electricity (Lüttgens et al., 2017).

Electrostatic charge can ignite combustible vapors as a result of the same sequence of physical processes shown in Figure 2.5.

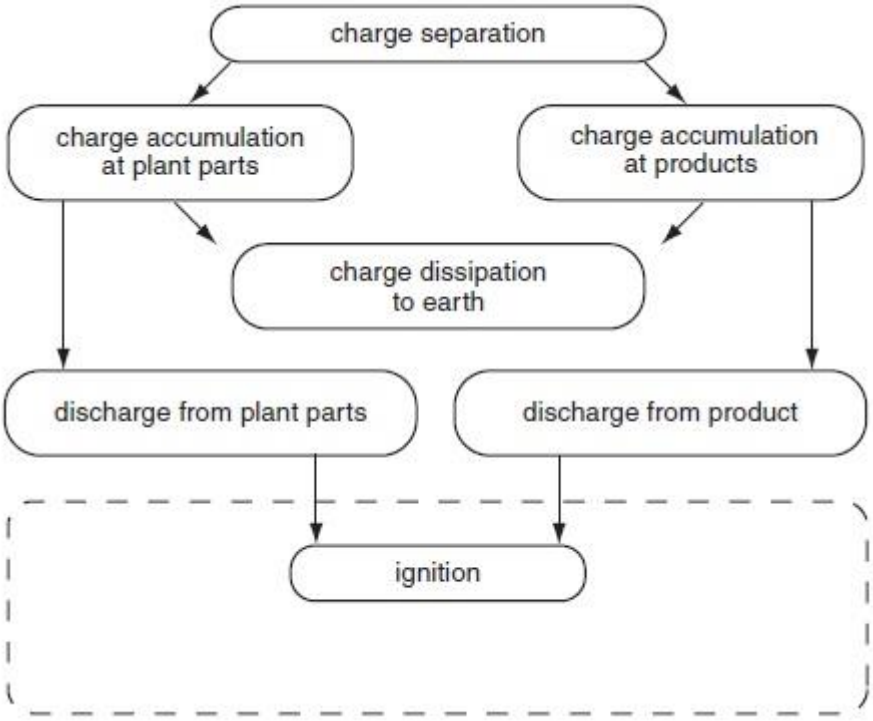

Figure 2.5. Ignition Process of Flammable Vapors by Electrostatic Electricity (Hattwig & Steen, 2004)

Even if the ignition process looks simple, it is very hard to define each step on the field since many different operations are conducted at the same time. Therefore, electrostatic charge accumulation is correspondent to the overall rate of charge separation and discharge.

In industrial plants, movement of conveyor belts, vehicle transportation and walk of workers on the insulating ground can cause electrostatic charge accumulation. It is

vital to notice that after the contact process, all surfaces which are in contact with each other are charged.

If the electrical field generated by charge accumulation reaches a higher value than the dielectric field strength which is 3 MV/m, electrostatic energy can be discharged. High energy discharge can cause the ignition of a flammable vapor-air mixture. Ignition of the explosive atmosphere is dependent on the amount of energy release and flammability of the chemical vapors that is correspondent to the MIE. In Figure 2.6, the physical parameters that affect the ignition process of flammable vapors by electrostatic electricity are shown. Electrical resistance of production equipment, products, materials and electrical connection to the ground are important parameters which have an influence on charge accumulation and discharge occurrence (Hattwig & Steen, 2004).

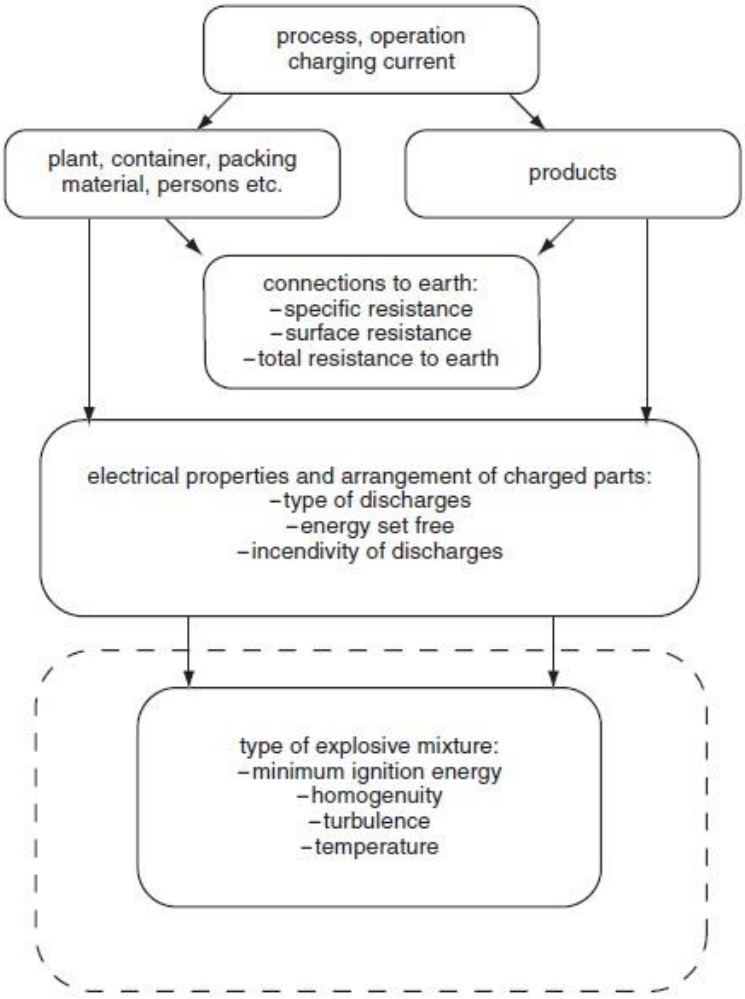

Figure 2.6. The Physical Parameters Affecting the Ignition Process of Flammable Vapors by Electrostatic Electricity (Hattwig & Steen, 2004)

2.3. JP-8 and Kerosene

Unrefined form of petroleum has a very limited range of direct use in industrial areas. Oil gains value after being transformed into commercial products in the refineries (Speight & El-Gendy, 2018). Liquid petroleum products can vary from highly volatile naphtha to lubricant oils which have very low volatility (Speight, 2014). Generally, physical characteristics are used to categorize liquid petroleum products (Speight & El-Gendy, 2018).

Kerosene (kerosine can also be used) is one of the liquid, colorless and flammable petroleum product with specific odor. It is commonly used for burning lamps, heating houses, fueling jet engines, solvent for greases and insecticides. In general, the term kerosene is wrongly used for describing fuel oils however fuel oil can be any type of liquid petroleum by-product which is used to obtain heat or power when burned (Speight & El-Gendy, 2018).

Table 2.4. *Petroleum Products (Speight & El-Gendy, 2018)*

Product	Lower Carbon Limit	Upper Carbon Limit	Lower Boiling Point (°C)	Upper Boiling Point (°C)
Refinery gas	C_1	C_4	-161	-1
Liquefied petroleum gas	C_3	C_4	-42	-1
Naphtha	C_5	C_{17}	36	302
Gasoline	C_4	C_{12}	-1	216
Kerosene/diesel fuel	C_8	C_{18}	126	258
Aviation turbine fuel	C_8	C_{16}	126	287
Fuel oil	C_{12}	$>C_{20}$	216	421
Lubricating oil	$>C_{20}$		>343	
Wax	C_{17}	$>C_{20}$	302	>343
Asphalt	$>C_{20}$		>343	
Coke	$>C_{50}$		>1000	

Kerosene is a chemical mixture of hydrocarbons. Constituents of kerosene vary according to their source. Mostly, kerosene contains various hydrocarbons with 10 to 16 carbon atoms (Speight, 2011). Table 2.4. shows carbon numbers of various petroleum products. Ghassemi et al. (2006) say that kerosene has very similar general properties to dodecane, $C_{12}H_{26}$. Table 2.5. demonstrates average formula of petroleum products. According to Chickos and Hanshaw (2004), enthalpy of vaporization of dodecane is 65.1 kJ/mol. Dodecane has a boiling temperature of 216 °C (Safety Data Sheet (SDS) – Thermo Fisher Scientific, 2018). Kerosene is more volatile than diesel oil but not more volatile than gasoline. Kerosene can be distilled between 150-300 °C. Flash point of kerosene is around 25 °C (Speight & El-Gendy, 2018).

Table 2.5. *Assumed Average Formula of Petroleum Fuels (Totten et al., 2003)*

Fuel	Assumed Average Formula
Aviation gasoline	$C_{7.3}H_{15.3}$
Aviation kerosene	$C_{12.5}H_{24.4}$
Gas oil	$C_{15}H_{27.3}$

Kerosene is mainly used as jet fuel in aviation. Some particular characteristics are needed to be used as aviation fuel such as high flash point for safe handling, low freezing point for cold weather usage and no mixing with water. Table 2.6 shows the heat of vaporization values for several oil products (Speight, 2017).

Table 2.6. *Heat of Vaporization of Oil Products (Speight, 2017)*

Product	Gravity, °API	Average boiling temp, °F	Heat of vaporization	
			Btu/lb*	Btu/gal*
Gasoline	60	280	116	715
Naphtha	50	340	103	670
Kerosene	40	440	86	595
Fuel oil	30	580	67	490

*Btu/lb × 2.328 = kJ/kg; Btu/gal × 279 = kJ/M^3

Jet fuel is light petroleum distillate and has different types for usage in jet engines. Commonly used jet fuels for military purposes are JP-4, JP-5, JP-6, JP-7 and JP-8. JP-8 is kerosene modeled fuel which is also used in civil aviation (Speight & El-Gendy, 2018). According to the U.S. Department of Defense (2015), JP-8 is a kerosene-type engine fuel which contains several additives such as fuel system corrosion and icing inhibitors.

Mainly, straight alkanes, branched alkanes and cycloalkanes are present in aviation fuels. A maximum of 20%–25% of fuel consist of aromatic hydrocarbons since they cause smoke after combustion. 5% of total fuel is limited to alkenes for JP-4. Approximately, the percentage of ingredients of aviation fuel are 32% of straight-

chain alkanes, 31% of branched alkanes, 16% of cycloalkanes and 21% of aromatic hydrocarbons (Speight & El-Gendy, 2018).

Table 2.7. *Properties of Hydrocarbon Products from Petroleum (Speight, 2011)*

	Molecular weight	Specific gravity	Boiling point °F	Ignition temperature °F	Flash point °F	Flammability limits in air % v/v
Benzene	78.1	0.879	176.2	1040	12	1.35-6.65
n-Butane	58.1	0.601	31.1	761	-76	1.86-8.41
iso-Butane	58.1		10.9	864	-117	1.80-8.44
n-Butene	56.1	0.595	21.2	829	Gas	1.98-9.65
iso-Butene	56.1		19.6	869	Gas	1.8-9.0
Diesel fuel	170-198	0.875			100-130	
Ethane	30.1	0.572	-127.5	959	Gas	3.0-12.5
Ethylene	28.0		-154.7	914	Gas	2.8-28.6
Fuel oil No. 1		0.875	304-574	410	100-162	0.7-5.0
Fuel oil No. 2		0.920		494	126-204	
Fuel oil No. 4	198.0	0.959		505	142-240	
Fuel oil No. 5		0.960			156-336	
Fuel oil No. 6		0.960			150	
Gasoline	113.0	0.720	100-400	536	-45	1.4-7.6
n-Hexane	86.2	0.659	155.7	437	-7	1.25-7.0
n-Heptane	100.2	0.668	419.0	419	25	1.00-6.00
Kerosene	154.0	0.800	304-574	410	100-162	0.7-5.0
Methane	16.0	0.553	-258.7	900-1170	Gas	5.0-15.0
Naphthalene	128.2		424.4	959	174	0.90-5.90
Neohexane	86.2	0.649	121.5	797	-54	1.19-7.58
Neopentane	72.1		49.1	841	Gas	1.38-7.11
n-Octane	114.2	0.707	258.3	428	56	0.95-3.2
n-Pentane	72.1	0.626	97.0	500	-40	1.40-7.80
iso-Pentane	72.1	0.621	82.2	788	-60	1.31-9.16
n-Pentene	70.1	0.641	86.0	569	-	1.65-7.70
Propane	44.1		-43.8	842	Gas	2.1-10.1
Propylene	42.1		-53.9	856	Gas	2.00-11.1
Toluene	92.1	0.867	321.1	992	40	1.27-6.75
Xylene	106.2	0.861	281.1	867	63	1.00-6.00

The most important characteristics for kerosene are flash point, fire point and boiling range. The flash point of kerosene is generally set above the average ambient temperature. The fire point is essential for determining fire prevention means. The distillation range is not a significant property however it can be seen as an indicator of viscosity. Additionally, pureness of the kerosene can be understood by the steady burning of the product over a time interval (Speight, 2011). Table 2.7. shows several properties of hydrocarbon products.

ACGIH (2015) states that kerosene/jet fuels, as total hydrocarbon vapor, have TLV-TWA of 200 mg/m^3. Additionally, exposures above the TLV-TWA value should not be allowed for more than 15 minutes. Kerosene has TLV –TWA of 30 ppm and an odor threshold of 0.1 ppm. Additionally, kerosene has a lower explosion limit (LEL) of 0.7% and an upper explosion limit (UEL) of 5% by volume. (Material Safety Data Sheet (MSDS) – John Duffy Energy Services, 2006)

According to the U.S. Department of Defense (2015), kerosene-type aviation turbine fuel, JP-8 should comply with the requirements given in the military standard MIL-DTL-83133J. Table 2.8 shows some requirements of MIL-DTL-83133J.

Table 2.8. *Chemical and Physical Requirement (U.S. Department of Defense, 2015)*

Property	**Min**	**Max**
VOLATILITY		
Distillation temperature, °C		
Initial boiling point		
10 percent recovered		205
20 percent recovered		
50 percent recovered		
90 percent recovered		
Final boiling point		300
Residue, vol percent		1.5
Loss, vol percent		1.5
Flash point, °C	38	
Density		
Density, kg/L at 15 °C or	0.775	0.840
Gravity, API at 60 °F	37.0	51.0

2.4. Fuel Servicing of Aircraft

Aircraft fuel servicing is the process of transfer of fuel to or from a fuel supply to or from an aircraft together with fueling connection and disconnection operation. Fueling operation supervisor must confirm that all fuel servicing operators are capable of conducting fueling operation safely by following technical orders under their supervision (USAF, 2013).

2.4.1. Electrostatic Hazards in Fuel Servicing and Static Grounding and Bonding

Aircraft fuel does not burn in liquid form but it burns in the gaseous state. Volatility is the ability of a liquid to transform into gaseous form and fuel can vaporize at low temperatures. Therefore, gaseous or vapor form of fuel has fire and explosion hazards during fuel servicing of aircraft (FAA, 2008).

Static electricity can be described as a buildup of electric charge on the uppermost layer of material (Wang, 2019). Static electricity can be formed by friction of two materials. Fuel flow inside a fueling pipeline generates electrostatic charging. Additionally, the structural frame of the aircraft accumulates static electricity due to friction in the air during the flight. Static electricity should be discharged before fueling operation otherwise, it reaches to ground through fueling pipeline and it can cause the ignition of fuel vapors.

There is always a hazard of fire and explosion due to electrostatic charges in fuel servicing of aircraft. The most effectual way of preventing electrostatic hazards is grounding or bonding. Grounding is the connection of metallic materials to ground. Bonding is the connection of two or more metallic materials to each other by a conductor to equalize electrostatic potential (FAA, 2008).

While filling the fuel tank, the electrical potential of fuel flow can increase up to thousands of volts. A spark discharged from pipelines, fittings or any other object can

ignite fuel vapor-air mixture. Any contaminant object in the fuel tank will accumulate the electrostatic charge and act as an electrical condenser. The potential needed for discharging from contaminant to fuel is much less than the amount necessary for discharge from fuel to tank. As a result, contamination of fuel dramatically increases the electrostatic hazards. If the fuel flow is kept under the allowable fueling rates, electrostatic charging does not occur (USAF, 2013). Table 2.9. shows maximum allowable fueling rates during fueling operation of aircrafts.

Table 2.9. *Maximum Allowable Fueling Rates (USAF, 2013)*

Nozzle / Hose / Pipe Diameter (inches)	Gallons / Minutes
0.75	32
1.50	125
2.00	225
2.50	352
3.00	470
4.00	627
5.00	783
6.00	940

2.4.2. Fueling Procedures

Two main procedures are applied during the fueling operation of aircraft. In small aircraft, fueling is conducted by over-the wing technique. In large aircraft, fueling is provided by single point technique. All fuel tanks of aircraft are filled from single point refuel (SPR) receptacle at the bottom of the wing. So that, time required for fueling aircraft is minimized, contamination of fuel is prevented and the ignition of fuel by static electricity is reduced. In general, fueling systems consist of fueling hose, control panel and gauges (FAA, 2008).

There are several precautions in order to prevent fire and explosion hazards during the fueling operation. Firstly, all electrical devices and electronic systems, including radar, must be closed down during fueling operation. Aircraft and fueling equipment must be grounded. Proper type of fire extinguishers must be available. Fueling operators are not allowed to carry any kind of equipment that can produce flame. The operator must wear antistatic safety shoes, clothes and eye protection (FAA, 2008). Operators shall carry a dead man control unit in order to stop fuel flow in case of emergency. Service operator shall report any type of probable hazard such as fuel leakage, spillage or spray, fault bonding/grounding of receptacles, visible spark from any source to the supervisor immediately.

Housekeeping of the work area is an important issue in aviation. Clean and tidy workplace is necessary for safe and effective operations in fueling stations, aircraft parking areas and servicing aprons. Safe fuel servicing can be provided by the prevention of fuel spills and removing ignition sources from fuel servicing stations.

Fuel servicing safety zone (FSSZ) must be established and retained during fueling operations. FSSZ covers 50 feet radius area centering fuel servicing components such as SPR, and 25 feet around fuel vent outlets. Figure 2.7 shows an example of a fuel servicing safety zone (FSSZ). Another aircraft next to FSSZ can keep its engine running as long as its thrust is not directed toward FSSZ (USAF, 2013). Throughout the fuel servicing of aircraft, all possible ignition sources such as ground servicing equipment are eliminated and kept away from FSSZ. Servicing equipment must be positioned so a clear path is maintained to allow fast evacuation of vehicles and staff in an emergency (USAF, 2018).

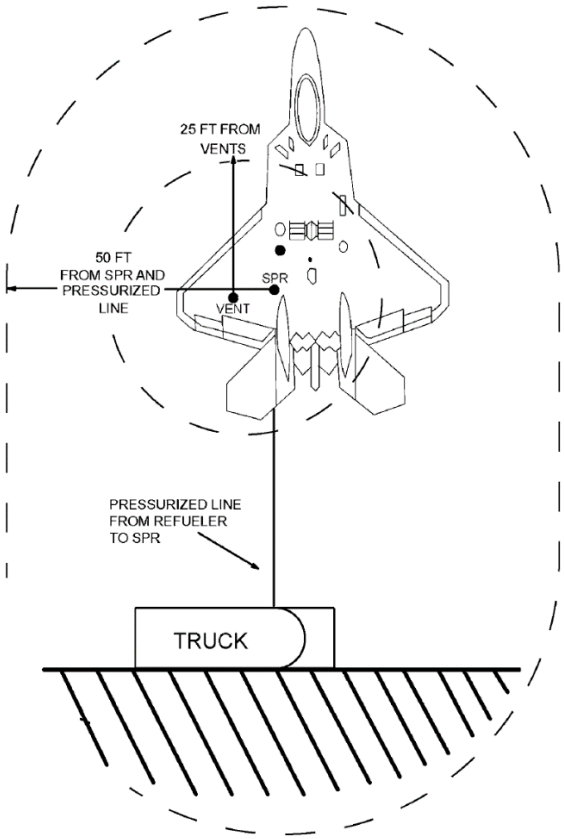

Figure 2.7. Fuel Servicing Safety Zone (FSSZ)

In the case of mobile fueling tank usage, the fuel tank must be parked in the direction of escape in an emergency. Hand break of the fuel truck must be set and wheels must be chocked. Aircraft must be grounded and then fuel truck must be grounded. Then, aircraft and fuel truck must be bonded by wire. Nozzle must be also grounded to the aircraft (FAA, 2008).

2.4.3. Fire Protection

Fire protection is crucial in fuel servicing of aircraft. Supervisors must establish and maintain a fire safety training program. All staff must be trained to understand their responsibilities and roles for the fire prevention program in the flight line. At the end

of every shift, field inspection should be carried out to ensure that there is no fire risk in the flight line (USAF, 2018). Supervisor should give briefing on emergency action plan to servicing operators before fueling service. The fire department must be notified before the fuel servicing operation (USAF, 2016). In case of fire or fuel leakage, fuel servicing operators are the first team of defense. Servicing operators must alert the fire department immediately and use available firefighting equipment until the fire department reaches to the area.

Fueling operation supervisor should ensure the proper type of fire extinguisher for fire class is available in the fuel servicing area. Fueling area fire extinguisher should be kept in a vertical position in order to increase firefighting effectiveness. Putting down fire extinguisher causes it to be unavailable to discharge all of its agents. The fire extinguishers should be used only for the initial knockdown of fire.

During the fueling operation in hangars, two fire extinguishers must be available within 100 feet of the hangar. The wheeled 150-pound Halon 1211 or Novec 1230 must be used as fire extinguishers in the hangars. Fire extinguishers must be replaced outside of 25 feet radius safety zone of the aircraft fuel vent outlet during fuel servicing of aircraft (USAF, 2013).

Supervisors must be sure of all fire extinguishers are inspected on a monthly basis and inspection records are documented. Extinguishers with nonconformity must be taken out of service and they must be replaced immediately. Fire extinguishers must be in designated points in the flight line. There must be no obstacles for access and visibility to fire extinguishers. The safe seal of fire extinguisher must be in place and not be deformed. The pressure gauge must be in the operable range. All staff must have knowledge about the fire alarm system, reporting an emergency and activation of the alarm system (USAF, 2018).

Warning signs must be hanged in visible places in the fueling area. Smoking and its materials are forbidden within the fuel servicing area and 6 m radius area around fueling systems (NFPA, 2003a).

Water suppression systems are not effective for fuel spillages. Water causes surrounding materials to become cooler however it also causes to spread of pool fire. In the case of a large amount of fuel spills, the drainage system is useful for mitigating the spread of burning fuels. The sprinkler system can be considered to be installed inside the drain system (NFPA, 2003b).

2.5. Modeling JP-8 Evaporation

Evaporation modeling is the most important subject for JP-8 spillage. All JP-8 spills include the evaporation process. However, the researches which have been carried out so far are insufficient to understand important concepts of oil spillage evaporation modelling (Fingas, 2013). It is very important to understand the evaporation process of oil to make an accurate prediction of evaporation rates of oil products in the case of oil spills (Fingas, 1995). The evaporation process can be described as the transformation of molecules from the liquid phase to the vapor phase under the boiling temperature of a substance. The kinetic energy of a liquid molecule is enough for moving away from the liquid surface to the vapor phase (Schaschke, 2014). In other words, the evaporation process can be described as liquid molecule movement from the liquid surface to the vapor phase. The air layer on the liquid surface is described as air boundary layer which has a thickness of less than 1 mm (Fingas, 2013). In general, the boundary layer can be described as a layer in a liquid where transfer activity is affected by characteristics of the surface below (Monteith and Unsworth, 2013). The most important concern about the air boundary layer is that it can affect the evaporation process. For the water evaporation process, the air boundary layer has an influence on the evaporation rate (Fingas, 2013). According to Fingas (2001), the oil evaporation rate is mainly dependent on the chemical composition of the oil compound. On the other hand, Haghighi et al. (2013) state that besides interior limitations, the air boundary layer has a restriction on the evaporation ratio of liquid substances. Some amount of water vapor can be held by air which is described as

relative humidity. If there is no wind and the air layer doesn't have movement, the water evaporation rate decreases since the air layer above the water is saturated. As a result, it can be said that the mechanism of water evaporation is regulated by the air boundary layer. Then, in the presence of wind, the evaporation rate of water is expected to increase (Fingas, 2013). On the other hand, most of the liquids which have air boundary layer evaporation regulation, evaporate very slowly to saturate the air boundary layer on the top of the surface (Fingas, 2011b).

On the contrary, the evaporation mechanism of some liquids are not regulated by air-boundary-layer since the evaporation rate is very slow for saturation of the air layer above the liquid. According to Fingas (2013), there are some liquids which have an evaporation mechanism regulated by molecular diffusion. Oil and fuels have diffusion regulated evaporation process since they consist of many different liquid compounds. As a result, the evaporation process of oils is not significantly influenced by increased spill area and wind velocity. The evaporation rate of water is linear with time since it is a single compound. On the other hand, oil products do not have a linear evaporation rate with respect to time (Fingas, 1997).

2.5.1. Historical Development of Oil Evaporation Modeling

According to Fingas (2011a), for liquids with air-boundary-layer evaporation model can be written as:

$$E \approx K\ C\ T_u\ S \tag{1}$$

In equation (1), E represents evaporation rate in mass/unit area, K represents mass transfer rate of evaporated fluid, C represents the concentration (mass/volume) of evaporated fluid, T_u is relative intensity factor of turbulence and S is the saturation factor (Fingas, 2013). As air above the liquid becomes more saturated evaporation rate of the liquid decreases (Fingas, 1998).

According to Fingas (1999), Sutton was one of the pioneers of the oil evaporation study. Fingas (2013) says that Sutton formed a model according to experimental data:

$$E = K\ C\ U^{7/9}\ {d_a}^{-1/9}\ Sc^{-r} \tag{2}$$

In equation (2), C represents the concentration of the evaporated liquid as mass per volume, U represents the velocity of wind, d_a is the pool area, Sc represents Schmidt number and r represents the experimental value between 0 and 2/3. The parameters in equation (2) are very similar to ones in equation (1). In equation (2), turbulence is described as multiplication of wind velocity, U, and Schmidt number, Sc (Fingas, 2013). Schmidt number can be found by theoretical study and empirical methodology (Yuan et al., 2017). Fingas (2013) states that the evaporation rate for oil was theoretically formulated for the first time by Blokker. Blokker assumed oil as a single component fluid. Distillation values and boiling points of all different liquid components in oil are provided to make an assumption on average vapor pressure. The Clausius-Clapeyron equation was used to calculate overall vapor pressure of oil components in the form as:

$$\log \frac{P_s}{P} = \frac{\Delta_{vap}H^0\ \mathrm{M}}{4.57}\left(\frac{1}{\mathrm{T}} - \frac{1}{T_s}\right) \tag{3}$$

In equation (3), P represents vapor pressure at T which is absolute pressure, P_s (760 mm Hg) represents vapor pressure at boiling point, T_s, $\Delta_{vap}H^0$ is the heat of evaporation as cal/g and M is the molecular weight.

According to Fingas (2013), $\Delta_{vap}H^0$M/(4.57 T_s) was considered as a constant value for hydrocarbons. Hence, the equation became as:

$$\log P_s/P = 5.0[(T_s - T)/T] \tag{4}$$

The pressure curve was obtained by using equation (4) and experimental data. In this calculation, Raoult's law was assumed to be valid providing that $\Delta_{vap}H^0$M is a function of evaporation percentage. Overall evaporation time was found by application of Pasquill's equation as:

$$t = \frac{\Delta h\, D^{\beta}}{K_{ev}\, U^{\alpha}} \sum \frac{1}{PM} \tag{5}$$

In equation (5), t represents total evaporation time in hours, Δh signifies a drop in thickness of layer in meters, D symbolizes oil spill diameter, β represents a meteorological coefficient (valued as 0.11), K_{ev} signifies atmospheric stability coefficient value given as 1.2×10^{-8}, α symbolizes a meteorological coefficient (valued as 0.78), P symbolizes the vapor pressure at absolute temperature (T) and M represents the molecular weight of the liquid. According to Fingas (2013), the results of equation (5) were not in correlation with data collected from the experiment conducted in a wind tunnel.

According to Jenkins (2008), The Clausius–Clapeyron equation can be expressed as:

$$\ln\left(\frac{P_2}{P_1}\right) = -\left(\frac{\Delta_{vap}H^0}{R}\right)\left[\frac{1}{T_2} - \frac{1}{T_1}\right] \tag{6}$$

If the exponential of the equation (6) is taken, then the equation yields a different form of the Clausius-Clapeyron equation such as (Jenkins, 2008):

$$\left(\frac{P_2}{P_1}\right) = exp\left\{-\left(\frac{\Delta_{vap}H^0}{R}\right)\left[\frac{1}{T_2} - \frac{1}{T_1}\right]\right\} \tag{7}$$

Fingas (2013) states that Mackay and Matsugu worked on oil evaporation modelling by combining the water evaporation model and empirical data. The model used for water evaporation was modified for oils by using the evaporation data of cumene. To formalize oil evaporation rate, evaporation rate of water and cumene were correlated as a wind velocity and pool areas function given the equation (Mackay & Matsugu, 1973):

$$K = c\, U^{0.78} X^{-0.11} \tag{8}$$

In order to obtain a constant value for equation coefficient c, Mackay and Matsugu observed evaporation of cumene for more than two days. Schmidt number is taken as 2.70 for cumene evaporation. It is important to notice that the dimension of c changes caccording to units used for mass transfer constant, K, wind velocity, U and pool

diameter, X which are m/h, m/h and m respectively. In the case of evaporation modelling different than cumene, a value of 0.0292 $Sc^{-0.67}$ can be used. Therefore, the equation (8) yields to (Mackay & Matsugu, 1973):

$$K = 0.0292\ U^{0.78} X^{-0.11} Sc^{-0.67} \quad (9)$$

According to Fingas (2013), Mackay and Matsugu say oil evaporation has complexity since there is a diffusion resistance of oil molecules. Empirical data on the oil evaporation rate was not in correlation with the results of calculated data which means diffusion resistance occurs. As a result, mass transfer constant is needed to model oil evaporation in spillages. The amount of evaporation of an oil spill in an environment can be determined by mass transfer constant (Goodwin et al., 1973). In order to test mass transfer constant methodology, Butler studied on an evaporation equation with mass transfer data available for specific conditions. In Butler's model evaporation is proportional to vapor pressure, P as shown :

$$dx/dt = -kP(x/x_0) \quad (10)$$

In equation (10), x represents the amount of specific oil product at time t, x_o symbolizes the amount of specific oil product at time t equals zero, k signifies experimental rate constant and P represents the vapor pressure of specific oil product (Fingas, 2013).

Butler also thought that P cannot represent the overall vapor pressure of the spillage since oil consists of various components. Also, there would not be big changes in activity constant during weathering. Accordingly, activity constants were included in the experimental rate constant k. For various oil products, P and k were considered as independent of the amount, x. As a result, the equation was derived to yield amount remaining after evaporation as:

$$x/x_0 = exp(-ktP/x_0) \quad (11)$$

After that, the regression line was used to predict model for vapor pressure of a single oil product:

$$P = exp(10.94 - 1.06\,N) \tag{12}$$

In equation (12), P is the vapor pressure in Torr and N is the carbon number of oil product. Then, equations (11) and (12) were combined given the formula:

$$x/x_0 = exp[-(k\,t/x_0)\,exp(10.94 - 1.06\,N)] \tag{13}$$

According to the equation (13), the weathered oil amount is formulated as a function of carbon number of oil product, N. If oil components are distributed uniformly, the equation (13) can estimate carbon number as a function of time where the known amount evaporated ($x = 0.5\ x_o$):

$$N_{1/2} = 10.66 + 2.17 \log kt/x_0 \tag{14}$$

The model was applied to some oil spills whose time of occurrence is known and the results were compared. The age prediction of the oil spill made by the equation was accurate. According to Fingas (2013), the equation was valid for water spillages also, but it was never preferred in modelling.

According to Fingas (2013), Mackay and Matsugu diffusion model is used by Yang and Wang to develop an evaporation model. Molecular diffusion is described as:

$$K = \frac{k_m(P_i - P_{i\infty})}{[R\,T_s]} \tag{15}$$

In equation (15), K represents mass transfer rate, k_m symbolizes a constant which involves all factors related to K, P_i signifies vapor pressure of oil compound, I, on the boundary, $P_{i\infty}$ signifies the vapor pressure of oil compound, I, at infinite altitude of the atmosphere, R represents molar gas constant and T_s absolute temperature of the oil layer on water. Yang and Wang (1977) also suggest the equation below:

$$K = a\,A^{\gamma}e^{qU} \tag{16}$$

In equation (16), A is the area of oil layer on water, U is the wind velocity and a, q and γ are experimental constants. Fingas (2013) says that research results indicated that, in the process of oil evaporation a surface film is formed on the oil layer, and it

caused an evaporation process to slow down. Before the film has formed on the oil layer ($\varrho_t/\varrho_o < 1.0078$):

$$K_{mb} = 69\ A^{-0.0055}\ e^{0.42U} \tag{17}$$

In equation (17), K_{mb} represents the constant which includes all factors concerning oil evaporation before the surface film. After the film has formed ($\varrho_t/\varrho_o > 1.0078$):

$$K_{ma} = 1/5\ k_{mb} \tag{18}$$

For equation (18), ϱ_o represents initial oil density, ϱ_t symbolizes oil density at time t and K_{ma} is the coefficient which includes all factors concerning oil evaporation after the surface film. According to Fingas (2013), research results showed that the film formed on the surface of the oil causes five times lower evaporation rate.

According to Drivas (1982), the model defined by Mackay and Matsugu has good accuracy to predict oil evaporation compared to the empirical data available in the literature. Reijnhart and Rose (1982) studied an equation to predict oil evaporation at sea level. Reijnhart and Rose model was as:

$$E = \alpha_1\ c_0 \tag{19}$$

In equation (19), E symbolizes evaporation rate of oil compound, α_1 represents coefficient which is the combination of wind speed and all factor in m/s and c_0 signifies the equilibrium concentration of vapor at the top layer of the oil (Reijnhart and Rose, 1982). According to Fingas (2013), research was conducted to compare test data and evaporation rates on the sea level. However, there is not a specific methodology to estimate equilibrium concentration, C_0.

According to Fingas (2013), Brighton redefined evaporation equation, and he studied on water evaporation with a similar approach to Sutton as:

$$E = K\ C_s\ U^{7/9}\ {d_1}^{-1/9}\ Sc^{-r} \tag{20}$$

In equation (20), E represents evaporation rate per unit area, K symbolizes experimental mass transfer coefficient, C_s signifies evaporating liquid concentration, d_1 represents pool length and r symbolizes an experimental constant value between 0 and 2/3.

Brighton (1985) states that evaporating liquid concentration, C_s, can be determined by the formula:

$$C_s = \frac{M\,P_v}{R\,T} \tag{21}$$

In equation (21), M is the molecular weight of the substance, P_v represents saturated vapor pressure, T is temperature and R is the gas constant.

According to Fingas (2013), Brighton thought that the formula can also comply with the fundamental dimensionless form including wind velocity, U, and roughness length, Z_0, which describes air-boundary-layer phenomena. In Brighton's analysis concentration is logarithmic above the surface which can be thought to be a more ideal approach than the results previously obtained. Brighton (1985) used a power profile for the estimation of turbulence, so the parameters above can be replaced into the equation:

$$U = \frac{u^*}{k}\,n \tag{22}$$

$$n = \left(\ln\frac{z_1}{z_0}\right) \tag{23}$$

In equation (22), u^* represents friction velocity, z_1 signifies height above the surface, z_0 symbolizes roughness length and n represents the power law dimensionless parameter. When the equations (22) and (23) were substituted into the evaporation model, the obtained equation was:

$$U\left(\frac{z}{z_1}\right)\frac{\delta y}{\delta X} = \frac{\delta}{\delta z}\left(\frac{k\,u^*\,z}{Sc}\right)\left(\frac{\delta C}{\delta z}\right) \tag{24}$$

In equation (24), z represents height above the surface, C symbolizes concentration of evaporated oil product, X is the size of the pool, k signifies von Karman coefficient obtained by K/u^* z and Sc represents the Schmidt number which was assumed as 0.85. The results of Brighton's model were evaluated and it was decided that some experimentation concluded with good results, however, data was not enough for testing the theory and control of the operation environment was poor (Brighton, 1990).

Fingas (2013) says that Tkalin described an evaporation model for oil at sea level as:

$$E_i = \frac{KMP_{oi}\,x}{RT} \tag{25}$$

In equation (25), E_i represents evaporation rate of oil compound i or total evaporation in kg/m^2s, K symbolizes mass transfer constant in m/s, M signifies molecular weight, P_{oi} represents vapor pressure of the oil compound i and x signifies the amount of the oil product i at time t. Experimental data was used to define parameters in the model:

$$P_{oi} = 10^3 e^A \tag{26}$$

In equation (26), A was described as:

$$A = -(4.4 + \log T_b)[1.803\,\{T_b/T - 1\} - 0.803\ \ln(T_b/T)] \tag{27}$$

In equation (27), T_b represents the boiling point of the oil product. Mass transfer constant was described as:

$$K = 1.25\ U\ 10^{-3} \tag{28}$$

According to Fingas (2013), Tkalin model for oil evaporation was confirmed by experimental results obtained from the literature.

Stiver and Mackay (1984) formulated an evaporation model, which is modified from Mackay and Matsugu's equation, is one of the most commonly used approach in oil spills. In the model, it was assumed that an oil is spilled and the evaporation rate was defined as:

$$E = KAP/(RT) \tag{29}$$

In equation (29), E represents the evaporative molar flux in mol/s, K symbolizes mass transfer constant under the wind effect in ms^{-1}, A represents the area in square meters, P symbolizes vapor pressure of the liquid as Pascal and T is the temperature as degree Kelvin. The equation was rearranged as:

$$dF_v/dt = K\ A\ P\ \ v/(V_0\ R\ T) \tag{30}$$

In equation (30), F_v represents the volume of the evaporated compound, v symbolizes the molar volume of the liquid in m^3/mol and V_0 signifies the volume of the spillage at the beginning in m^3. Then, equation (30) yields:

$$dF_v = [P\ v/(R\ T)](K\ A\ dt/V_0) \tag{31}$$

which was arranged to give:

$$dF_v = H\ d\theta \tag{32}$$

In equation (32), H represents Henry's law constant, and θ symbolizes evaporative exposure (Stiver and Mackay, 1984). In equation (31), $(K\ A\ dt/V_0)$ signifies the time-rate of evaporative exposure and was represented as $d\theta$ in equation (32). As it can be seen from the equation, the evaporative exposure is correspondent to time, area of spillage, the thickness of oil spill and mass transfer constant which is a function of the wind velocity. In other words, the evaporative exposure can be seen as the vapor volume ratio to initial fluid volume.

In equation (31), $[P\ v/(R\ T)]$ signifies H in equation (32) and H represents Henry's law constant. H is correspondent to temperature. Hence, θH represents the ratio of the amount of oil evaporated to the initial amount. In the case of pure fluids, H can be assumed as independent to F_v so equation (30) was rearranged as (Fingas, 2013):

$$F_v = H\ \theta \tag{33}$$

According to Fingas (2013), when K, A and temperature do not vary, the evaporation rate does not vary too, and the evaporation process can be thought as finished if θ gets to the level of 1/H.

In the case of fluid involving multiple compounds, H can be assumed as dependent on F_v. Therefore, H should be defined by using F_v to rearrange equation (31), that is, the vapor pressure variable can be described as a correlation with composition. In this situation, evaporation of the oil decreases as evaporation continues. Fingas (2013) says that equation (31) was rearranged by experimental data to obtain:

$$F_v = (T/K_1)\ln(1 + K_1\theta/T)\, exp(K_2 - K_3/T) \qquad (34)$$

In equation (34), F_v represents the ratio of the volume evaporated and $K_{1,\ 2,\ 3}$ symbolizes experimental coefficients. K_1 was found from the slope of the curve of F_v versus log θ by evaporation experiments. According to Fingas (2013), when θ is bigger than 10^4, the value of K_1 approaches the value of 2.3T divided by the slope. K_2 and K_3 were found separately by evaporation curvature at two different temperatures.

Fingas (2013) says that Hamoda and co-workers also studied evaporation in theory and conducted empirical researches. An approach was developed to understand how American Petroleum Institute gravity, API^o (expression for density), temperature and salinity affect mass transfers constant, K (Hamoda et al., 1989):

$$K = 1.68 \times 10^{-5}\ (API°)^{1.253}\ (T)^{1.80}\ e^{-0.1441} \qquad (35)$$

In equation (35), K represents mass transfer constant in cm/h, $API°$ symbolizes unitless density API parameter, and T signifies temperature as degree Celsius. Exponential values in the model were found from the results obtained from the experiments after multiple linear regression (Hamoda et al., 2013).

Quinn et al. (1990) provided an oil spill to make it evaporate in a conditioned medium and compared the evaporation records with former models such as Fick's diffusion law and the Clausius-Clapeyron equation. In this study, oil was separated into different components according to their boiling point. Every component was regarded as equal to an n-paraffin. Fractions of n-paraffin were decided by capillary gas-liquid chromatography. The evaporation rate in the field and evaporation rates obtained by

modelling were compared. Evaporative modelling gives very accurate results for film thickness from 10 μm to 1 mm until 4 weeks of weathering.

Bobra (1992) worked on oil evaporation modeling. The evaporation rates of different oil components were observed in numerous weathering conditions. The data collected from observations were evaluated regarding the formula given by Stiver and Mackay (1984). The formula was:

$$F_V = \ln[1 + B(T_G/T)\ \theta\ exp(A - B\,T_0/T)]\,\{T/BT_G\} \qquad (36)$$

In equation (36), F_V represents the ratio evaporated, T_G symbolizes the slope of the distillation curvature, A and B signifies unitless coefficients, T_0 is the boiling point of the oil product at the beginning and θ represents evaporative exposure. In order to understand the effectiveness of the model, empirical data and modeling results were compared where results were found to be low in accuracy (Bobra, 1992). The result of the study indicated that Stiver and Mackay evaporation model was accurate as the evaporation time reaches 8 hours. However, it was seen that after the period of 8 hours evaporation rate was overestimated. The overestimation could reach up to 10% of overall evaporation in the 24-hour period. The situation was mainly valid for light oil products. The Stiver and Mackay model was also decided to be in low accuracy in predicting oil evaporation in the beginning period (Fingas, 2013). According to Fingas (2013), Bobra stated that a big part of the oil evaporation curvature is logarithmic with time and this approach is much more accurate than equation (34).

In conclusion, developing an evaporation model for oil spills is a very challenging subject because of many different reasons. Firstly, oil product involves several compounds with different boiling points, vapor pressure and characteristics. Furthermore, oil evaporation is a diffusion regulated process but not an air-boundary-layer regulated process. Therefore, models used for water evaporation cannot be adapted to oil spill evaporation modeling.

2.5.2. Development of Diffusion-Regulated Models

According to Fingas (2013), air-boundary-layer models are not sufficient to explain long term evaporation of oils. In order to understand the concepts, Fingas (2013) conducted several experiments.

An experiment was conducted to understand if oil evaporation is air-boundary-layer regulated or not by measuring the wind effect on oil evaporation by equations (2) and (9). Oil evaporation experiments were conducted with ASMB (Alberta Sweet Mixed Blend), gasoline and water with different wind speeds. Water evaporation behavior was taken as the reference line in order to compare the results of the experiment. Three of the figures below show the evaporation rate of gasoline, ASMB and water respectively, regarding the loss of weight as a percentage versus various wind speed. According to Figure 2.8., Figure 2.9. and Figure 2.10., it can easily be seen that wind speed does not have an increasing effect on the evaporation rate of oil products.

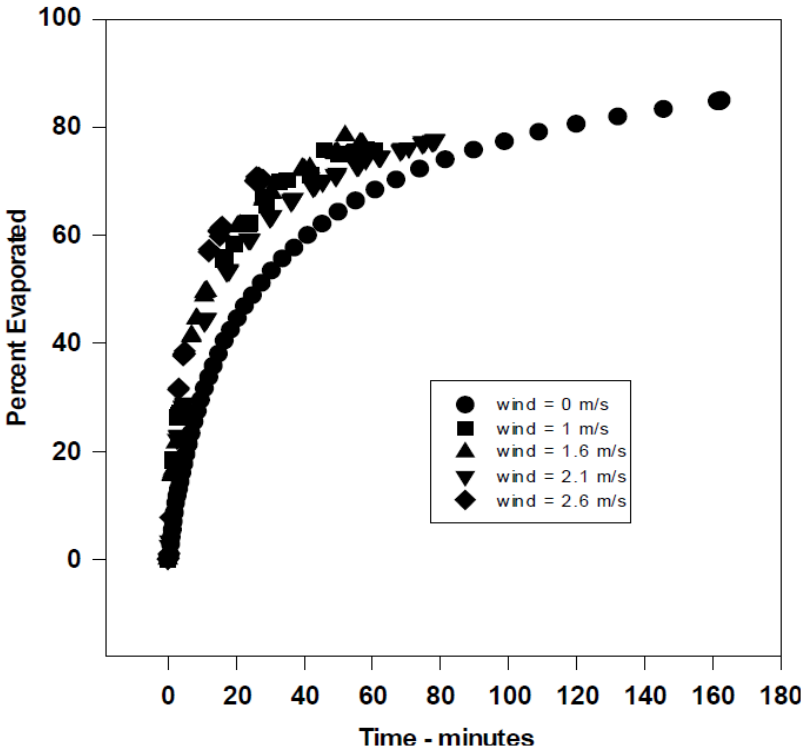

Figure 2.8. Evaporation Rates of Gasoline versus Various Wind Speed (Fingas 2013).

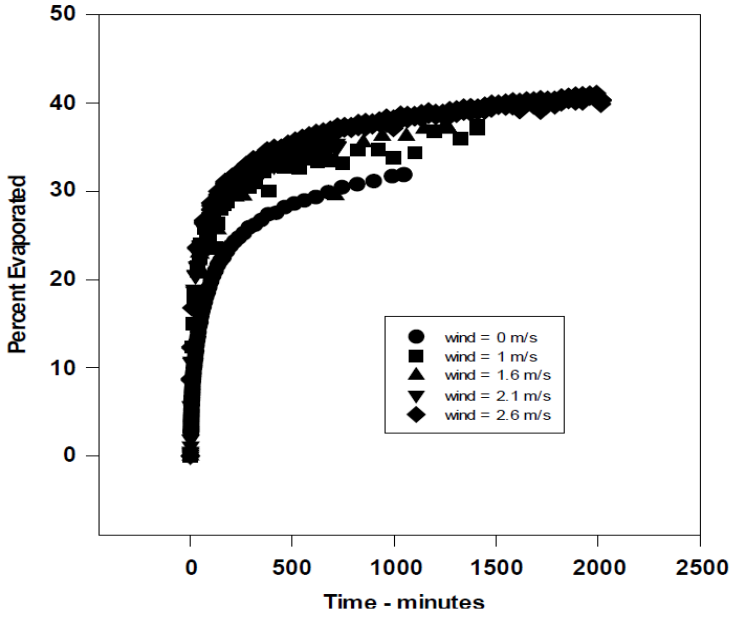

Figure 2.9. Evaporation Rates of ASMB versus Various Wind Speed (Fingas 2013).

There is only very little change in the evaporation rate from the 0 m/s wind speed to other wind speed levels. According to Fingas (2013), this can be explained by the stirring effect of wind but not in terms of air-boundary layer interaction.

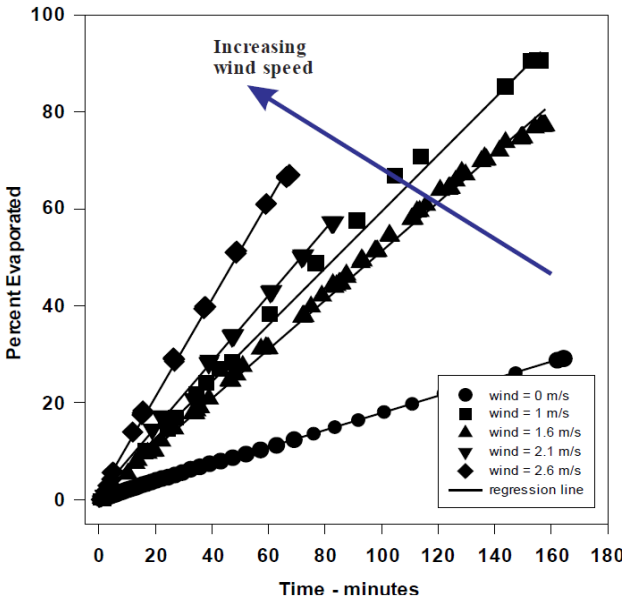

Figure 2.10. Evaporation Rates of Water versus Various Wind Speed (Fingas 2013).

On the other hand, it can be seen from the Figure 2.10. that there are dramatic changes in the evaporation rate of water as wind speed increases. According to Fingas (2013), it can be explained by the air-boundary-layer regulation evaporation model as it is mentioned before.

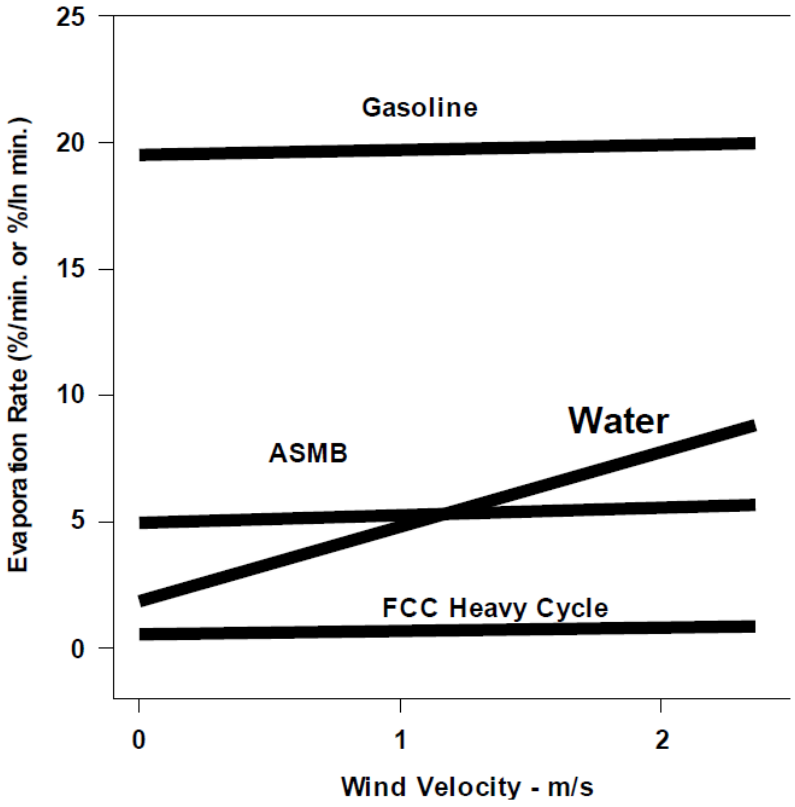

Figure 2.11. Wind Velocity versus Evaporation Rates (Fingas, 2013)

Figure 2.11 is obtained by correlation of data from the experiments. It can be seen from the lines that there is no correlation between wind speed and oil evaporation rates. On the other hand, there is a strong correlation between water evaporation and wind speed. As wind speed increases the evaporation rate of water also increases.

As a result of the experiment, it can be seen that the air-boundary-regulation model does not apply for the evaporation of oil products. However, the stirring effect of wind for evaporation at the beginning level should not be ignored.

Another important parameter for evaporation is the saturation concentration of oils. Saturation concentration is the maximum concentration of a liquid that can be soluble in the air. Table 2.10 shows the saturation concentration of different kinds of oil products and water. From the table, it is shown that water has a lower saturation concentration compared to oil products. According to Fingas (2013), this is due to the fact that oil products have not significant boundary layer limitations.

Table 2.10. *Saturation Concentration of Water and Hydrocarbons (Fingas, 2013)*

Substance	Saturation Concentration in g/m^3 at 25 °C
water	20
n-pentane	1689
hexane	564
cyclohexane	357
benzene	319
n-heptane	196
methylcyclohexane	192
toluene	110
ethylbenzene	40
p-xylene	38
m-xylene	35
o-xylene	29

According to Fingas (2013), there is an important difficulty in modelling of oil evaporation since every oil product has a different evaporation equation even in similar conditions. Therefore, it is important to have formerly obtained data to calculate the evaporation rate of oils. Fingas (2013) says that distillation data is used to characterize oils and it can be used to calculate the evaporation rate.

Oils and diesel fuels have different evaporation equations. Oils have evaporation rates as a logarithm with time. On the other hand, diesel fuels, like jet fuel which contains kerosene, have evaporation rate as a square root of time. According to Fingas (2013), the reason for this situation is that diesel oils contain only fewer number of compounds which have similar evaporation rates.

The data obtained from experiments at 15 °C were applied to temperature equations. So, the temperature equations were modified to give:

$$\%\, Evaporation = [B + 0.045(T - 15)] \ln(t) \quad (37)$$

In equation (37), B represents the equation factor at 15 °C, T symbolizes temperature in degrees Celsius and t signifies time as minute.

Fingas (1996) correlated distillation data by experiments so that evaporation rates of oils are found. It was seen that 180 °C is the optimum temperature for the correlation of distillation data to evaporation rates. Percentage evaporated at 180 °C was used to formulate the relationship between distillation and evaporation.

For oils which have a logarithm with time the equation yields as:

$$Percentage\ evaporated = 0.165(\%D) \ln(t) \quad (38)$$

And for diesel-like oils which have square root equation the equation yields as:

$$Percentage\ evaporated = 0.0254(\%D)\sqrt{t} \quad (39)$$

where %D is percentage distilled by weight at 180 °C and t is the time in minutes. Fingas (1996) combined the equations with the equations which were obtained before so that equations derived to as below:

For oils which have a logarithm with time:

$$Percentage\ evaporated = [0.165(\%D) + 0.045(T - 15)] \ln(t) \quad (40)$$

And for diesel-like oils which have a square root equation:

$$Percentage\ evaporated = [0.0254(\%D) + 0.01(T - 15)]\sqrt{t} \quad (41)$$

where %D is percentage distilled by weight at 180 °C, T is temperature in degrees Celsius and t is the time in minutes (Fingas, 1996).

Fingas (2013) says that thicker oil spills, more than 2 mm, evaporates much more slowly compared to thinner spills since they have diffusion regulated evaporation regulation. Oil compounds have to diffuse longer distances to evaporate in thicker spills. Additionally, it is totally different from the air-boundary-layer model.

Some experiments were conducted in order to see thickness effect on evaporation with light crude oil and ASMB. Fingas (2013) says that the most fitting equation can be obtained by a square root function for the thickness effect correction factor. The equation is as below:

$$Corrected\ equation\ factor = equation\ factor + 1 - 0.78 \times \sqrt{t} \quad (42)$$

where the corrected equation factor is a factor for oil thickness and t is the thickness of oil product in millimeter. Fingas (2013) also states that the equation (42) is valid for evaporation of oil spills with a thickness of more than 1.5 mm.

Fingas (2013) says that there is another important factor called bottle effect that has an impact on evaporation rates of oils. The evaporation rate is higher when oil is covered such as in a bottle than it is fully open. It can be explained by impermanent or partly air-boundary-layer regulated evaporation behavior of oil in the bottle. The bottle effect ends when the evaporation rate of oil product becomes low compared to the evaporation rate of oil vapor which evaporates from the bottle mouth.

According to Fingas (2013), it can be seen from the experiments that wind has a slight effect on the evaporation of oil with respect to the condition with no wind at all. This is the result of the stirring effect of wind which results in an increased diffusion rate of oil. However, the same effect does not apply to the evaporation rate of oil as the velocity of wind increases. As a result, it can only be observed in zero wind conditions.

2.5.3. Application and Comparison of Evaporation Models in Oil Spillages

According to Fingas (2013), evaporation equations are the most important concern in oil spillage modelling since the most important physical process that affects oil composition is evaporation. For many years, different equations are used for oil evaporation modelling. Nowadays, in evaporation modelling, the equations used are given as in Table 2.11 in which T is the temperature in degree Celsius and t is time in minutes.

Table 2.11. *Sample of Empirical Equations of Oil Evaporation (Fingas, 2013)*

Oil Type	Equation
Alaska North Slope	%Ev = (2.86 + .045T)ln(t)
Alberta Sweet Mixed Blend	%Ev = (3.24 + .054T)ln(t)
Arabian Medium	%Ev = (1.89 + .045T)ln(t)
Arabian Heavy	%Ev = (2.71 + .045T)ln(t)
Arabian Light	%Ev = (3.41 + .045T)ln(t)
Barrow Island, Australia	%Ev = (4.67 + .045T)ln(t)
Boscan, Venezuela	%Ev = (-0.15 + .013T)/t
Brent, United Kingdom	%Ev = (3.39 + .048T)ln(t)
Bunker C - Light (IFO~250)	%Ev = (.0035 + .0026T)/t
Bunker C - long term	%Ev = (-.21 + .045T)ln(t)
Bunker C (short term)	%Ev = (.35 + .013T)/t
California API 11	%Ev = (-0.13 + .013T)/t
Cano Limon, Colombia	%Ev = (1.71 + .045T)ln(t)
Chavyo, Russia	%Ev = (3.52 + .045T)ln(t)
Cold Lake Bitumen, AB Canada	%Ev = (-0.16 + .013T)/t
Delta West Block 97, USA	%Ev = (6.57 + .045T)ln(t)
Diesel - long term	%Ev = (5.8 + .045T)ln(t)
Diesel Fuel short term	%Ev = (0.39 + .013T)/t
Ekofisk, Norway	%Ev = (4.92 + .045T)ln(t)
Federated, AB, Canada	%Ev = (3.47 + .045T)ln(t)
Fuel Oil #5	%Ev = (-0.14 + .013T)/t
Gasoline	%Ev = (13.2 + .21T)ln(t)
Gulfaks, Norway	%Ev = (2.29 + .034T)ln(t)
Hout, Kuwait	%Ev = (2.29 + .045T)ln(t)
IFO-180	%Ev = (-0.12 + .013T)/t
Isthmus, Mexico	%Ev = (2.48 + .045T)ln(t)

Table 2.11. *Sample of Empirical Equations of Oil Evaporation (Cont'ed) (Fingas, 2013)*

Oil Type	Equation
Jet A1	%Ev = (.59 + .013T)/t
Komineft, Russian	%Ev = (2.73 + .045T)ln(t)
Lago, Angola	%Ev = (1.13 + .045T)ln(t)
Lago Treco, Venezuela	%Ev = (1.12 + .045T)ln(t)
Maya, Mexico	%Ev = (1.38 + .045T)ln(t)
Sahara Blend, Algeria	%Ev = (0.001 + .013T)/t
Sakalin, Russia	%Ev = (4.16 + .045T)ln(t)
Scotia Light	%Ev = (6.87 + .045T)ln(t)
South Louisiana	%Ev = (2.39 + .045T)ln(t)
Statfjord, Norway	%Ev = (2.67 + .06T)ln(t)
Taching, China	%Ev = (-0.11 + .013T)/t
Troll, Norway	%Ev = (2.26 + .045T)ln(t)
West Texas Intermediate	%Ev = (2.77 + .045T)ln(t)
West Texas Sour	%Ev = (2.57 + .045T)ln(t)

Researches on air-boundary-layer evaporation modelling of oil spills result in the wrong conclusion with respect to empirical values. In Figure 2.12, it can be easily seen that evaporation modeling of diesel product values of the air-boundary-layer model and experimental results are very close to each other in the case of no wind. However, diesel evaporation data obtained with various wind speeds result in big differences as much as 100% in a longer period of time such as 200 hours.

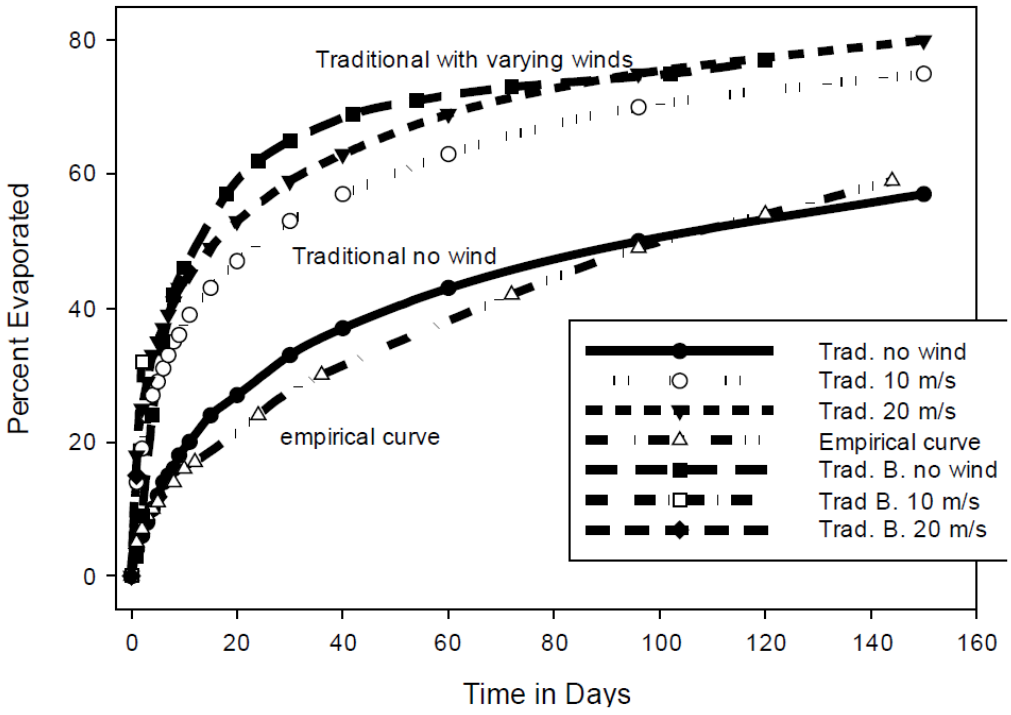

Figure 2.12. Evaporation Rate Modelling of Diesel Oil with Air-layer-boundary Equation (like equation (33)) versus Experimental Data Given in Table 11 (Fingas, 2013)

In Figure 2.13, the results of the evaporation modelling of Bunker C with two different air-layer-boundary equations and experimental data are given. The evaporation rates of models are almost the same until 8 hours. Nevertheless, in the case of varying winds levels, evaporation data obtained by air-layer-boundary equations have great differences with empirical data as much as 400% for a time period of 200 hours. As a result, air-layer-boundary models are not applicable for modelling Bunker C evaporation with wind condition as seen from the experimental data.

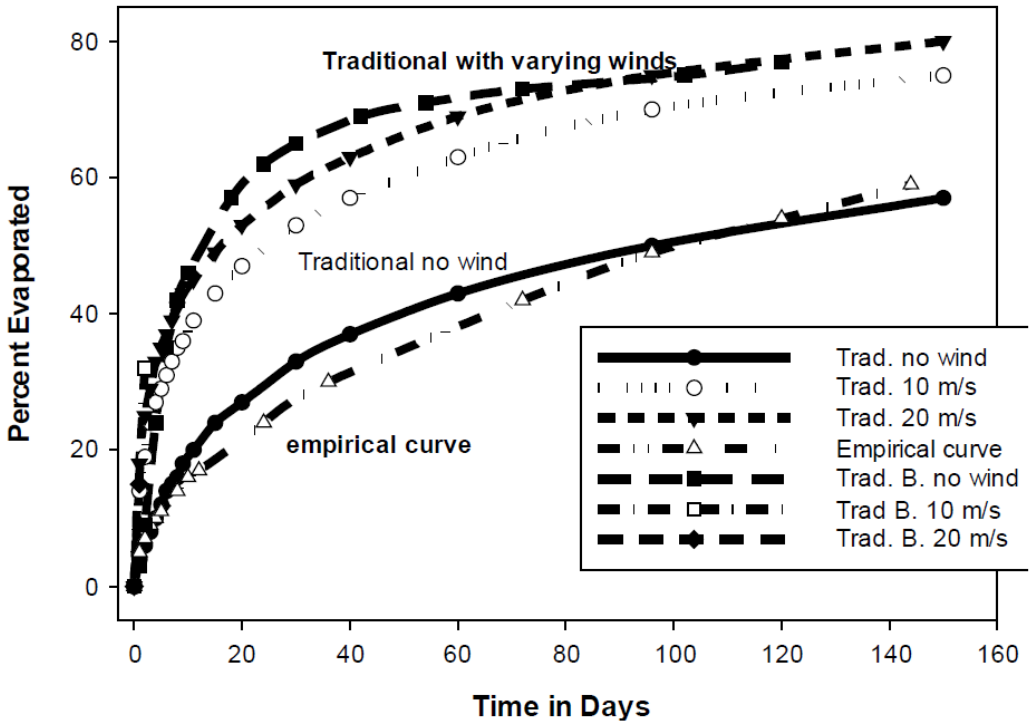

Figure 2.13. Evaporation Rate Modelling of Bunker C with Air-layer-boundary Equation (like equation (33)) versus Experimental Data Given in Table 11 (Fingas, 2013)

Thus, Fingas (2013) concludes that air-layer-boundary modelling of oil results in three main errors. Firstly and most importantly, with air-layer-boundary modelling, accurate long term evaporation rates cannot be obtained. Secondly, results in the case of different wind levels are impossible in reality. Finally, air-layer-boundary models do not give accurate evaporation rate curves for diesel oils. Fingas (2013) says that in order to obtain realistic results with air-layer-boundary equations, many researchers set maximum allowable evaporation value for long term evaporation modelling. For example, in Alberta of Pembina, an oil spill was analyzed by taking samples after 30 years and the evaporation rate was found to be 58%. In Figure 2.14, actual data, experimental prediction and air-layer-boundary modelling results are given. As it can be seen from the figure, actual analysis and empirical data are similar. However, the prediction made by air-layer-boundary modelling results in unrealistic values.

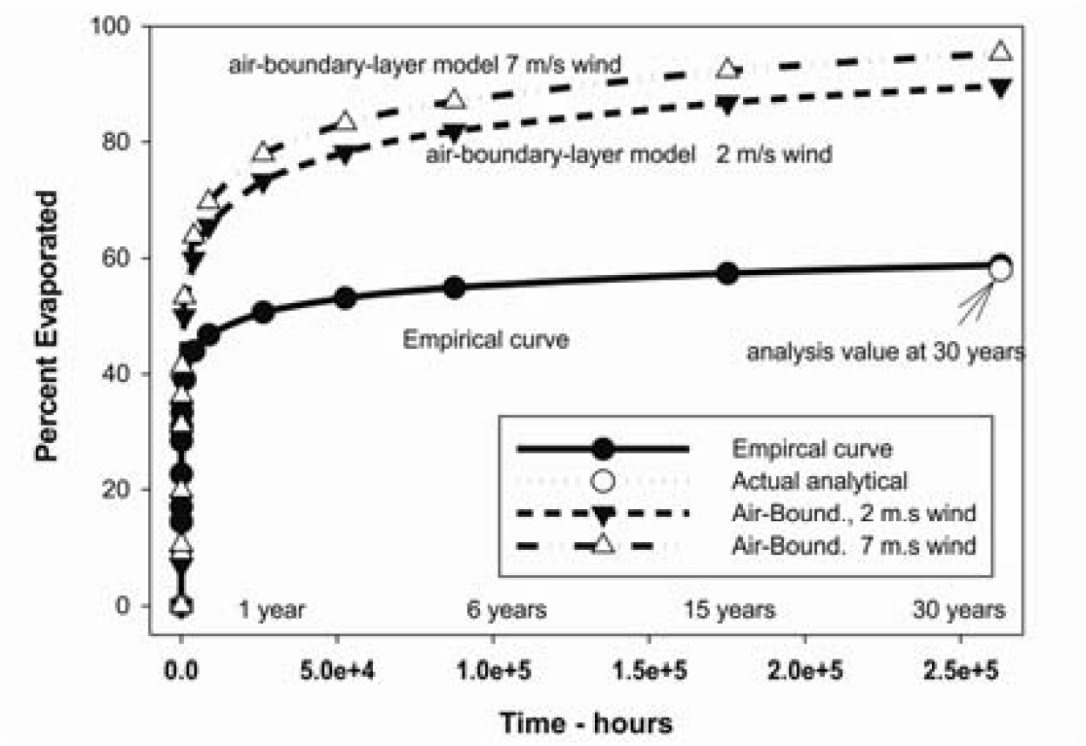

Figure 2.14. Evaporation Rate Modelling of Pembina Crude Oil with Air-layer-boundary Equation (like equation (33)) versus Real Data and Experimental Curve (Fingas, 2013)

In conclusion, the evaporation of oil cannot be modeled as an air-boundary-layer regulation. There are many experiments that show air-boundary-layer regulated modeling does not result in accurate evaporation rates. Hence, simpler evaporation modeling equations can be enough to describe the evaporation of oil products. Additionally, wind speed, turbulence of wind, area and scale size do not have major importance in oil evaporation modelling. In the oil evaporation process, the most important factors that should be taken into consideration are time and temperature.

The application of air-boundary-layer equations to predict oil evaporation for spillage gives unrealistic evaporation rates. According to Fingas (2013), there are three main reasons for inaccurate modeling results. First, air-boundary-layer equations do not provide accurate evaporation values for a long period of time. Second, the wind effect

causes the air-layer-boundary model to be in unreal rates. Third, air-boundary-layer models are not suitable for predict evaporation curves of oils like diesel.

Fingas (2013) states that diffusion-regulated equations are as accurate as empirical evaporation equations for oil products. Diffusion-regulated equations are used in the form given in equation (38). Fingas (2013) also says that diesel-like oils have the evaporation curve which follows the square root curve as given in equation (39).

According to Fingas (2013), in evaporation modeling, the best results can be achieved by using experimental equations as given in Table 2.11. If empirical equations are not present, distillation data can be used as given in equations (40) and (41).

According to Mackay and Wesenbeeck (2014), the evaporation rate is a concern for chemical exposure prediction in chemical spills. Evaporation rate and vapor pressure of substance have a relation. The relationship between evaporation rate and vapor pressure is established by Mackay and Wesenbeeck for several substances. Evaporation rate can be affected by numerous factors such as solar radiation, wind speed and humidity. However, these factors are not included in the determined formulation for the evaporation rate.

According to ideal gas law, on a solid and non-absorbing surface, a pure liquid substance has a saturated vapor concentration as indicated in equation (43) or (44).

$$C_s = P/RT \tag{43}$$

$$C_s = PM/RT \tag{44}$$

In equation (43) and (44), P is vapor pressure in Pa, M is molar weight in kg/mol, R is gas constant as 8.314 Pa m^3 /mol K and T is absolute temperature in K. Therefore, C_s is in mol/m^3 in equation (43) and kg/m^3 in equation (44).

Evaporation rate can be thought as the result of saturated vapor concentration and mass transfer constant, k as m/s which is the speed of transfer of saturated air from the liquid surface. Similar to Fick's law, diffusivity is D in m^2s^{-1} and diffusion path length

is Y in m, then k is equal to DY^{-1}. Thus, the evaporation rate is defined as molar flux and mass flux in equation (45) and (46) as:

$$E = Pk/RT \tag{45}$$

$$E = PMk/RT \tag{46}$$

In equation (45), evaporation rate, E is in mol/m^2s and in equation (46), E is in kg/m^2s.

Mackay and Wesenbeeck (2014) says that there is a correlation between E and P but not PM. The slope of the plot of log E versus log P is less than 1. This can be expressed by the absence of M in the correlation. Chemicals with higher molecular mass have lower volatility. If correlation is changed to evaporation rate in molar flux versus pressure than evaporation rate decreases and slope increases. E is modified to mol/m^2s and the slope of the plot is obtained closer to 1. Therefore, there is no need for a logarithmic correlation between E and P. The relationship between E and P can be expressed as simple and one parameter formula. Correlation between molar evaporation rate, E and pressure, P is given in the Figure 2.15.

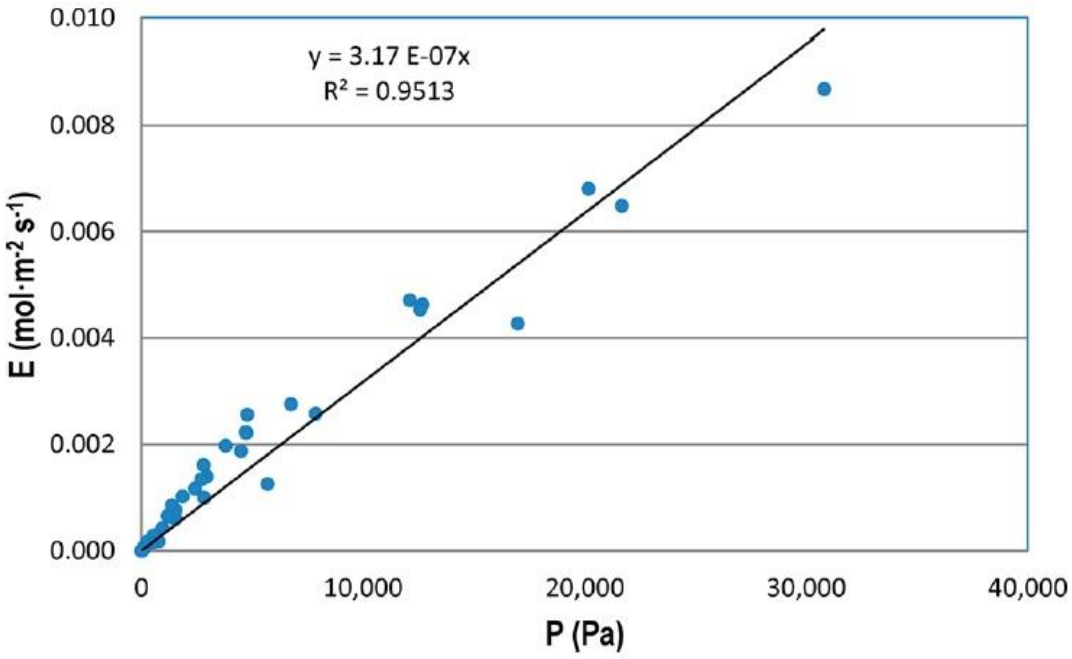

Figure 2.15. Plot of Molar Evaporation Rate, E vs. Pressure, P

According to Mackay and Wesenbeeck (2014), the correlation between the E and P can be expressed as:

$$E = 1464 \times P \times M \quad (47)$$

In equation (47), evaporation rate as mass flux, E, is in μg/m^{2}s, mean slope coefficient is 1464, vapor pressure, P, is in Pa and molar mass, M, is in g/mol. The mean slope correlation factor is modified by 10^9 μg/kg, 3600 s/h and 10^{-3} kg/g.

In Table 2.12, the modified slope coefficient, molar mass and vapor pressures of several substances are given.

Table 2.12. *Evaporation Rate Coefficients of Several Substances at 25 °C According to Equation 47 (Mackay and Wesenbeeck, 2014)*

Chemical Name	VP (Pa)	MW (g/mol)	ER (mg m^{-2} s^{-1})	Emass/(PxMW)
acetone	3.08 X 10^4	58,08	5.04 X 10^2	1015
benzene	1.27 X 10^4	78,11	3.62 X 10^2	1315
isobutyl acetate	2.41 X 10^3	116,16	1.36 X 10^2	1744
isobutyl alcohol	1.53 X 10^3	74,12	4.50 X 10^1	1426
n-butanol	9.46 X 10^2	74,12	3.19 X 10^1	1635
isobutyl isobutyrate	6.27 X 10^2	144,22	4.30 X 10^1	1712
cyclohexanol	9.20 X 10^1	100,16	7.05 X 10^0	2755
cyclohexanone	5.39 X 10^2	98,15	2.89 X 10^1	1967
diacetone alcohol	1.65 X 10^2	116,16	8.20 X 10^0	1537
diethyl ketone	4.71 X 10^3	86,13	1.93 X 10^2	1710
diisobutyl ketone	2.23 X 10^2	142,24	1.60 X 10^1	1815
ethyl acetate	1.26 X 10^4	88,11	4.00 X 10^2	1298
ethanol (100%)	7.86 X 10^3	46,07	1.19 X 10^2	1181
ethyl amyl ketone	2.60 X 10^2	128,22	2.24 X 10^1	2424

Table 2.12. *Evaporation Rate Coefficients of Several Substances at 25 °C According to Equation 47 (Cont'ed) (Mackay and Wesenbeeck, 2014)*

Chemical Name	VP (Pa)	MW (g/mol)	ER ($mg\ m^{-2}\ s^{-1}$)	Emass/(PxMW)
ethylbenzene	1.28×10^{3}	106,17	6.82×10^{1}	1812
ethyl lactate	5.00×10^{2}	118,13	1.80×10^{1}	1096
n-hexane	2.02×10^{4}	86,18	5.87×10^{2}	1215
isophorone	5.73×10^{1}	138,21	2.17×10^{0}	988
mesityl oxide	1.46×10^{3}	98,15	7.23×10^{1}	1820
methanol	1.70×10^{4}	32,04	1.37×10^{2}	905
nitroethane	2.80×10^{3}	75,07	1.21×10^{2}	2078
nitromethane	4.77×10^{3}	61,04	1.57×10^{2}	1936
1-nitropropane	1.37×10^{3}	89,09	7.62×10^{1}	2247
n-octane	1.85×10^{3}	114,23	1.17×10^{2}	1993
n-propyl acetate	4.49×10^{3}	102,13	1.92×10^{2}	1504
isopropyl alcohol	5.69×10^{3}	60,1	7.56×10^{1}	796
n-propyl alcohol	2.83×10^{3}	60,1	6.00×10^{1}	1271
tetrahydrofuran	2.17×10^{4}	72,11	4.68×10^{2}	1078
toluene	3.80×10^{3}	92,14	1.82×10^{2}	1873
p-xylene	1.17×10^{3}	106,17	7.00×10^{1}	2024
dodecane	1.23×10^{1}	170,34	2.75×10^{-1}	474
n-octanol	1.73×10^{1}	130,23	3.75×10^{-1}	599
tridiphane	2.93×10^{-2}	320,43	1.98×10^{-3}	759
trifluralin	1.47×10^{-2}	335,29	4.41×10^{-4}	322
pendimethalin	4.00×10^{-3}	281,31	2.89×10^{-4}	924
2,4-D	2.67×10^{-3}	221,04	1.86×10^{-4}	1135
diazinon	1.49×10^{-3}	304,35	2.52×10^{-4}	2004
toxaphene	5.33×10^{-4}	413,82	5.53×10^{-5}	902
dieldrin	6.59×10^{-4}	380,91	4.78×10^{-5}	685

According to Table 2.12, dodecane has an evaporation rate equation as:

$$E = 474 \times P \times M \quad (48)$$

In equation (48), E is the evaporation rate in $\mu g/m^2 s$, vapor pressure, P, is in Pa and molar weight is in g/mol.

The purposed methodology offers linear regression with one parameter. In practice, the evaporation rate can be affected by several environmental factors such as wind speed, temperature and radiation. If environmental factors are taken into account, the correlation becomes more accurate but more complex to handle. However, simple approaches can be used for checking data obtained from the field. Unfortunately, this approach can be applied to estimate the evaporation of pure substances.

2.6. Dispersion of Air Pollutants

Air pollutants do not stay at their discharge point. Atmospheric motions and physical conditions move particles emitted in the air. Therefore, it is important to understand the mechanism which affects the dispersion process of airborne particles (Spellman & Stoudt, 2013). The concentration of a contaminant at a specific location is correspondent to several factors such as emission rates, distance from the source and meteorological conditions (Abdel-Rahman, 2008).

2.6.1. Weather

Atmospheric conditions significantly affect pollutant concentration, in a positive or negative manner, particularly on the local scale (Spellman & Stoudt, 2013). Variation of atmospheric factors can cause the concentration of a substance in the air to be affected by 10 times even in a case of steady wind flow. Obviously, meteorological factors are significant for accurate modeling of air pollution dispersion. On the other hand, mainly microscale atmospheric conditions are concern with air dispersion

modelling. Atmospheric conditions on the larger scale have also an effect on dispersion, however, their effect is only significant for pollution with a longer period of time than 1 hour (De Visscher, 2014).

Meteorological conditions affect substance concentration in the air mechanically and chemically. Weather conditions can ease airborne substances to precipitate mechanically which causes a decrease in concentration. Particle concentration in the air is diluted by wind which brings clean air. Air and the pollutant contained by air rise as the sun heat up the upper atmosphere.

Atmospheric factors such as wind and turbulence can mix two different air contaminants which give a chemical reaction and form another hazardous substance (Spellman & Stoudt, 2013).

2.6.2. Turbulence

Turbulence in the air is a significant factor which affects air dispersion of contaminants. Since turbulence provides fresh air to the contaminated air mixture, the concentration of pollutants decreases. Turbulence is caused by wind speed which is a result of temperature difference in the atmosphere proportional to elevation. Therefore, turbulence is related to stability which is correspondent to vertical temperature distribution in the atmosphere (Spellman & Stoudt, 2013). Stability means the tendency or resistance of air to move vertically which is crucial for pollution dispersion (Nesaratnam and Taherzadeh, 2014). In other words, if air resists vertical movement it can be regarded as stable, if air develops vertical motion then it can be assumed to be unstable (Boubel et al., 1994).

Pasquill (1961) categorized atmospheric stability classes into six different groups. Pasquill's stability classes are shown in Table 2.13. Sutherland et al. (1986) states that stability class can also be decided qualitatively from atmospheric conditions by practical skills.

Table 2.13. *Pasquill's Atmospheric Stability Classes*

Pasquill stability class	Condition
A	extremely unstable
B	moderately unstable
C	slightly unstable
D	neutral
E	slightly stable
F	moderately stable

Pasquill (1961) also proposed key characteristics for deciding the stability category of the atmospheric conditions. Table 2.14 shows the key characteristics of the stability categories.

Table 2.14. *Key to Stability Categories*

Surface wind speed (at 10 m) m/sec	Insolation			Night	
	Strong	Moderate	Slight	Thinly overcast or ≥4/8 low cloud	≤3/8 cloud
<2	A	A-B	B	-	-
2-3	A-B	B	C	E	F
3-5	B	B-C	C	D	E
5-6	C	C-D	D	D	D
>6	C	D	D	D	E

Atmospheric stability classes are used to define the dispersion rate of airborne contaminants (Chapman, 2017). Spellman & Stoudt (2013) says that stable meteorological conditions results in low wind speeds accordingly lower level of turbulence. Therefore, low turbulence has an adversary effect on the dispersion of contaminants (Spellman & Stoudt, 2013). On the contrary, if rising pollutants do not reach stable atmospheric conditions then they are diluted by turbulence which ease the dispersion of contaminants (Hanna et al., 1982).

2.6.3. Topography

Topography has an important effect on airflow patterns and dispersion of pollutants from point and area sources (Spellman & Stoudt, 2013). Complex topographical structures in a region have a powerful influence on wind patterns which cause alteration in the stability of atmospheric conditions affecting contaminant dispersal (Valdenebro et al., 2014).

According to Nesaratnam and Taherzadeh (2014), buildings cause turbulence which has an effect on pollutant dispersion. Wind is divided into two parts in the front part of the building and as a result, the distributed wind covers the structure twice its height by upwards and five to ten times its height by downwind direction. Figure 2.16 shows the effect of a building to the flow of wind.

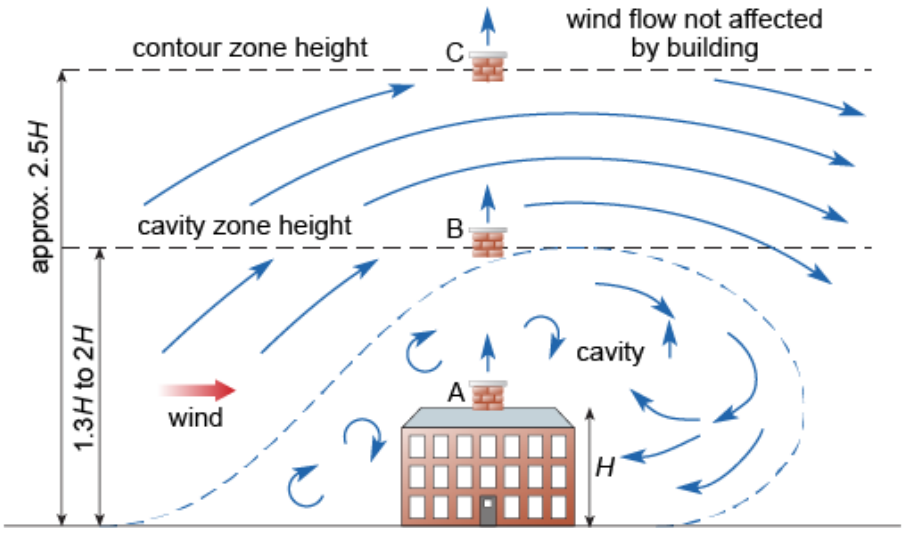

Figure 2.16. The Effect of a Building to the Flow of Wind

Temperature change, pressure change and friction which is related to surface roughness, affects wind speed (Godish, 2004). The effect of urban, suburbs and rural

areas on wind speed is shown in Figure 2.17 (Turner, 1994). At the top height of each wind profile, surface effect is over and the gradient wind starts. The highest level for the urban area is 500 m, 350 m for the suburban area and 250 m for the rural area (Godish, 2004).

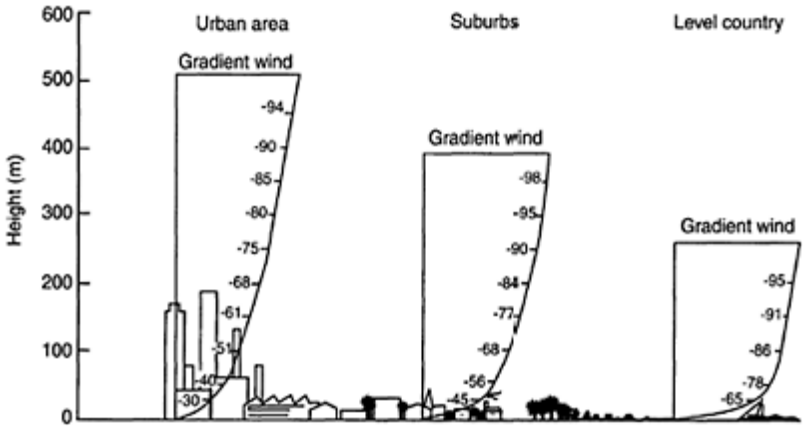

Figure 2.17. Effect of Urban, Suburbs and Rural Areas on Wind Speed (Turner, 1994)

2.6.4. Dispersion Models

According to Lim et al. (2012), Global Burden of Disease research shows that one of the most important health problem in the world is caused by exposure to environmental and indoor air contaminants. Russell et al. (2014) say that the number of evidences showing the adversary effect of air pollution is increasing. For establishing legislative precautions to air pollution, estimation of the scale of the health impact and prediction of economical cost is needed (Brandt et al., 2014). Scientists and governmental foundations have been doing researches in scientific and legislative means in order to comprehend the air pollution problem (Namdeo et al., 2012). Currently, health experts conducting a study to establish a procedure which involves air quality modelling in order to connect air pollution to several health problems (Russell et al., 2014).

Air dispersion modeling continues to be developed for over decades (Sriram et al. 2006). There are many different models for air dispersion varying from simple Gaussian plume models to complex computational fluid dynamics models (De Visscher, 2014). Air dispersion modelling provides an estimation of the concentration of pollutants at a specific distance from the pollution source (Spellman & Stoudt, 2013). De Visscher (2014) claims that generally basic air dispersion models have more accuracy in pollutant concentration prediction than complex models. Though, every dispersion model has a handicap and high accuracy is not certain. In general, high accuracy can be reached by correct model selection regarding model requirements and circumstances. Singh (2018) says that there are five different models available for air pollutant dispersion:

1. Box Model
2. Gaussian Model
3. Lagrangian Model
4. Eulerian Model
5. Dense gas model

According to Artana et al., (2014), some scientists also examine hybrid models which are a combination of different dispersion models.

Currently, the most widely used model of air dispersion estimation is Gaussian Plume Model and its modified versions (Sriram et al. 2006). According to Spellman & Stoudt (2013), during air dispersion modelling four-step procedure is recommended to follow:

1. Determine the rate, duration and location of the emission
2. Decide the best suitable model to conduct dispersion modelling study
3. Calculate the concentration of pollutant at the specific location
4. Determine possible outcomes according to the modelling process.

2.6.5. Box Model

Markiewicz (2006) claims that the box model is the simplest model among all other dispersion models. According to the box model, the atmosphere is thought to be separated into equal size of numerous boxes (Indra et al., 2004). It is assumed that emission from the source is constant over a distance Δx. It is also assumed that the concentration of the pollutant is constant in the box due to uniform mixing. In the box, the wind velocity is taken as a constant value. In the box model, mixing height is tought to be increasing with respect to time. Thus, the box model equation can be expressed as (Hanna et al., 1982):

$$\Delta x\, z_i\, \frac{\partial C}{\partial t} = \Delta x\, Q + u\, z_i (C_b - C) + \Delta x\, \frac{\partial z_i}{\partial t}\, (C_a - C) \qquad (49)$$

Change in the C with time	=	source	+	change due to horizontal advection	+	change due to mixing layer growth and vertical advection

In equation (49), Q represents the emission rate in mass per unit time per unit area, C_b and C_a symbolize concentrations upwind and above the mixing height respectively. In steady-state conditions, C_b, $\frac{\partial C}{\partial t}$ and $\frac{\partial z_i}{\partial t}$ is equal to 0 hence, the equation (49) yields to:

$$C = \frac{\Delta x\, Q}{z_i\, u} \qquad (50)$$

Box model diagram can be seen in Figure 2.18.

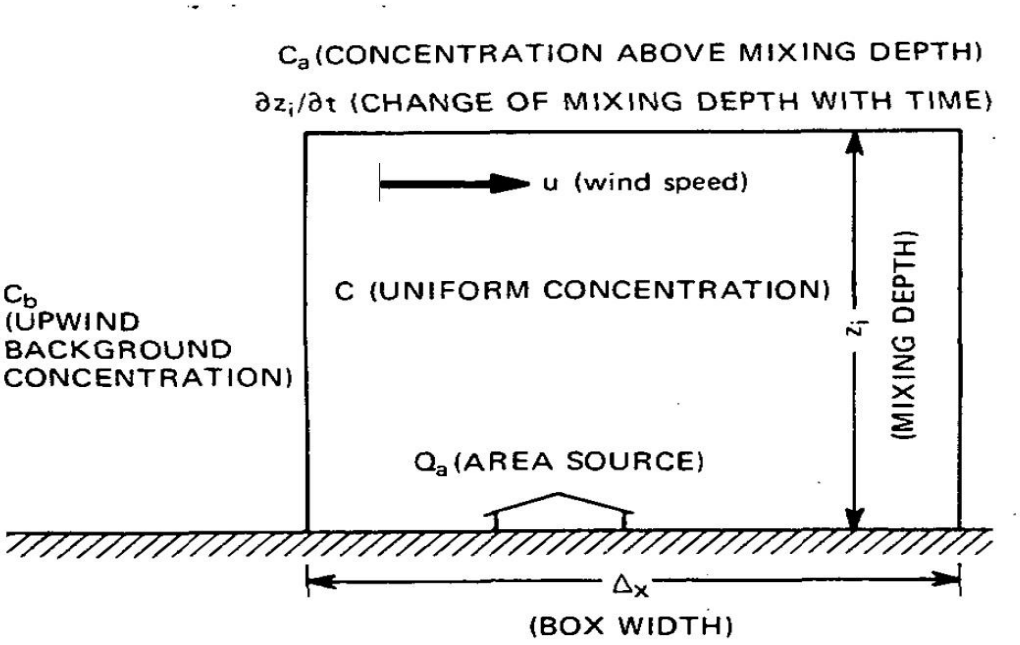

Figure 2.18. Box Model Diagram (Hanna et al., 1982)

Hanna et al. (1982) state that generally governmental foundations use the box model for detecting some specific substances to take into consideration solely among a group of hazardous chemicals. In general, the box model is regarded as a fundamental approach for dispersion modelling and good results have been obtained. On the other hand, Spellman & Stoudt (2013) claim that since assumptions in the box model are very simple, the accuracy of the model is limited in air dispersion estimation.

2.6.6. Gaussian Model

The first and most widely used air dispersion model is Gaussian model. It is assumed that the dispersion of pollutants has a Gaussian distribution model. In general, the Gaussian model is applied to steady-state air pollutant emission from the sources at ground-level or at a specific height (Spellman & Stoudt, 2013). The Gaussian model can be used for calculations to determine the concentration of the pollutant emitted from a source (Beychok, 2005). Empirically, the model can be defined drawn as

standard deviation of concentration in y and z-axis correspondent to atmospheric stability classes and downwind distance from the emission point (Singh, 2018).

In case of modeling emissions from ground level area sources, it can be assumed that there are many point sources which have individual emissions. All emissions from each point source in the area can be combined by assuming that there is an initial horizontal standard deviation, σ_{y0}. A virtual distance, x_y, can be determined to give horizontal standard deviation, σ_{y0}. This value is used to determine σy according to atmospheric stability class. After that, model for point source can be used to determine σ_y as a function of $x + x_y$. According to this theory, area source can be thought as a crosswind line source with a Gaussian distribution. The initial horizontal standard deviation, σ_{y0}, for an area source can be calculated by $\sigma_{y0} = s/4.3$, where s is the length of the area source (Turner, 1994).

According to Indra et al. (2004), in Gaussian modelling of a plume of a single stack, the assumptions made are as:

1. Distribution of concentration in the plume is Gaussian in both y and z-axis
2. Wind velocity, u, and wind direction is constant
3. Continuous and constant emission rate of pollutant, Q
4. Dispersion in x-axis is negligible
5. The pollutant does not have a chemical reaction
6. Steady-state and homogeneous transportation of pollutants
7. Topography is negligible

On the other hand, Singh (2018) mentions additional assumptions such as:

1. There is no background pollution
2. Mass is preserved by reflection from the ground

Hence, the Gaussian dispersion model can be expressed as:

$$C = \frac{Q}{2\pi u \sigma_y \sigma_z} exp\left(-\frac{y^2}{2{\sigma_y}^2}\right) exp\left[-\frac{(z-h)^2}{2{\sigma_z}^2}\right] \quad (51)$$

In equation (51), C represents the concentration of the pollutant at a given point, Q symbolizes the emission rate of the pollutant, u is the wind velocity, σ_y signifies horizontal dispersion parameter, σ_z is the vertical dispersion parameter, h is the effective height (De Visscher, 2014).

Figure 2.19 shows the Gaussian dispersion model (Nesaratnam and Taherzadeh, 2014).

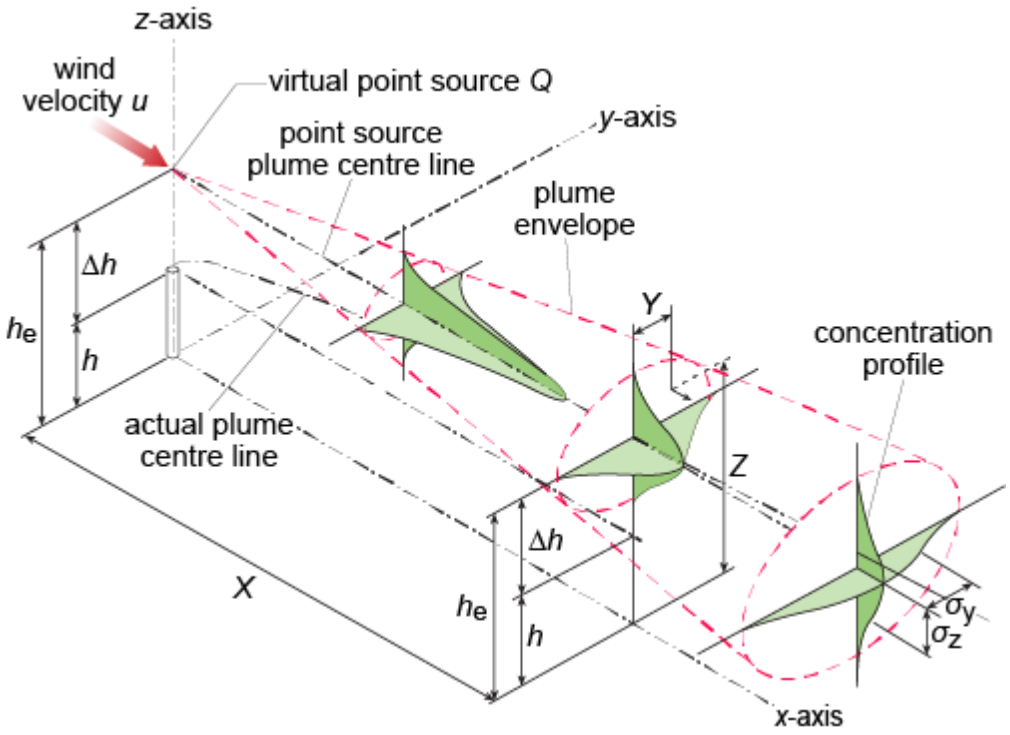

Figure 2.19. Gaussian Dispersion Model (Nesaratnam and Taherzadeh, 2014).

According to the assumption of mass is preserved by reflection from the ground, a reflected source is added to the equation and equation (51) yields (De Visscher, 2014):

$$C = \frac{Q}{2\pi u \sigma_y \sigma_z} exp\left(-\frac{y^2}{2{\sigma_y}^2}\right)\left\{exp\left[-\frac{(z-h)^2}{2{\sigma_z}^2}\right] + exp\left[-\frac{(z+h)^2}{2{\sigma_z}^2}\right]\right\} \quad (52)$$

Figure 2.20 shows non-buoyant Gaussian dispersion model from a ground source. Figure 2.21 demostrates reflected source due to ground reflection.

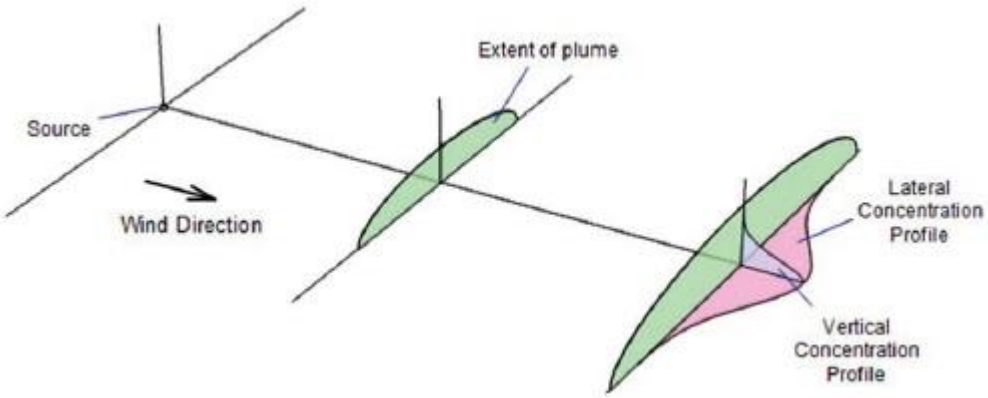

Figure 2.20. Non-buoyant Gaussian Dispersion from a Ground Source (Pursuer et al., 2016).

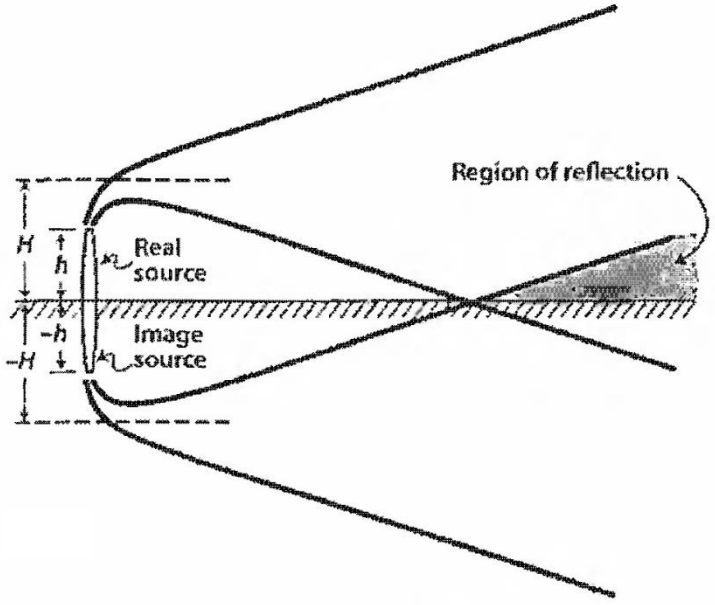

Figure 2.21. Reflected source due to ground reflection (Cooper and Alley, 2011)

From the equation (52), it can be concluded that (De Visscher, 2014):

1. The pollution concentration is correspondent to the emission rate
2. The pollution concentration has inverse proportion to wind velocity: high velocity of wind results in low pollutant concentration
3. In the case of the plume rise is affected by emission and wind speed, hence, the first two conclusions are only approximations.

According to Hanna et al. (1982), it should also be considered what would happen if wind velocity, u, is measured as zero in the Gaussian model. Hanna et al. (1982) states that anemometers can give a measurement result as u≈0 near the surface however it should be suitable to take u as 0.5 m/s since it is not possible for the wind to stop completely at the surface of the ground.

In general, the main concern is the ground level concentration of pollutant regarding public health. At ground level, where z=0, the equation is derived to (Nesaratnam and Taherzadeh, 2014):

$$C = \frac{Q}{\pi u \sigma_y \sigma_z} exp\left(-\frac{y^2}{2{\sigma_y}^2}\right) exp\left(-\frac{h^2}{2{\sigma_z}^2}\right) \quad (53)$$

Nesaratnam and Taherzadeh (2014) also state that the maximum concentration of the pollutant can be observed at the center line of the plume, where y=0, therefore equation (53) can be written as:

$$C = \frac{Q}{\pi u \sigma_y \sigma_z} exp\left(-\frac{h^2}{2{\sigma_z}^2}\right) \quad (54)$$

If the emission is at ground level and there is no effective plume rise, h=0, then the equation is derived to (Godish, 2004):

$$C = \frac{Q}{\pi u \sigma_y \sigma_z} \quad (55)$$

In the Gaussian dispersion model, in order to determine pollutant concentration at the desired downwind distance, two stages of calculation should be conducted (Singh, 2018):

1. Effective height should be calculated by adding plume rise at specific downwind distance from the pollutant source to the height of the source.
2. Pollutant concentration at the desired downwind distance by applying the Gaussian dispersion model.

2.6.7. Dispersion Parameters

In the Gaussian dispersion model, σ_y and σ_z symbolize the standard deviation of the horizontal and vertical dispersion parameters respectively. Bigger value of dispersion parameter, σ, results in wider distribution. Accordingly, the plume spreads wider as the downwind distance from the pollution source increases and dispersion parameters have bigger values. In other words, dispersion parameters are correspondent to value of downwind distance, x (Nesaratnam and Taherzadeh, 2014).

Godish (2004) says that the increase in the ratio of dispersion coefficients is proportional to meteorological parameters, specifically atmospheric stability. In the atmospheric stability of class A, the amount of increase is maximum for dispersion coefficients. On the other hand, in the atmospheric stability of class F, the degree of increase is minimum for dispersion coefficients. Generally, σ_y is not affected by inversion conditions, hence, σ_y has a bigger value than σ_z. Dispersion coefficients, σ_y and σ_z, can be found from Figure 2.22 and Figure 2.23 respectively.

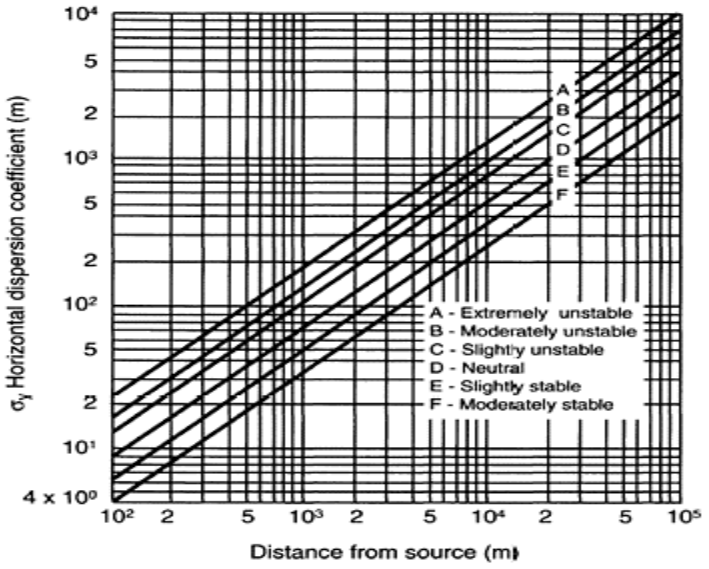

Figure 2.22. Horizontal Dispersion Coefficient, σ_y , vs. Downwind Distance, x (Godish, 2004).

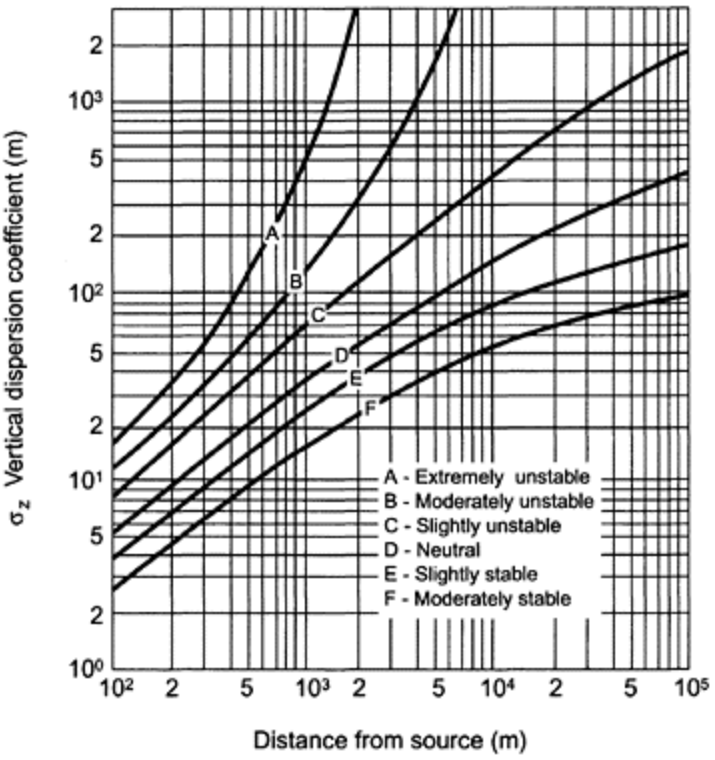

Figure 2.23. Vertical Dispersion Coefficient, σ_z , vs. Downwind Distance, x (Godish, 2004).

According to De Visscher (2014), there are various different experimental formulations to define Pasquill's dispersion coefficient graphs. Briggs (1973) claims that diffusion coefficients are a function of atmospheric stability classes. De Visscher (2014) says that Briggs (1973) formulated equations for σ_y and σ_z calculation as:

$$\sigma_y = \frac{ax}{(1+bx)^c} \tag{56}$$

$$\sigma_z = \frac{dx}{(1+ex)^f} \tag{57}$$

In equation (56) and (57), a, b, c, d, e and f are experimental coefficients (De Visscher, 2014). Depending on micrometeorological rules c and f are assumed as 0.5, however, it is not valid for f in extremely stable or extremely unstable atmospheric conditions (De Visscher, 2014). Table 2.15 shows experimental coefficients determined by Briggs (1973) for rural and urban areas.

Table 2.15. *Experimental Coefficients Determined by Briggs (1973) (De Visscher, 2014).*

Rural						
	σ_y			σ_z		
Stability Class	a	b	c	d	e	f
A	0.22	0.0001	0.5	0.2	0	-
B	0.16	0.0001	0.5	0.12	0	-
C	0.11	0.0001	0.5	0.08	0.0002	0.5
D	0.08	0.0001	0.5	0.06	0.0015	0.5
E	0.06	0.0001	0.5	0.03	0.0003	1
F	0.04	0.0001	0.5	0.016	0.0003	1
Urban						
	σ_y			σ_z		
Stability Class	a	b	c	d	e	f
A-B	0.32	0.0004	0.5	0.24	0.0001	- 0.5
C	0.22	0.0004	0.5	0.2	0	-
D	0.16	0.0004	0.5	0.14	0.0003	0.5
E-F	0.11	0.0004	0.5	0.08	0.0015	0.5

In order to have an idea about the accuracy of the Briggs' equation, dispersion coefficients graph according to downwind distance for rural terrain is given in Figure24 (a) and (b) (De Visscher, 2014).

Martin (1976) formulized an equation for σ_y and σ_z as:

$$\sigma_y = aX^b \tag{58}$$

$$\sigma_z = cX^d + f \tag{59}$$

In equation (58) and (59), a, c, d and f are stability coefficients, b is constant which is equal to 0.849.

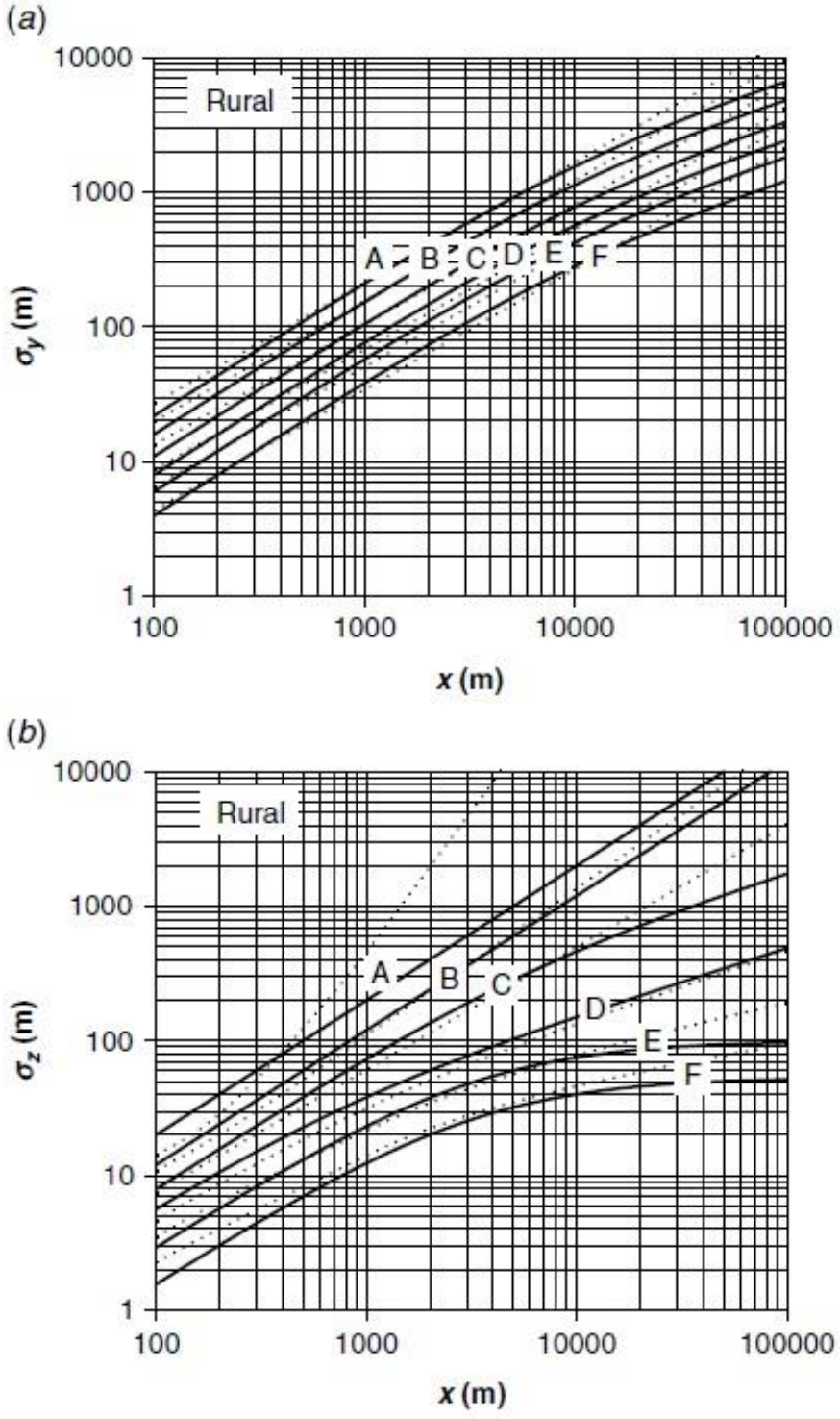

Figure 2.24. (a) Horizontal, σ_y , and (b) vertical, σ_z , Dispersion Coefficients Formulated by Briggs (1973) (solid lines) and Martin (1973) (dotted lines) vs. Downwind Distance, x in Rural Area (De Visscher, 2014)

2.6.8. Lagrangian Model

Lagrangian model can be used as another technique for pollutant dispersion modelling. In the Lagrangian model, particle movement is correspondent to instantaneous flow (Zannetti,1990). According to Weber (1982), distinct air parcels are monitored and concentration is calculated for every single parcel in Lagrangian modelling. The conception of air parcel is frequently used in atmospheric science. An air parcel can be described as a volume of air which is sufficiently big to contain the adequate number of molecules to have characteristics such as density, temperature and contaminant concentration (Lin, 2012). The Lagrangian particle trajectory model complies with the similar assumptions made by puff dispersion models (Walcek, 2002). Figure 2.25 shows the movement of a particle in the random walk model.

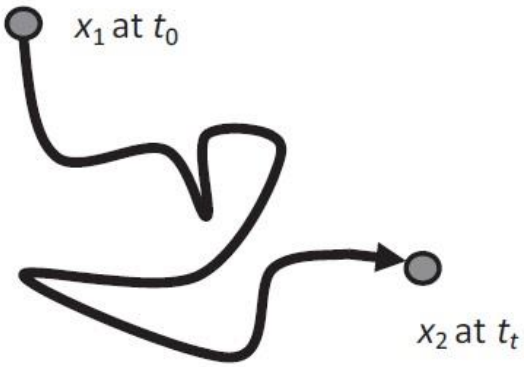

Figure 2.25. Movement of a Particle in the Random Walk Model (Vallero, 2014)

Movement of a particle in the random walk model can be formulated by Lagrangian approach as:

$$\vec{v} = [x(t), y(t), z(t)] \tag{60}$$

The Lagrangian model calculates statistics of the trajectories of particles representing the entire plume to determine pollutant dispersion (Vallero, 2014). Figure 2.26 shows Lagrangian Model for a vertical column of boxes.

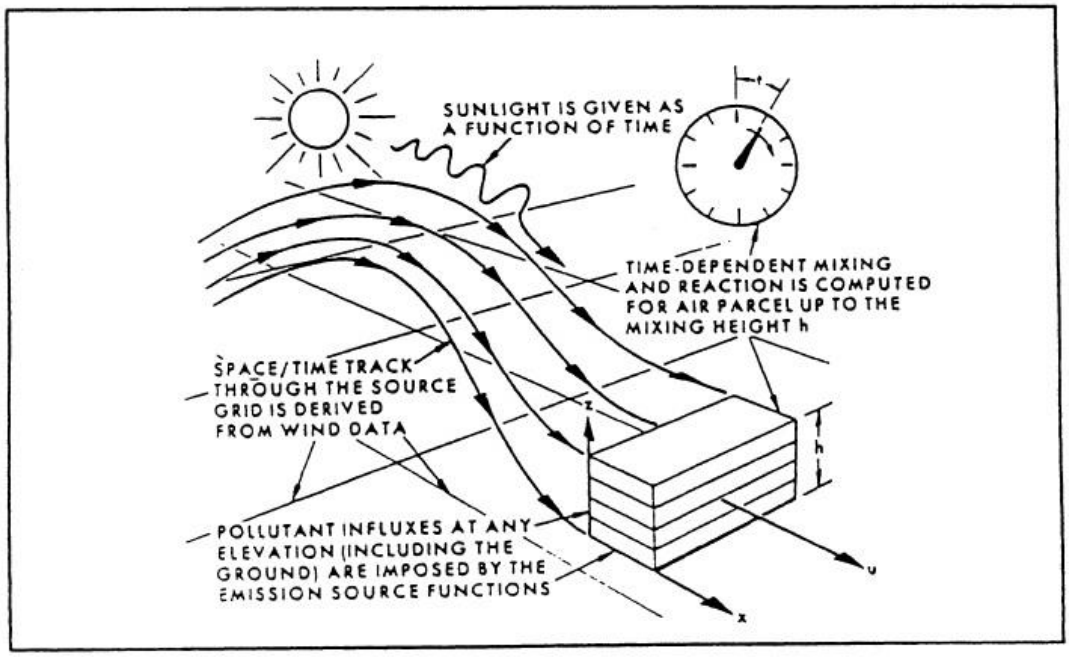

Figure 2.26. Lagrangian Model for a Vertical Column of Boxes (Zannetti,1990).

In the Lagrangian model, assumptions are similar to puff dispersion models. In puff model, pollutant is emitted from the source and disperses in the air by constant wind speed and diffusivities. Additionally, pollutant dispersion is constrained by ground level, z=0, at the bottom and planetary boundary layer (PBL) at the top in the vertical dimension. The Lagrangian model describes the concentration of the pollutant in the center of the puff as:

$$C_{(x,y,z)} = \frac{Q}{(2\pi)^{3/2}\sigma_y\sigma_z}\, exp\left(\frac{-(x-x_c)^2-(y-y_c)^2}{2\sigma_y}\right)\left[exp\left(\frac{-(z-z_c)^2}{2\sigma_z}\right) + exp\left(\frac{-(z+z_c)^2}{2\sigma_z}\right)\right] \quad (61)$$

In equation (61), x_c and y_c is the center of the puff, z_c puff dispersion height, σ_y and σ_z are horizontal and vertical dispersion coefficients respectively (Singh, 2018).

2.6.9. Eulerian Model

Anfossi and Physick (2004) say that there are two fundamental approaches for air dispersion modelling which are Eulerian models and Lagrangian models. In Eulerian models, the reference system is fixed with respect to the pollution source, on the other hand, the reference system follows the instantaneous flow in Lagrangian models (Harrop, 2002).

The Eulerian model assumes that the amount of contaminant of concentration of c(x, y, z, t) is conserved. Therefore, the Eulerian model yields to:

$$\frac{\partial c}{\partial t} = -V\nabla c + D\mathrm{i}\nabla^2 c + S_n \qquad (62)$$

In equation (62), Di symbolizes the molecular diffusivity constant which is $1{,}5\text{x}10^{-5}$ m^2/s for air, $\nabla^2 = \partial^2/\partial x^2 + \partial^2/\partial y^2 + \partial^2/\partial z^2$ signifies the Laplacian operator, ∇ represents the gradient operator, S_n is source or sink term (Zannetti,1990).

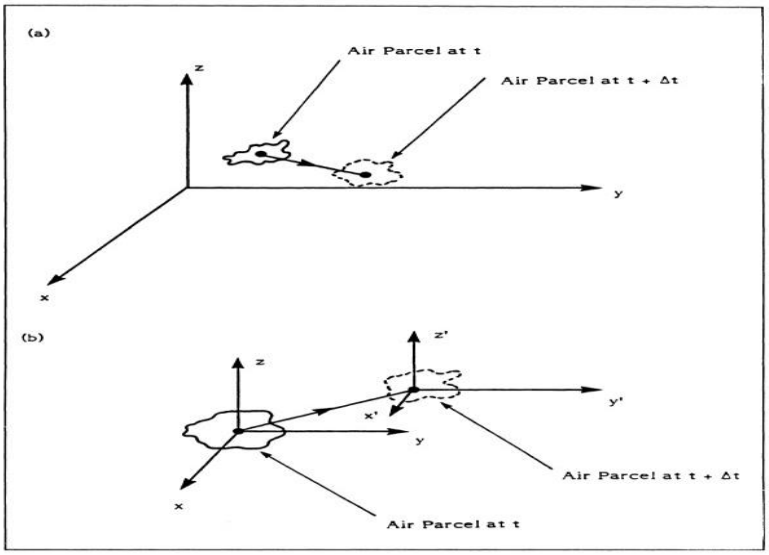

Figure 2.27. Scheme of Reference Frame for Eulerian (a) and Lagrangian (b) dispersion Model (Zannetti,1990)

According to Singh (2018), characteristics of the atmosphere such as temperature, pressure and concentration of pollutants can be monitored by Eulerian modelling. Eulerian dispersion model is not accurate at short distances modelling because turbulent eddies cannot be neglected regarding downwind distance between pollution source and the receptor. In contrast, the Lagrangian dispersion model is more accurate for monitoring pollutant concentration on small scales. Eulerian dispersion model has more accuracy on the regional scale. Additionally, Eulerian dispersion model calculations need more computer work than Lagrangian models (De Visscher, 2014). Scheme of reference frame for Eulerian and Lagrangian dispersion model can be seen in Figure 2.27.

2.6.10. Dense Gas Model

Emission of pollutants will have an impact starting from the pollution source and the effect of the pollutant will reduce at downwind locations. The biggest adverse effects can be revealed by toxic or explosive gas emissions. Therefore, gas dispersion modeling should be conducted in order to forecast pollution effects. In general, atmospheric effects enhance dispersion and decrease adverse effects caused by hazardous gas. This phenomenon is valid for buoyant dispersion from elevated sources. Nevertheless, for dense gases, dispersion is reduced and the effect area is more considerable at ground level.

There are many gas pollutants, which are denser than air such as chlorine and LPG. Thus, dense gas modelling is an important issue (Deaves, 1992). Traditional air dispersion models are not accurate for evaluation of the outcome of gas emissions which are denser than air (Spicer & Havens, 1989). Dense gases have a tendency to stay at ground level (Deaves, 1992). As a result, they cause higher safety risks in operational areas. According to Deaves (1992), obstacles have a more significant effect on dense gas dispersion than on elevated emission sources.

The dense gas dispersion model is a numerical model which can be applied to atmospheric dispersion of hazardous gases. The dense gas dispersion model is applicable to non-buoyant, ground level, continuous, sudden, and time-variant emissions (EPA, 2002). The dense gas dispersion model can be applied to short-term releases such as 1 hour or shorter time periods and the area of effect can be estimated. The dense gas dispersion model is beneficial in case of an excessive amount of hazardous dense gas releases. The frequently applied dense gas dispersion model are DEGADIS, SLAB and HEGADIS (Singh, 2018).

DEGADIS can be used for modelling aerosol dispersion with predefined concentration and density ratio. In DEGADIS, the relation between the concentration and density of aerosol is correspondent to mole fraction, concentration and mixture density. SLAB model is applicable to evaporating pools and stack releases. SLAB model is used for the estimation of downwind centerline concentration and pollutant puff dimensions (Zapert et al., 1991).

CHAPTER 3

STATEMENT OF PROBLEM

JP-8 is a widely used jet propellant in the aviation sector. In the aerospace industry, fueling operations have a risk of JP-8 spillage due to breakage or leakage in fueling stations. JP-8 vapor is hazardous to health in case of human exposure, flammable and can explode in the presence of various ignition sources such as open flames, sparks and static electricity. Therefore, it is important to understand the evaporation and dispersion process of JP-8 as well as the physical and environmental factors affecting evaporation and dispersion.

By modeling JP-8 evaporation, concentration, percentage and flammability of the air-vapor mixture can be known at a specific time and distance after the leakage of the fuel. Dispersion modeling can be used to determine the concentration of flammable and hazardous vapors in the air at the time given. The physical and environmental factors such as the amount of spillage, spillage area, wind speed and temperature affect the dispersion of particles in the air.

The aim of this study is to model evaporation and dispersion of JP-8 spill according to the environmental and physical factors and to determine the effects of these factors on possible outcomes. Therefore, evacuation zones can be determined, precautions for explosion prevention can be clarified and a scientific approach to explosion protection can be established in the aerospace industry for oil spills.

CHAPTER 4

METHODOLOGY

4.1. Introduction

In this current study, JP-8 spill scenario is based on a real accident happened during the fueling operation of an aircraft in the aerospace industry. In modelling, the environmental and physical conditions are taken into consideration regarding real accident area circumstances.

For fueling of aircraft in the fueling station, two operators connected fueling pipe to the aircraft and started fueling operation. Just after starting fueling, two operators left the fueling station for 30 minutes lunch break. During the fueling operation, due to the failure in the gasket of the fuel pump's pipeline, 4,6 tons of JP-8 leaked. Fortunately, all JP-8 fuel discharged into the secondary containment of the fuel tank. Fueling tank is next to fueling hangar in open air area. Additionally, JP-8 spill fully filled secondary containment tank. However, there was no failure alarm in the fueling system and all operators were at the lunch break for 30 minutes. After the break, the spill alarm was given and the spillage was cleaned up by the spill response team at the end of 5 hours of intervention.

In this thesis, after a spillage due to a failure in the fueling system, evaporation and dispersion of JP-8 under different physical and environmental conditions are modelled, effects of physical and environmental factors are observed, evacuation zones and precautions for fire and explosion prevention are defined.

A steady-state model representing the evaporation of the spillage of JP-8 and atmospheric dispersion of JP-8 vapors has been established. The spill of JP-8 is estimated as an instantaneously-formed pool of liquid. In order to determine the concentration of JP-8 vapors downwind of the spillage, two main models are used in

the study. Firstly, the evaporation of JP-8 into the atmosphere is modelled. Atmospheric and chemical properties are used to calculate the vapor formation of JP-8. The ingredients of JP-8 assumed to be 100% of kerosene. The evaporation rate of JP-8, calculated through the evaporation model, is regarded as the emission rate for the atmospheric dispersion model. The JP-8 spill is assumed to be a ground level, single and constant point source for air dispersion calculation. The concentration of JP-8 vapors is modelled as a function of downwind distance. The air dispersion model of JP-8 provides concentration contour plots of JP-8 at an elapsed time, elevation and distance. The effects of each physical and environmental parameter on JP-8 concentration are modelled and discussed respectively.

4.2. Fueling Operation Area and Fuel Spill Accident Conditions

During the spill accident, physical and environmental factors have an effect on JP-8 evaporation and dispersion. Physical and environmental parameters can be listed as:

- Amount of spill
- Spillage area
- Ambient temperature
- Wind speed in the open air
- Atmospheric stability class
- Land Characteristic

At the time of the spill accident, the values of the physical and environmental factors affecting dispersion are given in the Table 4.1.

Table 4.1. *The Values of the Physical and Environmental Factors*

Parameter	Value
Spillage amount	4,608 tons (5760 lt)
Spill area	28,8 m^2
Dimensions of the secondary containment	6,4 m x 4,5 m x 0,2 m
Ambient Temperature	30 °C
Dimensions of the fuel station building	20 m x 30 m x 6,5 m
Wind velocity in the open air	5 m/sec
Insolation	Slight
Land characteristic	Rural
Duration of evaporation until clean up	5 hours

4.3. Evaporation Model of JP-8

The main aim of JP-8 evaporation modelling is to calculate the amount of chemical vapors emitted from the stationary and instantaneously-formed spill due to failure in the pipeline. The area of the spill pool is assumed to occur instantaneously after breakage and remains constant during the evaporation process. The evaporation rate of JP-8 is dependent on time, atmospheric conditions such as temperature, wind velocity and chemical properties of substances in JP-8 composition. For calculation purposes, the oil spilled is considered as a pure substance of kerosene.

It is assumed that JP-8 in the pipeline leaked from the gasket rupture at atmospheric conditions. Therefore, kerosene is considered as at ambient temperature and no heat transfer occurs between chemical spillage and secondary containment. Additionally, the evaporation amount from the pool is limited by the mass transfer mechanism.

Mass transfer evaporation rate, due to wind blowing over the spill pool, is considered as constant since the mass transfer rate is independent of time. Furthermore, all oil vapors are thought to be emitted to the atmosphere. According to the above

assumptions, several model is used and compared for oil evaporation and dispersion calculation.

In Stiver and Mackay model, spilled oil the evaporation rate was formulated as:

$$E = KAP/(RT) \tag{29}$$

In equation (29), E represents the evaporative molar flux in mol/s, K symbolizes mass transfer constant under the wind effect in ms^{-1}, A represents the area in square meters, R symbolizes the gas constant [8,314 $Pa.m^3/(mol.K)$], T signifies temperature (K) and P symbolizes vapor pressure of the liquid (Pa).

As an alternative model for evaporation calculation, the Brighton evaporation model is also used. Brighton redefined evaporation equation, and he studied on water evaporation with a similar approach to Sutton as:

$$E = K\, C_s\, U^{7/9}\, {d_1}^{-1/9}\, Sc^{-r} \tag{20}$$

In equation (20), E represents evaporation rate per unit area, K symbolizes experimental mass transfer coefficient, C_s signifies evaporating liquid concentration which is thought of as pure kerosene, d_1 represents pool length in meters which is 4,5 and r symbolizes an experimental constant value between 0 and 2/3. In this current work, Schmidt number is assumed as 2.70 and r is taken as 1/3. Tkalin mass transfer constant equations are used to determine K.

C_s is determined by the formula:

$$C_s = \frac{M\, P_v}{R\, T} \tag{21}$$

In this current work, the evaporation model of Tkalin is also used for the evaporation calculation of JP-8. Tkalin described an evaporation model for oil at sea level as:

$$E_i = \frac{KMP_{oi}\, x}{RT} \tag{25}$$

In equation (25), E_i represents evaporation rate of oil compound i or total evaporation in kg/m^2s, K symbolizes mass transfer constant in m/s, M signifies molecular weight,

P_{oi} represents vapor pressure of the oil compound i and x signifies the amount of the oil product i at time t. Experimental data was used to define parameters in the model:

$$P_{oi} = 10^3 e^A \tag{26}$$

In equation (26), A was described as (Fingas, 2013):

$$A = -(4.4 + \log T_b)[1.803\,\{T_b/T - 1\} - 0.803\ \ln(T_b/T)] \tag{27}$$

In equation (27), T_b represents the boiling point of the oil product. K is described as:

$$K = 1.25\ U\ 10^{-3} \tag{28}$$

JP-8 evaporation is also modelled according to empirical equations given in Table 2.11. Since JP-8 is diesel-like fuel, the empirical equation of diesel–long term evaporation is used. According to Fingas, diesel fuel evaporation has an empirical equation is given as:

$$\%Ev = \ (5.8 + 0.045\ T)\ /\ \ln(t) \tag{63}$$

In Equation (63), T is the temperature in degree Celsius and t is time in minutes.

In this study, in order to obtain evaporation cure of pure kerosene, Clausius-Clapeyron equation was used to calculate vapor pressure in the form as:

$$\log\frac{P_s}{P} = \frac{\Delta_{vap}H^0\ \mathrm{M}}{4.57}\left(\frac{1}{\mathrm{T}} - \frac{1}{T_s}\right) \tag{3}$$

In equation (3), P represents vapor pressure at T which is absolute pressure, P_s represents vapor pressure at boiling point, T_s. In this case, P_s equals to 1 atm. T_s is considered as 192°C which is the average value of lower and highest boiling point given in Table 2.4. $\Delta_{vap}H^0$ is the heat of evaporation as cal/g. Heat of evaporation is determined as 86 Btu/lb. When unit conversion is done 86 Btu/lb × 2,328 = 200,208 J/g which is equals to 47,849 cal/g is obtained. M is the molecular weight. Since kerosene is mainly equivalent to dodecane, $C_{12}H_{26}$, molecular weight is taken as 170 g/mol.

According to Fingas (2013), $\Delta_{vap}H^0$M/(4.57 T_s) was considered as a constant value, 5±0.2, for hydrocarbons. Hence, the equation became as

$$\log P_s/P = 5.0[(T_s - T)/T] \quad (4)$$

Equation (4) is also used for calculation of the vapor pressure of spilled JP-8.

The Clausius–Clapeyron equation can be also expressed as:

$$\ln\left(\frac{P_2}{P_1}\right) = -\left(\frac{\Delta_{vap}H^0}{R}\right)\left[\frac{1}{T_2} - \frac{1}{T_1}\right] \quad (6)$$

If the exponential of the equation (6) is taken, then the equation yields a different form of the Clausius-Clapeyron equation such as (Jenkins, 2008):

$$\left(\frac{P_2}{P_1}\right) = exp\left\{-\left(\frac{\Delta_{vap}H^0}{R}\right)\left[\frac{1}{T_2} - \frac{1}{T_1}\right]\right\} \quad (7)$$

Equation (7) is also used in order to obtain the vapor pressure curve of kerosene. Heat of vaporization of kerosene is given as 86 Btu/lb in Table 2.6. In order to convert Btu/lb to KJ/kg, 86 Btu/lb multiplied by the conversion factor, 2.328, and 200,208 J/g is obtained. The gas constant, R, is equal to 8,314 J/(mol.K).

In order to model oil evaporation in spillages, mass transfer constant is needed to be calculated. There are several different approaches to calculate the mass transfer constant.

In this thesis, Mackay & Matsugu method is used to determine mass transfer constant. In Mackay & Matsugu method, mass transfer constant is formulized as a function of wind velocity and pool areas given the equation:

$$K = 0.0292\ U^{0.78}X^{-0.11}Sc^{-0.67} \quad (9)$$

In equation (9), K represents mass transfer constant (meter/hour), U is wind velocity in meter/hours and X symbolizes pool diameter in meters. Regarding the information given in Table 5.1, X is accepted as equal to the shortest side of the secondary

containment which is 4,5 m. Schmidt number is assumed as 2.70 according to Mackay & Matsugu (1973).

For calculation of mass transfer constant Hamoda formulation is also used. In Hamoda and co-workers study, mass transfers constant, K, is given as:

$$K = 1.68 \times 10^{-5} \, (API°)^{1.253} \, (T)^{1.80} \, e^{-0.1441} \qquad (35)$$

In equation (35), K represents mass transfer constant in cm/h, $API°$ symbolizes unitless density API parameter and T is temperature as degree Celsius.

Tkalin's evaporation model is also used for mass transfer constant determination. According to Tkalin's evaporation model, mass transfer constant, K, in m/s, is described as:

$$K = 1.25 \, U \, 10^{-3} \qquad (28)$$

Mackay & Wesenbeeck purposed an evaporation rate equation for dodecane as:

$$E = 474 \times P \times M \qquad (64)$$

In equation (64), E is the evaporation rate in $\mu g/m^2 s$, vapor pressure, P, is in Pascal and molar weight is in g/mol.

4.4. Dispersion Model of JP-8

In this study, the Gaussian dispersion model is used as a dispersion model of oil vapors. The air dispersion model takes into account the atmospheric conditions, type of source and emission rate to calculate downwind concentrations. Oil vapors are considered as transported by the prevailing wind at constant speed and direction.

The area of the spill is used as a ground-level, single and constant point source in the air dispersion model. The emission rate is determined by the evaporation rate obtained from the evaporation model. During the evaporation process, the evaporation rate is thought to be constant. It is also assumed that the atmospheric turbulence is stationary and homogeneous. Wind speed and direction are taken as constant during dispersion.

Moreover, the mass of vapors is assumed to be preserved by reflection from the ground.

The Gaussian dispersion model can be expressed as:

$$C = \frac{Q}{2\pi u \sigma_y \sigma_z} exp\left(-\frac{y^2}{2{\sigma_y}^2}\right)\left\{exp\left[-\frac{(z-h)^2}{2{\sigma_z}^2}\right] + exp\left[-\frac{(z+h)^2}{2{\sigma_z}^2}\right]\right\} \quad (52)$$

In equation (52), C represents the concentration of the pollutant at a given point, Q symbolizes the emission rate of the pollutant which is equal to the evaporation rate of kerosene, u is the wind velocity. σ_y signifies horizontal dispersion parameter and σ_z is the vertical dispersion parameter which are both a function of x, downwind distance and atmospheric stability class. h is the effective height. For chemical spillage, effective height, h, is regarded as zero. Therefore, the Gaussian dispersion model can be written as:

$$C = \frac{Q}{2\pi u \sigma_y \sigma_z} exp\left(-\frac{y^2}{2{\sigma_y}^2}\right)\left\{exp\left[-\frac{(z)^2}{2{\sigma_z}^2}\right] + exp\left[-\frac{(z)^2}{2{\sigma_z}^2}\right]\right\} \quad (65)$$

In this current work, dispersion parameters, σ_y and σ_z, is determined according to Pasquill's method and Briggs formulation.

According to Pasquill's atmospheric stability classes method, lateral and vertical standard deviations are corresponding to atmospheric turbulence and wind speed. Therefore, atmospheric stability class is chosen according to Table 2.14.

In this thesis, horizontal and vertical dispersion coefficients at the 100 m 200 m 300 m 400 m and 500 m of downwind distance from the source are calculated. Pasquill's horizontal and vertical dispersion coefficients are determined from Figures 2.22. and 2.23. respectively.

According to Briggs formulation, σ_y and σ_z can be expressed as:

$$\sigma_y = \frac{ax}{(1+bx)^c} \quad (56)$$

$$\sigma_z = \frac{dx}{(1+ex)^f} \quad (57)$$

In equation (56) and (57), a, b, c, d, e and f are experimental coefficients which are chosen from Table 2.15. depending on meteorological and terrain data.

CHAPTER 5

RESULTS AND DISCUSSIONS

5.1. Results and Discussions for Evaporation Modelling

In evaporation modelling, it is necessary to calculate vapor pressure and mass transfer constant. There are several different approaches for vapor pressure and mass transfer constant calculation. Firstly, in this current thesis, four different model is applied for vapor pressure calculation. Secondly, three different equations are used for mass transfer constant determination. Finally, five evaporation models are applied to calculate the evaporation rate of the JP-8 spill. All results are compared and most suitable approaches are selected to be used in oil evaporation modelling regarding physical and environmental conditions of the spill accident.

5.2. Vapor Pressure Calculation

In this current thesis, the vapor pressure of the JP-8 spill is calculated according to Blokker's, Fingas', Jenkins' and Tkalin's model. Each model is used to obtain vapor pressure of JP-8 spill at 30^{o}C and vapor pressure line of kerosene versus varying temperatures. The results of vapor pressure calculation are given in Table 5.1 and each model application is discussed respectively.

Table 5.1. *Vapor Pressure of Kerosene According to Various Models*

Model	**Vapor Pressure mm Hg at 30 °C**
Blokker	96,2842
Fingas	51,1439
Jenkins	6,5642
Tkalin	0,0109

5.2.1. Blokker's Model

In Blokker's model, the molecular weight, M, heat of vaporization, $\Delta_{vap}H^0$, and constant value of 4.57 are used for vapor pressure calculation. In this current study, oil is assumed as a single component fluid as kerosene and kerosene is considered mainly equivalent to dodecane, $C_{12}H_{26}$. However, in reality, JP-8 consists of several compounds which have different molecular weights and heat of vaporization values. This approximation can be seen as a disadvantage of Blokker's vapor pressure calculation. According to Blokker (1964), the Clausius-Clapeyron equation (3), vapor pressure line versus temperatures between 0 °C and 60 °C is given in Figure 5.1.

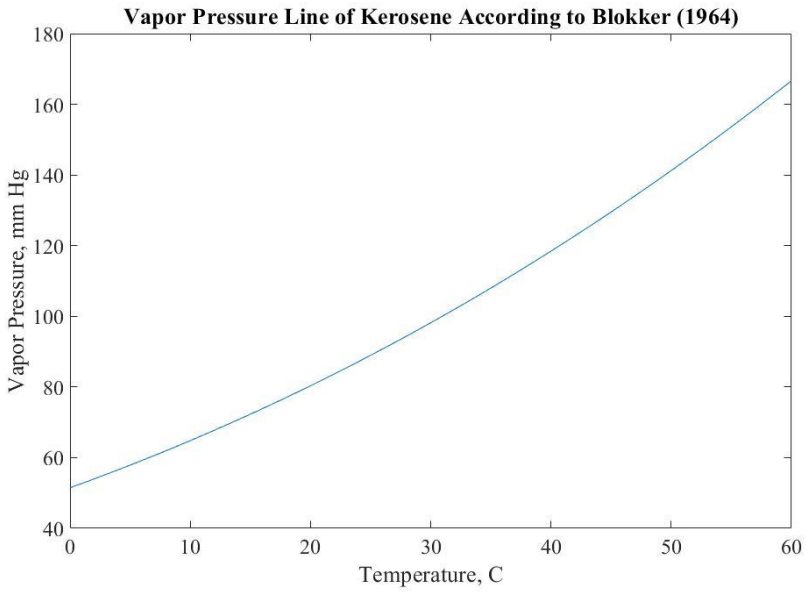

Figure 5.1. Vapor pressure line of kerosene according to Blokker

5.2.2. Fingas (2013) Model

In Fingas (2013) model, $\Delta_{vap}H^0$M/(4.57 T_s) was considered as a constant value which is equal to 5. However, in practice, this assumption is not valid for every hydrocarbon. Considering JP-8 which involves different types of hydrocarbons with different

$\Delta_{vap}H^0$M/(4.57 T_s) ratios, this approximation can be considered as a drawback of the model. According to Fingas (2013), equation (4), vapor pressure line versus temperatures between 0 °C and 60 °C is given in Figure 5.2.

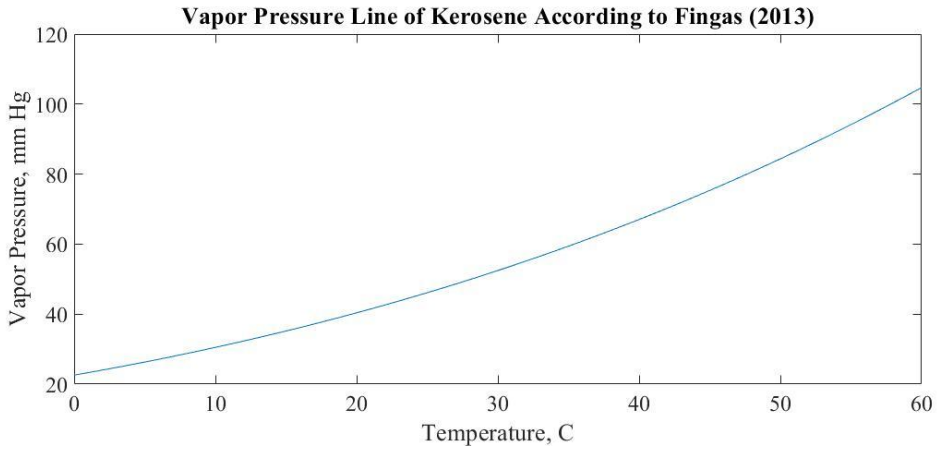

Figure 5.2. Vapor pressure line of kerosene according to Fingas (2013)

5.2.3. Jenkins (2008) Model

In Jenkins (2008) model, heat of vaporization and gas constant is used for the vapor pressure equation. In this study, since JP-8 is regarded as pure kerosene, heat of vaporization of kerosene is used in calculation. Yet, JP-8 consists of different types of compounds with different heat of vaporization values. This fact can be thought as the downside of the model. According to Jenkins (2008), equation (7), vapor pressure line versus temperatures between 0 °C and 60 °C is given in Figure 5.3.

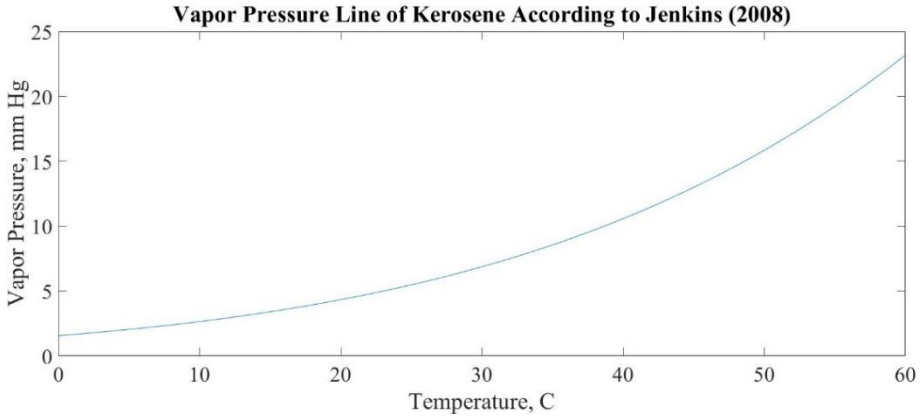

Figure 5.3. Vapor pressure line of kerosene according to Jenkins (2008)

5.2.4. Tkalin's Model

In Tkalin's model, the boiling point of the oil product is used for vapor pressure calculation. In this work, JP-8 is regarded as pure kerosene and the boiling point is taken as 192 °C. In practice, the boiling point of the JP-8 can be different from the boiling point of kerosene. This assumption can be regarded as the negative side of the model. In addition, the pressure values obtained from the Tkalin model look very low compared to other models. Therefore, Tkalin's model is not suitable for evaporation modeling of the JP-8 spill. According to Tkalin's model, equation (25) and (26), vapor pressure line versus temperatures between 0 °C and 60 °C is given in Figure 5.4.

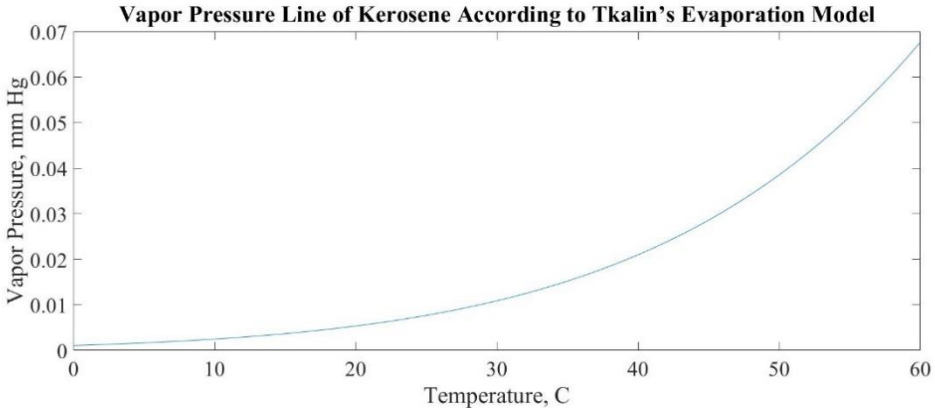

Figure 5.4. Vapor pressure line of kerosene according to Tkalin's Evaporation Model

5.3. Mass Transfer Constant Calculation

In this current work, the mass transfer constant of kerosene is determined according to Mackay & Matsugu, Tkalin's and Hamoda's model. Each model is applied to mass transfer constant calculation at spillage conditions. Mass transfer constant variation graph is drawn with respect to different wind speeds and temperatures. The results of mass transfer constant calculations are given in Table 5.2 and the results of each model are discussed separately.

Table 5.2. *Mass Transfer Constant of Kerosene According to Various Models*

Model	**Mass Transfer Constant m/s**
Mackay & Matsugu	0,0084
Tkalin	0,0075
Hamoda	$0{,}0021 \times 10^{-3}$

5.3.1. Mackay & Matsugu Formulation for Mass Transfer Constant

In Mackay & Matsugu formulation, mass transfer constant is correspondent to wind velocity, pool diameter and Schmidt number. As wind velocity increases mass transfer constant also increases. Mackay & Matsugu formula yields K values similar to Tkalin model. According to Mackay & Matsugu formulation, equation (9), K values versus various wind velocities are given in Figure 5.5.

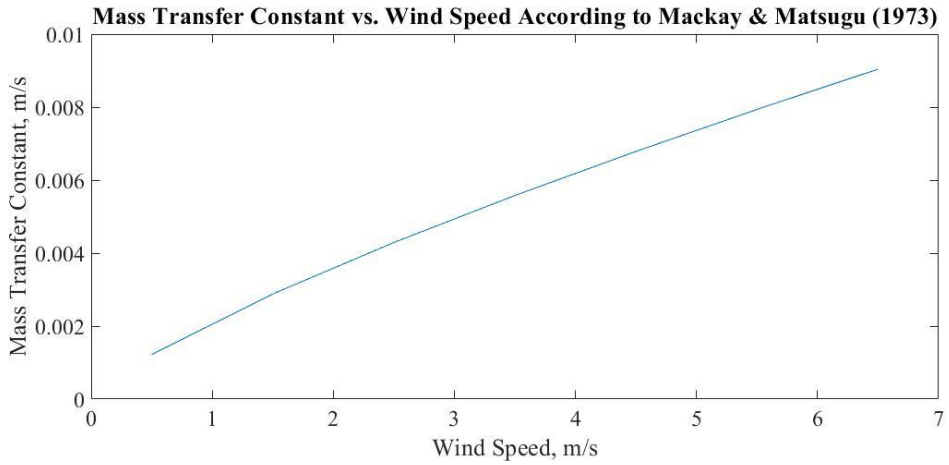

Figure 5.5. Mass Transfer Constant vs. Wind Speed According to Mackay&Matsugu (1973)

5.3.2. Hamoda Formulation for Mass Transfer Constant

In the Hamoda formula, mass transfer constant depends on API° density and temperature. API° value is chosen as 44 which is the average of minimum and maximum acceptable API^{o} density values at 60 °F given in Table 8. However, the evaporation rate is calculated at 30 °C. This acceptance is the shortcoming of the model. Moreover, the results of the mass transfer constant formula are very low compared to other models. As a result, Hamoda formulation for mass transfer constant calculation for oil JP-8 spill evaporation modeling is not significant. According to Hamoda formula, equation (35), mass transfer constant versus temperatures between 0 °C and 60 °C is given in Figure 5.6.

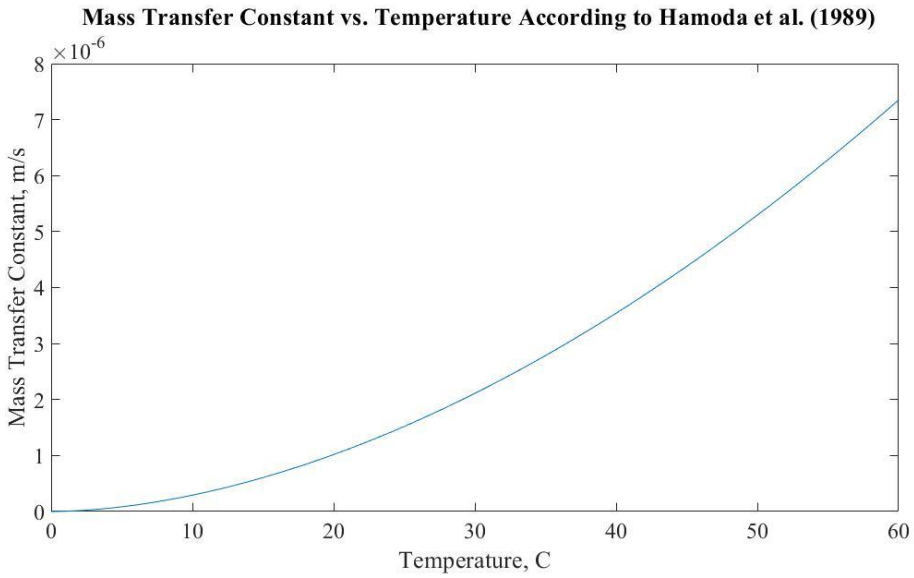

Figure 5.6. Mass Transfer Constant vs. Temperature According to Hamoda et al. (1989)

5.3.3. Tkalin's Formulation for Mass Transfer Constant

Tkalin's formula for mass transfer constant calculation is very simple. In Tkalin's model, mass transfer constant is only correspondent to wind velocity. In the model, mass transfer constant increases as wind velocity increases. The mass transfer constant values found by Tkalin's model is very similar to mass transfer constant values of Mackay and Matsugu. According to Tkalin's evaporation model, mass transfer constant, K, in m/s, versus wind speed graph is given in Figure 5.7.

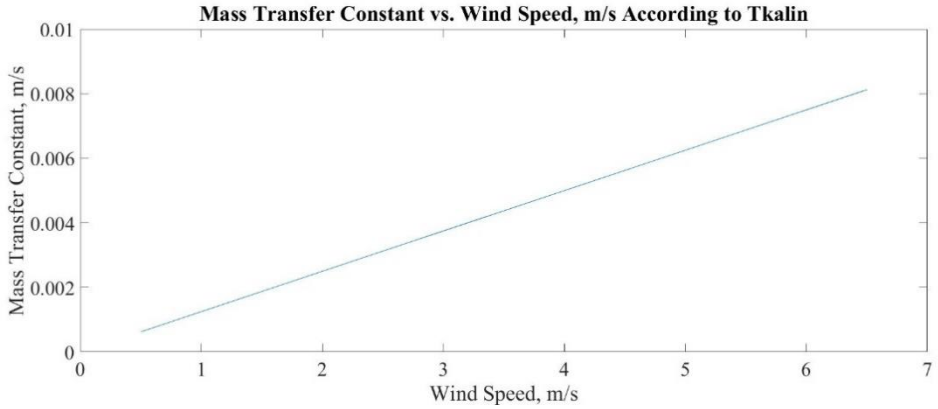

Figure 5.7. Mass Transfer Constant vs. Wind Speed According to Tkalin's Evaporation Model

5.4. Evaporation Calculation

In this study, the evaporation rate of the JP-8 spill is calculated according to Stiver and Mackay, Mackay and Wesenbeeck, Brighton, Tkalin and empirical equation model. Five models are used to determine the evaporation rate at spill condition. Evaporation rates are given in Table 5.3 and each evaporation model is argued respectively.

Table 5.3. *Evaporation Rate of JP-8 spill According to Various Models*

Model	**Evaporation Rate kg/s**
Stiver and Mackay	1,4366
Brighton	3,5722
Tkalin	97,3526
Mackay and Wesenbeeck	0,044

5.4.1. Stiver and Mackay Evaporation Model

In Stiver and Mackay evaporation model, the evaporation rate is related to mass transfer constant, spillage area and vapor pressure. Mass transfer constant is determined by Tkalin's model. The vapor pressure of the JP-8 spill is calculated by

the Clausius-Clapeyron equation given in Jenkin (2008). The evaporation rate obtained by Stiver and Mackay model is more lower than Brighton and Tkalin evaporation models. Still, the heat of vaporization assumption of JP-8 can be different from the value in practice. Additionally, JP-8 consists of several hydrocarbons so it is expected that the evaporation rate is not a constant value. At the beginning of the spill, more volatile hydrocarbons are expected to evaporate in high rates than less volatile hydrocarbons evaporate slowly. Therefore, the JP-8 evaporation rate is expected to decrease eventually.

5.4.2. Tkalin's Evaporation Model

In Tkalin's evaporation model, the evaporation rate is dependent on mass transfer constant, molecular weight, vapor pressure, the amount of component and temperature. Tkalin's mass transfer approach results in sensible values. On the contrary, Tkalin's model for evaporation rate yields very high results for the JP-8 spill. Additionally, the molecular weight of kerosene is considered similar to dodecane however JP-8 consists of several hydrocarbon components. This weakness of the model causes the model to yield very high evaporation rates. Additionally, Tkalin's model gives a constant evaporation rate for the JP-8 spill. Though, the JP-8 evaporation rate is expected to decrease as time increases. Thus, Tkalin's evaporation model is not appropriate for JP-8 spill evaporation modelling.

5.4.3. Brighton's Evaporation Model

In Brighton's evaporation model, the evaporation rate depends on mass transfer constant, saturated vapor concentration at pool surface, wind velocity and pool diameter. Mass transfer constant is calculated by Tkalin's equation. Saturated vapor concentration is dependent on the molecular weight and saturated vapor pressure of kerosene. Saturated vapor pressure, which is determined by Jenkin's model, is

proportional to the heat of vaporization. In this current work, assumed molecular weight and heat of vaporization values of JP-8 can be different in practice since JP-8 consists of many different compounds. In addition, Brighton's model yields a constant evaporation rate which is not desired for oil evaporation modelling. These assumptions can be seen as the handicaps of Brighton's evaporation model. Thus, Brighton's evaporation model is not appropriate for JP-8 spill evaporation modelling.

5.4.4. Evaporation Modelling with Empirical Equation

In the empirical equation model, the evaporation rate is dependent on temperature and time. According to the empirical evaporation equation, until the end of cleaning up of JP-8 spill 40,7820% of the total amount of spillage evaporated which equals an amount of 1.879,2345 kg. Evaporation rate decreases logarithmically and the highest evaporation rate is obtained as 2,0074 kg/s in the third minute after the spill.

In reality, it is expected for the evaporation rate of JP-8 spill to decrease as time elapses since more volatile hydrocarbons evaporate first and less volatile hydrocarbons evaporate more slowly. Thus, the result of the empirical equation model is realistic. However, in evaporation calculation, diesel long term empirical equation is chosen. This assumption can be seen as a drawback for the model. It would be more accurate to determine specific empirical equation for JP-8 evaporation calculation. Additionally, emission rate is constant in vapor dispersion modelling. Therefore, a constant evaporation rate is needed to be used in dispersion model. Percentage evaporated and evaporation rate versus time graphs according to the empirical equation model is given in Figure 5.8 and Figure 5.9 respectively.

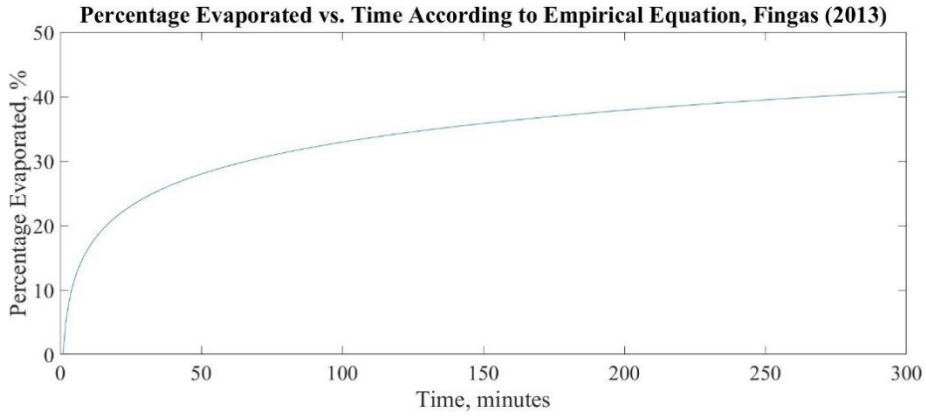

Figure 5.8. Percentage Evaporated vs. Time According to Empirical Equation

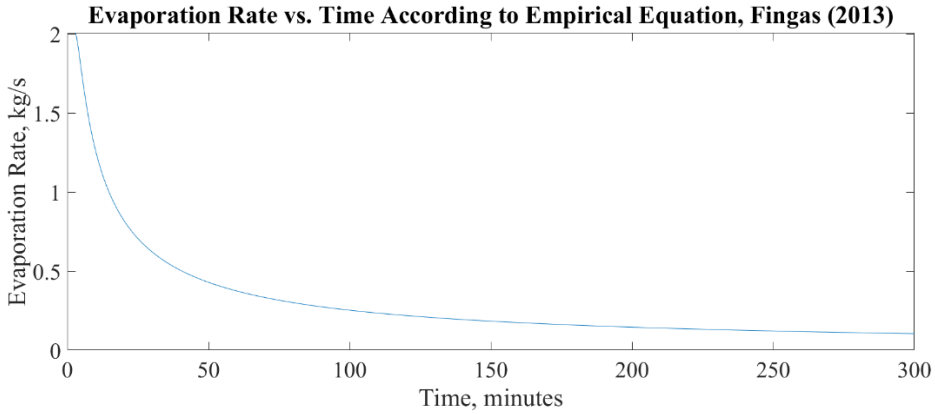

Figure 5.9. Evaporation Rate vs. Time According to Empirical Equation

According to the empirical evaporation model, evaporation percentage and evaporation rate of JP-8 spill at various minutes are given in Table 5.4.

Table 5.4. *Percentage Evaporated and Evaporation Rate at Various Time After Spill*

t (minutes)	Percentage Evaporated %	Evaporation Rate kg/s
2	4,9560	1,8998
3	7,8551	2,0074
4	9,9120	1,8998
8	14,8680	1,4249
17	20,2575	0,9136
22	22,1010	0,7702
33	25	0,5808

5.4.5. Mackay and Wesenbeeck Evaporation Model

Mackay and Wesenbeeck purposed an evaporation rate equation for dodecane as:

$$E = 474 \times P \times M \tag{64}$$

In equation (64), E is the evaporation rate in μg/m^{2}s, vapor pressure, P, is in Pa and molar weight is in g/mol. The molecular weight of dodecane is 170 g/mol and vapor pressure is 18,9763 Pa at 30 °C.

In Mackay and Wesenbeeck model, evaporation is correspondent to the molecular weight and vapor pressure of dodecane. The vapor pressure of dodecane is calculated by the Clausius-Clapeyron equation of Jenkins (2008). Saturated vapor pressure, which is determined by Jenkin's model, is proportional to the heat of vaporization. In this study, the assumed molecular weight of dodecane and heat of vaporization values can be a different value than JP-8 since JP-8 consists of several compounds. In addition, Mackay and Wesenbeeck model yields a constant evaporation rate which is the lowest value for oil evaporation modelling. These assumptions are the negative side of the Mackay and Wesenbeeck model.

In literature, there are oil evaporation models concerning about oil spills at sea and on soil. Wind has an mixing effect on oil spills at sea. On the other hand, in case of oil spill on soil, oil is absorbed by soil. These cases have an effect on evaporation rate of oil spill. However, these situations are not the concern for this current study.

Tkalin proposed an evaporation model for oil spills at sea. Oil spills at sea forms a thin layer on sea surface. In Tkalin's model, evaporation rate is correspondent to spill amount. Therefore, all oil spill is subject to evaporation process. Yet, it is not the case for oil spill accident in this study. In empirical equation model, evaporation rate decreases logarithmically with time. However, in dispersion model it is needed to use a constant evaporation rate. In Brighton model, evaporation rate calculation is derived from the water evaporation model. In water evaporation, characteristics of the air layer above the water surface has an effect on evaporation rate. Though, in oil evaporation, evaporation rate is not affected by air boundary layer. Oil has different evaporation mechanism from water. In Stiver and Mackay's model, evaporation rate of oil is dependent to vapor pressure. On the other hand, in Mackay and Wesenbeeck' evaporation model, evaporation rate is correspondent to vapor pressure and molecular weight but not only vapor pressure. This approach increases the prediction accuracy for evaporation rate of the spilled substance.

In vapor dispersion modelling, Mackay and Wesenbeeck equation method is used to calculate vapor concentrations as emission rate since it is considered as the best suitable, easiest and most accurate approach.

5.5. Results and Discussions for Dispersion Modelling

In dispersion modelling, it is important to determine horizontal dispersion coefficient, σ_y, and vertical dispersion coefficient, σ_z, according to downwind distance. Two different methodology is used for dispersion coefficient determination. Results of two methodologies are compared. After that, JP-8 vapor concentration dispersion is calculated by using the Gaussian dispersion model.

5.5.1. Determination of σ_y and σ_z According to Pasquill's Atmospheric Stability Classes Method

In consideration of the information given in Table 4.1, insolation is slight and the wind velocity is 5 m/s, atmospheric stability class is determined from Table 5.5 as D.

Table 5.5. *Key to Stability Categories*

Surface wind speed (at 10 m) m/sec	Insolation			Night	
	Strong	Moderate	**Slight**	Thinly overcast or ≥4/8 low cloud	≤3/8 cloud
<2	A	A-B	B	-	-
2-3	A-B	B	C	E	F
3-5	B	B-C	C	D	E
5-6	C	C-D	**D**	D	D
>6	C	D	D	D	E

For comparison of two methodologies, dispersion coefficients at the 100 m 200 m 300 m 400 m and 500 m of distance away from the source is calculated. According to Pasquill's method horizontal and vertical dispersion coefficients are determined from Figures 5.10 and 5.11 respectively.

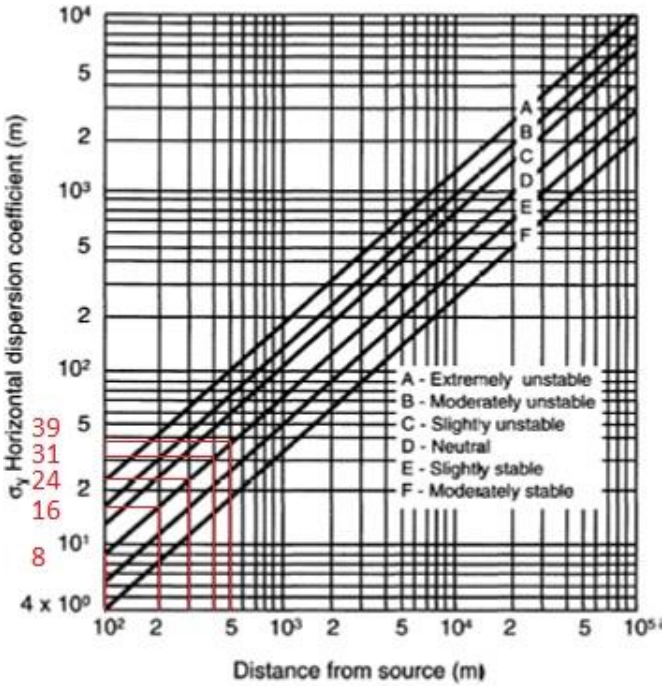

Figure 5.10. Horizontal dispersion coefficient, σ_y , vs. Downwind distance, x (Godish, 2004).

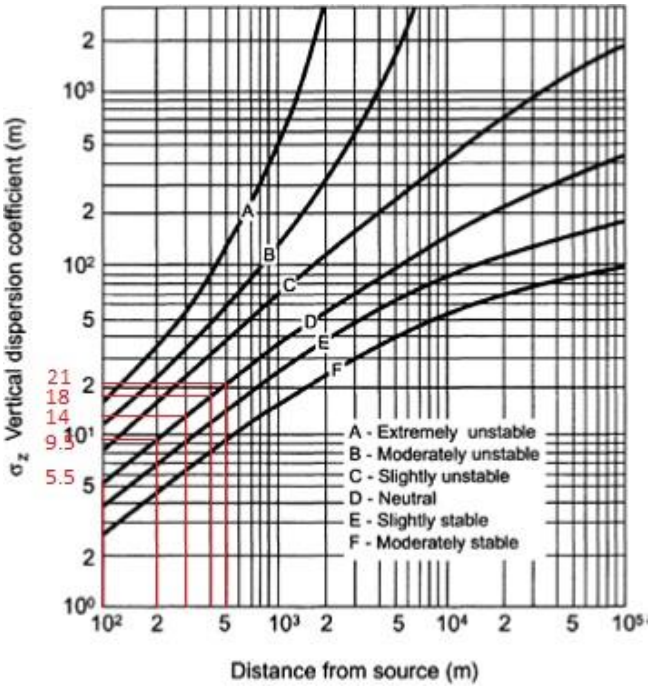

Figure 5.11. Vertical dispersion coefficient, σ_z , vs. Downwind distance, x (Godish, 2004).

According to Pasquill's dispersion coefficient estimation model, σ_y and σ_z, is determined as in Table 5.6 given below:

Table 5.6. *σ_y and σ_z Values According to Pasquill's Model.*

Downwind Distance, x (m)	σ_y (m)	σ_z (m)
100	8	5.5
200	16	9.5
300	24	14
400	31	18
500	39	21

In Pasquill's model, σ_y and σ_z values are determined by just looking at the graphs and selected manually. This approach can lead to some accuracy errors in the determination of dispersion coefficients.

5.5.2. Calculation of σ_y and σ_z According to Briggs Formulation

The stability class is determined as D and the terrain is rural. Therefore, experimental coefficients of Briggs formula, a, b, c, d, e and f can be determined from Table 5.7 as 0.08, 0.0001, 0.5, 0.06, 0.0015 and 0.5 respectively.

Table 5.7. *Experimental coefficients determined by Briggs*

Rural						
	σ_y			σ_z		
Stability Class	a	b	c	d	e	f
A	0.22	0.0001	0.5	0.2	0	-
B	0.16	0.0001	0.5	0.12	0	-
C	0.11	0.0001	0.5	0.08	0.0002	0.5
D	**0.08**	**0.0001**	**0.5**	**0.06**	**0.0015**	**0.5**
E	0.06	0.0001	0.5	0.03	0.0003	1
F	0.04	0.0001	0.5	0.016	0.0003	1
Urban						
	σ_y			σ_z		
Stability Class	a	b	c	d	e	f
A-B	0.32	0.0004	0.5	0.24	0.0001	- 0.5
C	0.22	0.0004	0.5	0.2	0	-
D	0.16	0.0004	0.5	0.14	0.0003	0.5
E-F	0.11	0.0004	0.5	0.08	0.0015	0.5

According to Briggs dispersion coefficient formula, σ_y and σ_z, is determined as in Table 5.8 given below.

Table 5.8. *σ_y and σ_z Values According to Briggs Formula*

Downwind Distance, x (m)	σ_y (m)	σ_z (m)
100	7.9603	5.5950
200	15.8424	10.5247
300	23.6479	14.9482
400	31.3786	18.9737
500	39.0360	22.6779

The comparison of the σ_y and σ_z values obtained from Paquill's and Briggs' model are given in Table 5.9.

Table 5.9. *Comparison of σ_y and σ_z Values According to Briggs Formula and Pasquill's Method*

Downwind Distance, x (m)	σ_y (m)		σ_z (m)	
	Briggs	Pasquill	Briggs	Pasquill's
100	7.9603	8	5.5950	5.5
200	15.8424	16	10.5247	9.5
300	23.6479	24	14.9482	14
400	31.3786	31	18.9737	18
500	39.0360	39	22.6779	21

According to Table 5.9, it can be seen that Pasquill and Briggs' models result in close values for σ_y and σ_z. Therefore, both approaches can be used in oil vapor dispersion models.

5.5.3. Application of Gaussian Dispersion Model

In dispersion modelling, emission source is assumed as ground level point source. Gaussian Dispersion modelling is conducted by gaussianPlume MATLAB code which is provided by Bien (2009).

In the Gaussian dispersion model, the distribution of JP-8 vapor concentration is correspondent to emission rate, wind velocity, horizontal and vertical dispersion coefficients. JP-8 vapors are dispersed through prevailing wind direction and diluted as carried away from the source. The concentration distribution of JP-8 vapors is Gaussian in the horizontal and vertical axis.

In order to determine the concentration levels of JP-8 vapors in the spill area, the evaporation rate of the JP8 spill is taken as the emission rate in the dispersion modeling. According to dispersion modeling, contour plots of the vapor concentration of JP-8 regarding the spill accident scenario are given in Figure 5.12.

According to Figure 5.12, the vapor concentration of the JP-8 spill exceeds 7000 ppm in a region of just below 0,4 meter height and up to 3 m downwind distance from the source. Additionally, the vapor concentration of JP8 exceeds 30 ppm, TLV-TWA value for kerosene, in a region of just below 2,6 meters height, up to 3,8 meters in both vertical sides and up to 55 m downwind distance from the source in the prevailing wind direction.

In Figure 5.12 it can be seen that flammable vapor concentration in the air reaches the lower explosive limit (LEL) which is 0,7% by volume, 7000 ppm, in the air for kerosene. Therefore, the explosive zone is formed and can be ignited by any kind of ignition source. On the other hand, kerosene concentration exceeds the TLV-TWA value of 30 ppm for a distance of 55 m from the spill in the wind direction. Also, vapor concentration is well above the odor threshold of kerosene, 0.1 ppm, until 100 meters away from the spill in the wind direction.

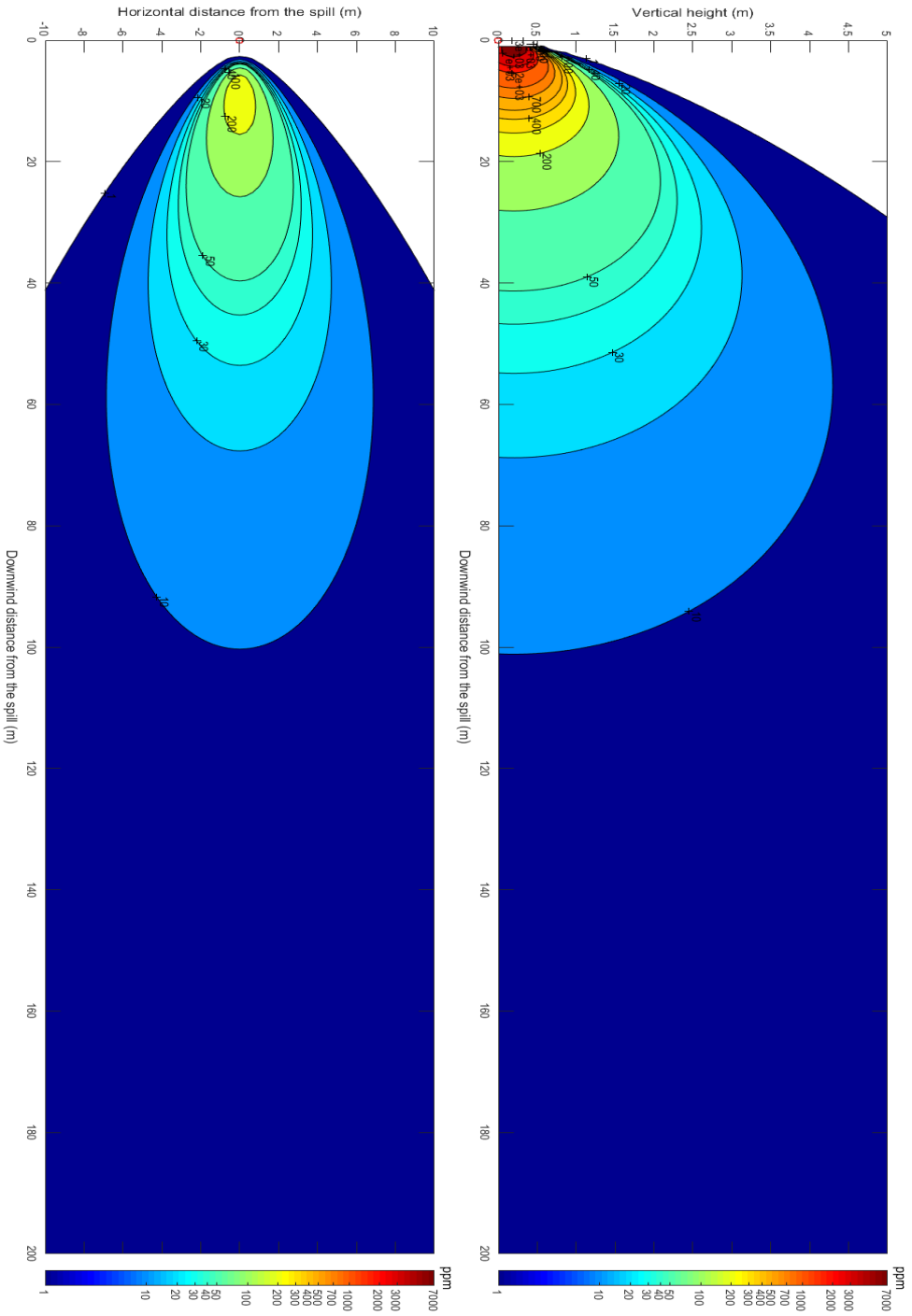

Figure 5.12. JP-8 Vapor Concentration vs. Downwind Distance

5.6. The Effect of Amount of Spill and Spillage Area

In Mackay and Wesenbeeck model, the evaporation rate is given as units of $\mu g/m^2 s$. Therefore, the spillage area has an effect on the evaporation rate. According to Mackay and Wesenbeeck evaporation equation, evaporation rate raises as the area of spill increases.

In the empirical equation, the evaporation rate is correspondent to temperature and time. Therefore, the amount of spill and spillage area has no effect on the dispersion of the vapor concentration of the JP-8 spill.

Additionally, in the Brighton model, the evaporation rate is correspondent to pool diameter. As pool diameter increases evaporation rate also increases. On the other hand, in Stiver and Mackay model, the evaporation rate is in direct correlation with the amount of spilled fuel and the spillage area.

Furthermore, in Tkalin's model, the evaporation rate is dependent on the amount of spill. As the amount of spill increases evaporation rate also increases. Accordingly, higher evaporation rates result in higher JP-8 vapor concentration in the ambient air.

In case of constant spill area, such as spill into secondary containment pool, the amount of spillage does not affect the evaporation rate. On the contrary, in the case of open ground spillage, the spillage area is dependent on various factors such as the shape of the surrounding terrain and the amount of spill. On flat terrain, a bigger amount of spill causes liquid material to spread wider area so spill area increases as the amount of spill increases. In this study, the spillage area is constant and the amount of spill has no effect on the spillage area because of the secondary containment pool.

5.7. The Effect of Temperature

Temperature is an important parameter in evaporation calculation. In the empirical equation model, the evaporation rate is directly proportional to temperature. According to the empirical equation, in high temperatures, the percentage of

evaporation of the liquid substance will be higher. As a result, as temperature increases, the evaporation rate also increases.

Mackay and Wesenbeeck evaporation model is directly proportional to vapor pressure. The vapor pressure of a substance is dependent on temperature. As temperature increases, vapor pressure also increases. Therefore, temperature has an important effect on the vapor concentration of JP-8.

In dispersion modelling, the evaporation rate is taken as the emission rate of JP-8 vapors from the spillage. According to the Gaussian dispersion model, the vapor concentration of JP-8 is directly proportional to the emission rate of vapors from the spill. As a result, JP-8 vapor concentration in the air also increases as temperature increases.

In order to see the effect of temperature on JP-8 vapors dispersion, dispersion model is carried out at 10 °C and 40 °C ambient temperature. Results of JP-8 vapor dispersion model for 10 °C and 40 °C is given in Figure 5.13 and Figure 5.14 respectively.

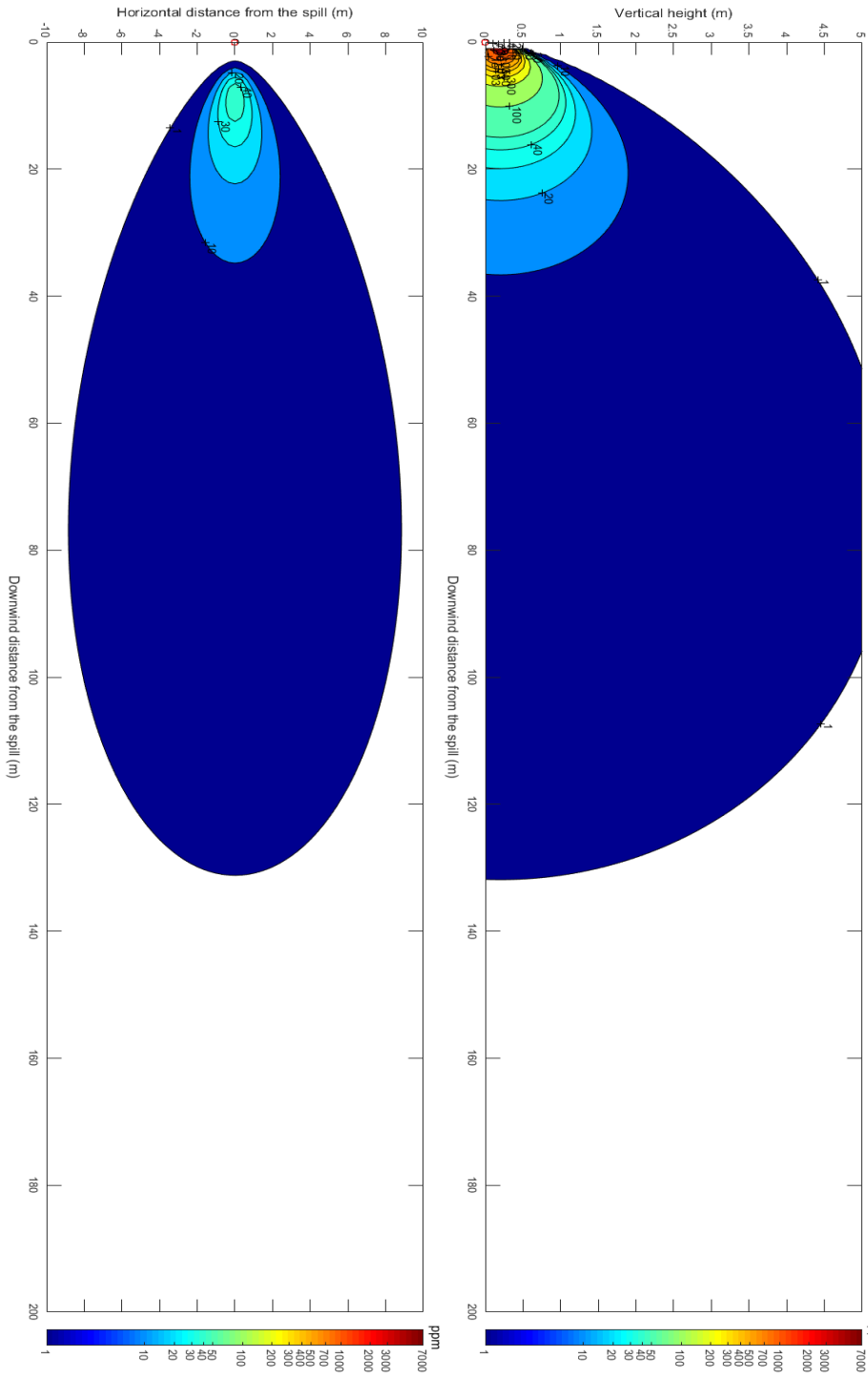

Figure 5.13. Vapor Concentration vs. Downwind Distance at 10 °C Temperature

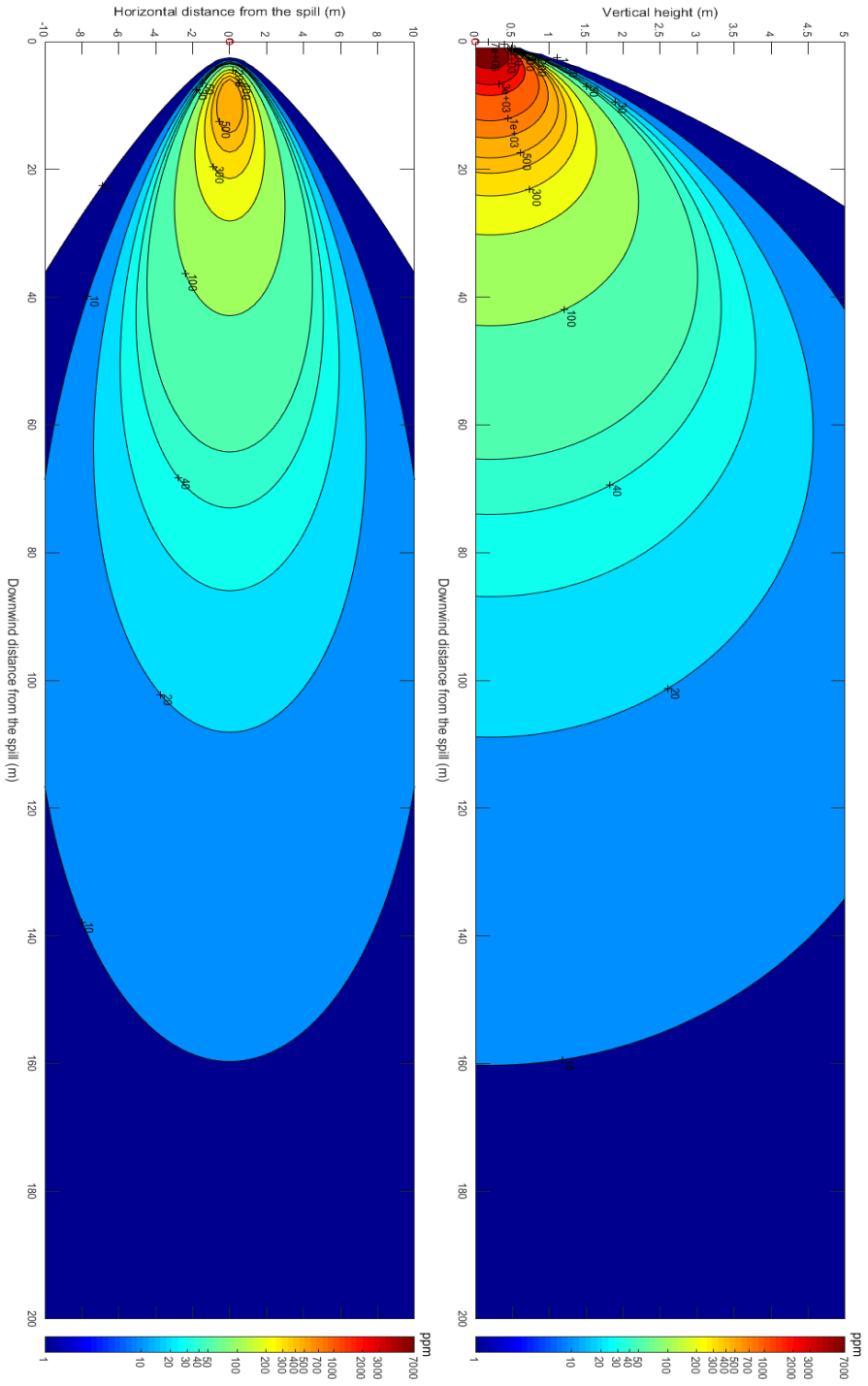

Figure 5.14. Vapor Concentration vs. Downwind Distance at 40 °C Temperature

5.8. The Effect of Wind Speed in The Open Air

In the empirical equation model, the wind has no effect on the evaporation rate. However, in Tkalin's model, wind speed is used for mass transfer constant calculation. According to Tkalin's model, mass transfer constant increases with higher wind speed values.

In Stiver and Mackay evaporation model, the evaporation rate is directly proportional to mass transfer constant. In Stiver and Mackay model, mass transfer constant is calculated according to Tkalin's model. Since mass transfer constant is directly proportional to wind velocity, an increase in mass transfer constant results in an increased evaporation rate. On the contrary, in Mackay and Wesenbeeck evaporation model, evaporation rate is independent of wind speed.

In dispersion modelling, as wind speed increases the JP-8 vapors disperse to more distant location which causes lower values in concentration. On the other hand, in low wind speed conditions, JP-8 vapor concentration is not diluted and reaches up to very high concentration. Therefore, wind speed has a major effect on vapor concentrations in dispersion modelling. Figures 5.15 and 5.16 show the vapor concentrations distribution in downwind distance at 0.5 m/s and 6 m/s respectively.

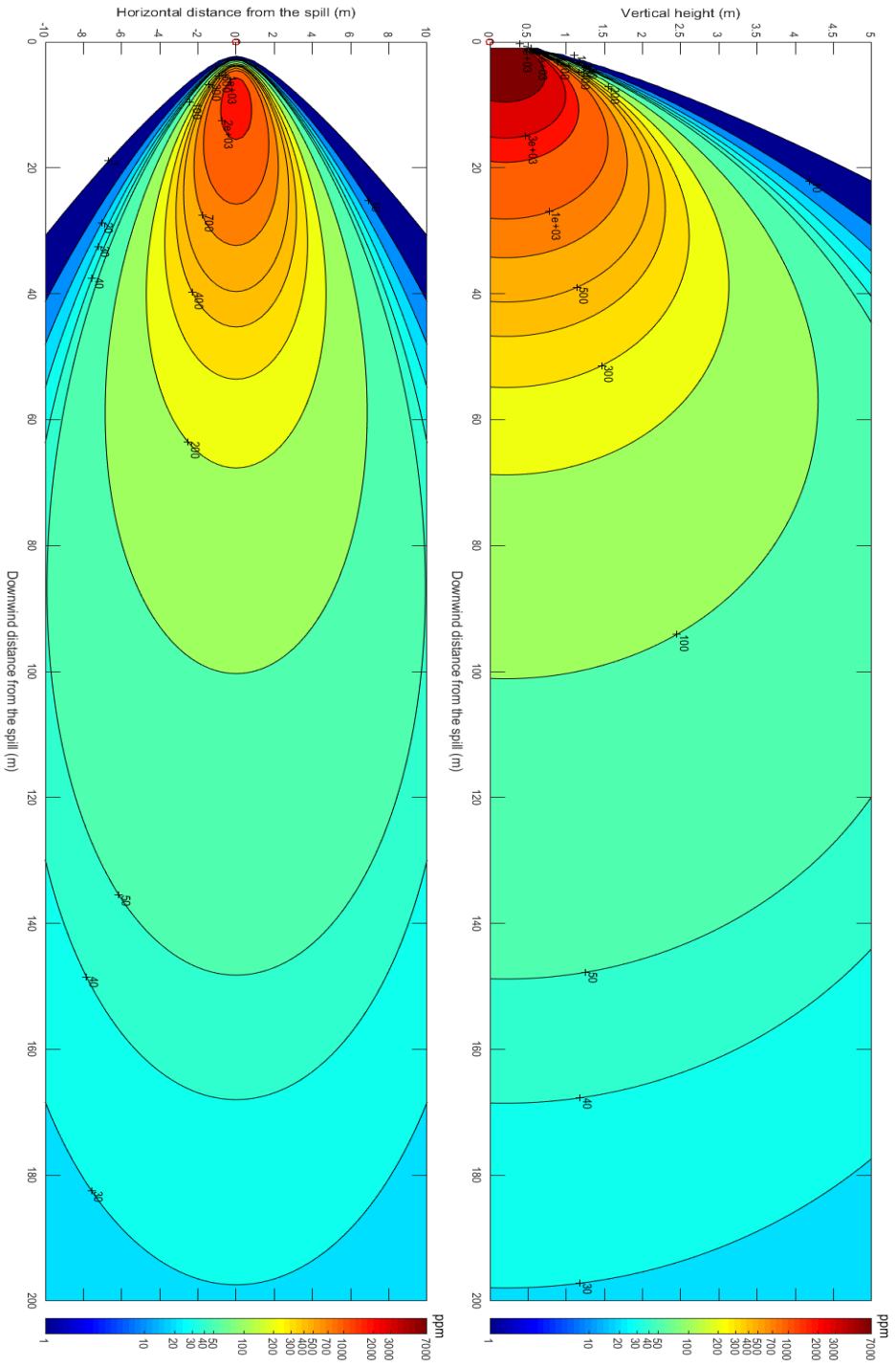

Figure 5.15. Vapor Concentration vs. Downwind Distance at 0.5 m/s Wind Speed

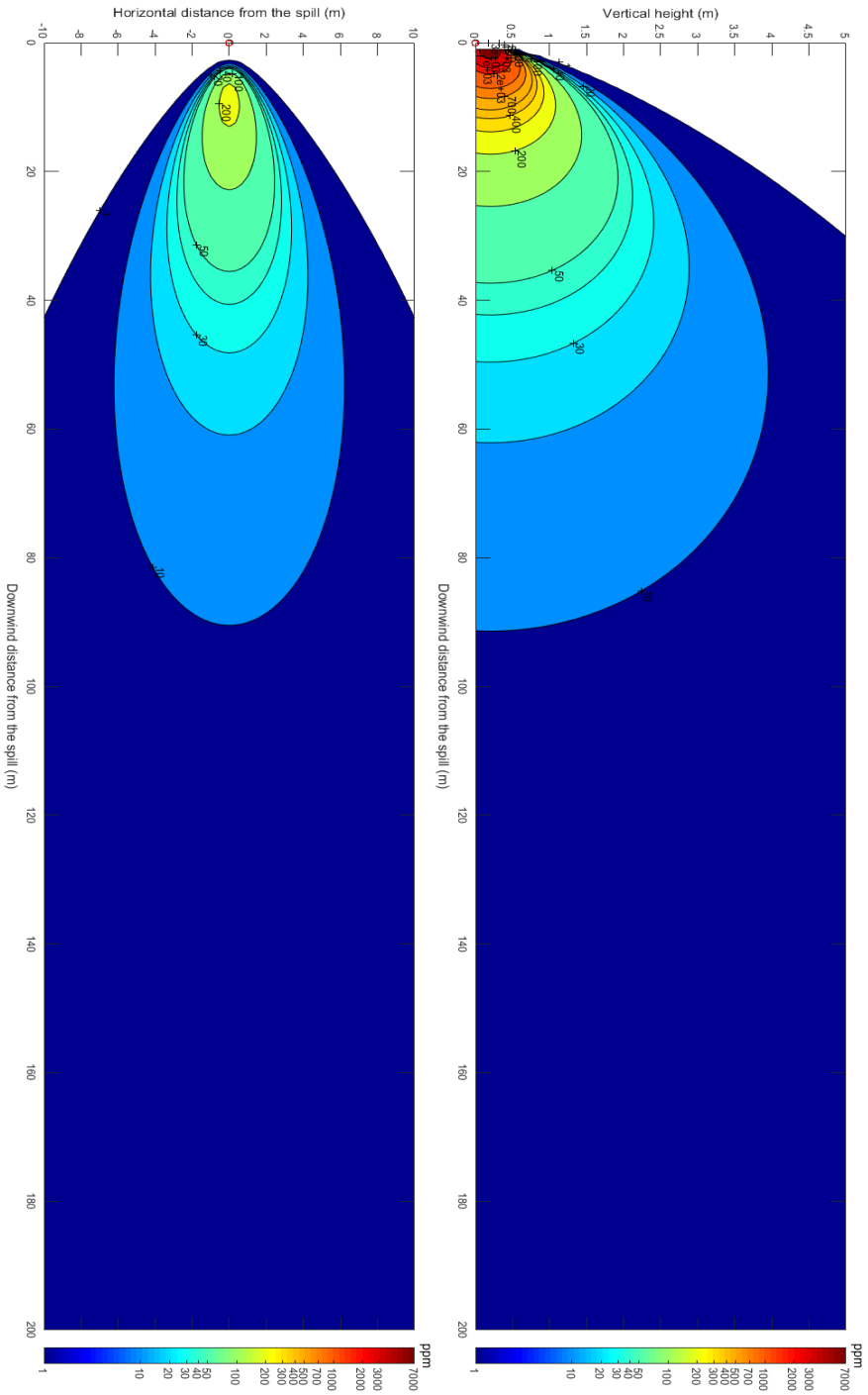

Figure 5.16. Vapor Concentration vs. Downwind Distance at 6 m/s Wind Speed

5.9. The Effect of Atmospheric Stability Class

The stability of weather increases from A class to F class. The most unstable weather condition is A class, on the other hand, the most stable weather condition is F class. In the Gaussian dispersion model, vapor concentrations are reversely proportional to dispersion coefficients in both vertical and horizontal directions. In the unstable weather condition, the JP-8 vapors disperse more in both vertical and horizontal direction which causes lower vapor concentration. In contrast, in stable weather conditions, dispersion will be lowered and concentation of JP-8 vapor is observed in higher values.

5.10. The Effect of Land Characteristic

Land characteristic has an important effect on the dispersion of chemical vapors. Structures on terrain can cause alteration in wind pattern which results in a change in atmospheric stability.

As building height increases, wind moves upward direction causing an increase in dispersion of JP-8 vapors. Therefore, in urban terrain, the vapor concentration of JP-8 will be at lower levels.

5.11. Model Accuracy and Limitations

In this current thesis, two main models are used for the dispersion modelling of JP-8 vapors. Firstly, the evaporation rate of JP-8 is determined then the dispersion of JP-8 vapors is calculated.

In evaporation modelling, the vapor pressure of JP-8 is calculated according to a single component liquid evaporation. However, in reality, JP-8 consists of many different components. As the more volatile material evaporates first, the liquid composition will change with time. As a result, the rate of evaporation will fall as evaporation proceeds.

Still, in this work, the evaporation rate is assumed as constant for four evaporation models.

In mass transfer constant calculation according to Tkalin' model, wind speed is considered as constant. However, wind speed can vary during the evaporation process which causes evaporation rate to fluctuate.

Additionally, the latent heat of vaporization varies with temperature. However, in this study, the heat of vaporizations is taken as the value obtained from the kerosene boiling point at 1 atm.

Furthermore, in this current study, it is assumed that there is no heat transfer occurs between the oil, atmosphere and ground. Since oil temperature determines the vapor pressure of kerosene, the evaporation rate of JP-8 will also be affected. In order to obtain accurate evaporation modelling, it is very important to take heat transfer into consideration.

In this current work, it is also assumed that the atmospheric turbulence is stationary and homogeneous. Wind speed and direction are taken as constant during dispersion. However, this assumption is not possible in practice. Atmospheric turbulence, wind speed and direction change continuously which makes impossible to obtain accurate dispersion prediction.

CHAPTER 6

CONCLUSION

Evaporation and dispersion modelling of oil spills is a very challenging subject. There are many different models with some pros and cons. Every model can give different results depending on the chemical and physical conditions of the oil spill. So, there is no best model for evaporation and dispersion calculation of oil spillages. The most important point in evaporation and dispersion estimation is to choose the most suitable model according to the incident scenario. If appropriate evaporation and dispersion model is applied to the oil spills, the vapor concentration prediction can be done accurately. Otherwise, unrealistic modeling results can be encountered.

In mass transfer constant calculation, in contrast to Hamoda formula, Mackay and Tkalin approaches yield almost similar results. Hamoda formula for mass transfer constant calculation results in very low values compared to other models. Therefore, Mackay and Tkalin model for mass transfer calculation is suitable for oil spill evaporation modeling. Especially, Tkalin formulation for mass transfer constant is very easy to apply if wind speed is known.

For vapor pressure calculation, four different vapor pressure calculation method is applied to the spill of JP-8. Blokker, Fingas and Jenkins models are based on the Clausius-Clapeyron equation expect from Tkalin's model. Tkalin' model for vapor pressure calculation yields very low values. Therefore, Tkalin's model is not suitable for vapor pressure calculation in JP-8 spill evaporation modelling. On the other hand, Blokker, Fingas and Jenkins models yield more realistic results. Blokker model gives the highest value for vapor pressure, then Fingas and Jenkins models come respectively. Since it is widely used and easy to apply, the Jenkins model is preferable for vapor calculation in JP-8 spill evaporation modelling.

In evaporation modelling, Stiver and Mackay, Brighton, Tkalin, empirical model and Mackay and Wesenbeeck model are used. Tkalin's model results in very high values so it is not applicable for JP-8 spill evaporation modelling. In contrast, Stiver and Mackay, Brighton and empirical models yield acceptable evaporation rates. Brighton model gives the highest evaporation rate for JP-8 evaporation, then Stiver and Mackay and empirical method come respectively. The empirical equation gives logarithmic curvature for the evaporation rate. However, in dispersion modelling, the emission rate is needed to be constant. Since Mackay and Wesenbeeck model is easy to apply and has higher accuracy, it is superior for evaporation modelling of JP-8 spill.

For vapor dispersion calculation, the Gaussian dispersion model is used. In the Gaussian dispersion model, vapor concentrations have Gaussian distribution along the horizontal and vertical axis. By using the Gaussian dispersion model, the variation of vapor concentration from the maximum value to minimum value can be drawn as contour plots. Also, the vapor concentration of the JP-8 spill can be specified at a particular point in the downwind and crosswind position at a given time. According to the Gaussian dispersion model, the highest vapor concentration is obtained in the centerline of downwind direction where y is equal to zero.

According to JP-8 spill dispersion modelling, in the horizontal axis, the highest vapor concentration reaches 200 ppm at a distance of 2 meters for both sides. Additionally, the risk for the toxic health effect of JP-8 appears until 55 meters away from the spill in the wind direction. After 55 meters away from the spillage, vapor concentrations drop below 30 ppm which is TLV-TWA for kerosene. In the vertical axis over the spill point, vapor concentrations exceed 7000 ppm which is LEL for kerosene. Consequently, an explosion can occur in the presence of an ignition source in the explosive zone. Furthermore, vapor concentration is well above the odor threshold of kerosene, 0.1 ppm, more than 100 meters away from the spill in the wind direction.

In conclusion, the Gaussian dispersion model can be useful for determining the risk level and possible outcomes of oil spill accidents. It is helpful to establish safe

operations in the aviation sector by clarifying the extent of hazards, understanding the level of the risk of spill accidents. Additionally, it helps to predict the range of explosive zone. Furthermore, evacuation zones can be declared in emergency response plans for immediate evacuation during the spill accident. Therefore, by this current study, ways of fast and efficient response to the oil spills can be determined and adverse health effects of an oil spill to the public can be minimized in the aviation sector.

CHAPTER 7

RECOMMENDATION

The main objective of the present work is to estimate the possible safety risks of the JP-8 spill in the aviation sector. In order to evaluate possible outcomes of JP-8 spill accident, evaporation and dispersion models are used. By using these models, the area affected by the spill is revealed and the level of adverse effects is determined. However, the models which are used in this current work have several limitations and assumptions. The accuracy of evaporation and dispersion models can be decreased by model limitations and assumptions.

In evaporation modelling, JP-8 is assumed as a pure substance which consists of kerosene. Additionally, kerosene is assumed to have some similar molecular properties with dodecane. In the evaporation rate calculation, the empirical evaporation equation of dodecane is used. These assumptions lower the accuracy of evaporation modeling. It is well-known that JP-8 contains many different chemicals with different chemical and physical properties. In future studies, for obtaining more accurate evaporation modelling results, the evaporation equation for JP-8 can be determined empirically.

There are various different evaporation and dispersion models. Different models should be applied to model dispersion of the JP-8 spill. So, the results of different models can be compared and the most suitable approach can be decided more accurately.

Evaporation and dispersion models requires a lot of data input and include complex numbers for calculation. It can be useful to use computer programs for easily predicting the concentration of chemical vapors emitted from the spill accident. So

that, important information can be obtained for the emergency response team for understanding the level of the hazard and for clarifying the evacuation zone.

In the aviation industry, lots of chemicals are used in production and flight lines in huge amounts. Because of this reason, similar modelling studies should be conducted for other hazardous chemicals for assessment of safety risks and for determining safety measures.

Spill accidents can happen in different climate conditions. Evaporation and dispersion modelling should be conducted for different atmospheric conditions. Therefore, the emergency response plan can be determined according to the worst-case scenario.

According to the dispersion model, within the area of 55 m radius from the oil spill, buildings involving employees are needed to be evacuated immediately and entrance to the spill area should be forbidden after the spill. TLV-TWA of kerosene is 30 ppm and exposures above the TLV-TWA should not be allowed more than 15 minutes otherwise adverse health effects can be observed.

In order to conduct safe fueling operations, safety instructions should be declared to the operators. Necessary training should be given to operators. Operators without training and knowledge should not be allowed to work at fueling stations. Operators should be provided a dead man control unit in order to stop fueling operation in case of emergency. Warning sign for explosive zone and static grounding should be present at the station. Emergency phone numbers should be known by the operators and the emergency call numbers should be hanged in the fuel station. Emergency response plans should be documented and declared to operators. The emergency response team should be determined, roles and responsibilities should be declared to team members. Evacuation drills should be conducted regularly in the buildings close to the fueling station.

During the fueling operations, access to the fueling areas should be limited. The fire department should be noticed before the fueling operations and should be present at the station during fueling. Fire extinguishers should be provided to the fuel station in

enough numbers. Fire alarm and smoke detection systems should be installed to fuel station. For early response, hydrocarbon sensors detecting vapor concentrations can be also installed to the fueling station. Also, installation of automatic blockage valves for shutting the system down in case of system failure can prevent leakage.

The area where spill can occur and explosive zone can be formed, should be colored to attract the attention of operators. In this zone, access to ignition sources should be forbidden. In order to discharge static electricity, grounding plates should be replaced at the fueling station. The outwear of operators should be made of antistatic material to prevent static charging in the explosive zone. During fueling operation, aircraft and fuel tanks should be connected and grounded.

REFERENCES

Abdel-Rahman, A. A. (2008). On the atmospheric dispersion and Gaussian plume model. Proceedings of the 2nd International Conference on Waste Management, Water Pollution, Air Pollution, Indoor Climate, pp. 31-39.

ACGIH (American Conference of Governmental Industrial Hygienists). (2015). 2015 TLVs and BEIs Based on the Documentation of the Threshold Limit Values for Chemical Substances and Physical Agents and Biological Exposure Indices. Cincinnati, OH: Signature Publications.

API (American Petroleum Institute). (2003). Ignition risk of hydrocarbon liquids and vapors by hot surfaces in the open air (3rd ed., p. 3). Washington: American Petroleum Institute.

Anfossi, D. and W. Physick (2004). Lagrangian Particle Models. Air Quality Modeling – Theories, Methodologies, Computational Techniques, and Available Databases and Software. Vol. II – Advanced Topics. The EnviroComp Institute and the Air & Waste Management Association.

Artana, K. B., Pratiwi, E., Dinariyana, B., Pitana, T., Masroeri, A. A., Ariana, M., Arifin, M. D. (2014). Enhancement on Methodology for Estimating Emission Distribution at Madura Strait by Integrating Automatic Identification System (AIS) And Geographic Identification System (GIS), Proceedings of the 3rd International Symposium of Maritime Sciences. Nov. 10-14, 2014, Kobe, Japan.

Baker, Q.A. et al. (2010). Guidelines for vapor cloud explosion, pressure vessel burst, BLEVE, and flash fire hazards (2nd ed., p. 54). Hoboken, N.J: Wiley.

Beychok, M. R. (2005). Fundamentals of stack gas dispersion. Newport Beach, CA.

Bien, H. (2009). gaussianPlume [MATLAB Code]. Retrieved from https://www.mathworks.com/matlabcentral/fileexchange/13279-gaussianplume?s_tid=srchtitle

Bobra, M. (1992). A study of the evaporation of petroleum oils. Environment Canada, Environmental Protection Directorate, River Road Environmental Technology Centre.

Boubel, R. W., Vallero, D., Fox, D. L., Turner, B., & Stern, A. C. (1994). Fundamentals of air pollution. San Diego: Elsevier.

Brandt, J., Silver, J.D., Christensen, J.H., Andersen, M.S., Bønløkke, J.H., Sigsgaard, T., Geels, C., Hansen, K.M., Kaas, E. and Frohn, L.M. (2014). Air Quality Effects on Human Health. Air Pollution Modeling and its Application XXIII, pp. 7-15

Briggs G.A. (1973). Diffusion Estimation of Small Emissions. Contribution No. 79, Atmospheric Turbulence and Diffusion Laboratory, Oak Ridge, TN.

Brighton, P. W. M. (1985). Evaporation from a plane liquid surface into a turbulent boundary layer. Journal of Fluid Mechanics, 159(-1), 323.

Brighton, P. W. M. (1990). Further verification of a theory for mass and heat transfer from evaporating pools. Journal of Hazardous Materials, 23(2), 215–234.

British Standards Institution (2008). Explosive atmospheres - Explosion prevention and protection. London, U.K..

BP Process Safety Series (2006) - Hazards of Electricity and Static Electricity (6th Edition). Institution of Chemical Engineers. Retrieved from https://app.knovel.com/hotlink/toc/id:kpBPPSSHEI/bp-process-safety-series-2/bp-process-safety-series-2

Chapman, H. (2017). "Performance Test of the Pasquill Stability Classification Scheme". University of Wisconsin-Milwaukee. Retrieved from http://dc.uwm.edu/etd/1453

Chickos, J.S. and Hanshaw, W. (2004). Vapor Pressures and Vaporization Enthalpies of the n-Alkanes from C31 to C38 at T= 298.15 K by Correlation Gas Chromatography. Journal of Chemical & Engineering Data, 49(3), 620-630.

Cooper, C.D. and Alley, F.C. (2011). Air Pollution Control, 4th ed., Long Grove: Waveland Press.

Crowl, D. A. and Louvar, J. F. (2011). Chemical Process Safety Fundamentals with Applications. 3rd ed. Upper Saddle River, NJ: Prentice Hall.

De Visscher, A. (2014). AIR DISPERSION MODELING Foundations and Applications. Hoboken, New Jersey: John Wiley & Sons, Inc.

Deaves, D.M., Dense gas dispersion modelling. Journal of Loss Prevention in the Process Industries Volume 5, Issue 4, 1992, Pages 219-227.

Drivas, P.J., "Calculation of Evaporative Emissions from Multicomponent Liquid Spills", Environmental Science and Technology, Vol. 16, pp. 726-728, 1982.

Environmental Protection Agency (EPA), (2002). Dense Gas Dispersion Model (DEGADIS). (2002, December 10). Retrieved January 14, 2019, from https://cfpub.epa.gov/si/si_public_record_Report.cfm?Lab=&dirEntryID=2904

Federal Aviation Administration (FAA), (2008). Aviation Maintenance Technician Handbook – General. Washington: U.S. Government Printing Office (GPO). Retrieved April 10, 2019, from https://www.faa.gov/regulations_policies/handbooks_manuals/aircraft/

Fingas, M.F. (1995). "A Literature Review of the Physics and Predictive Modelling of Oil Spill Evaporation", Journal of Hazardous Materials, Vol. 42, pp.157-175, 1995.

Fingas, M. (1996). The evaporation of oil spills: Prediction of equations using distillation data. Spill Science & Technology Bulletin, 3(4), 191–192.

Fingas, M.F. (1997). "Studies on the Evaporation of Crude Oil and Petroleum Products: I. The Relationship between Evaporation Rate and Time", Journal of Hazardous Materials, Vol. 56, pp. 227-236, 1997.

Fingas, M.F. (1998). “Studies on the evaporation of crude oil and petroleum products II. Boundary layer regulation”, Journal of Hazardous Materials, Volume 57, Issues 1–3, January 1998, Pages 41-58.

Fingas, M. F. (1999). The Evaporation of Oil Spills: Development and Implementation of New Prediction Methodology. International Oil Spill Conference Proceedings: March 1999, Vol. 1999, No. 1, pp. 281-287.

Fingas, M. F. (2001). The Basics of Oil Spill Cleanup. (2.nd ed., pp.) Boca Raton: Lewis Publishers.

Fingas, M. F. (2004). Modeling evaporation using models that are not boundary-layer regulated, Journal of Hazardous Materials, Volume 107, Issues 1–2, Pages 27-36.

Fingas, M. F. (2011a). Oil and Petroleum Evaporation. J. Pet. Sci. Res. 2. 426-459.

Fingas, M. F. (2011b). Oil Spill Science and Technology - Prevention, Response, and Cleanup. Burlington: Elsevier.

Fingas, M. F. (2013). “Modeling Oil and Petroleum Evaporation”, Journal of Petroleum Science Research (JPSR), Vol. 2, pp. 104-115, Issue 3, July 2013.

Ghassemi, H., Baek, S. W., & Khan, Q. S. (2006). Experimental Study On Evaporation Of Kerosene Droplets At Elevated Pressures And Temperatures. Combustion Science and Technology, 178(9), 1669–1684.

Godish, T. (2004). Air Quality. (4th ed., pp.78-79). Boca Raton: Lewis Publishers.

Goodwin, S. R., Mackay, D., & Shiu, W. Y. (1976). Characterization of the evaporation rates of complex hydrocarbon mixtures under environmental conditions. The Canadian Journal of Chemical Engineering, 54(4), 290–294.

Groh, H. (2004). Explosion protection (pp. 8-10). Amsterdam: Elsevier/Butterworth Heinemann.

Haghighi, E., E. Shahraeeni, P. Lehmann, and D. Or (2013), Evaporation rates across a convective air boundary layer are dominated by diffusion, Water Resour. Res., Volume49, Issue3, March 2013 Pages 1602-1610

Hamoda, M. F., Hamam, S. E. M., & Shaban, H. I. (1989). Volatilization of crude oil from saline water. Oil and Chemical Pollution, 5(5), 321–331.

Hanna, R. S., Briggs, G. A., Hosker, R. P. (1982). Handbook on Atmospheric Diffusion. U.S.: Technical Information Center, U.S. Department of Energy.

Harrop, O. D. (2002). Air Quality Assessment and Management - A Practical Guide. London: Spon Press.

Hattwig, M., & Steen, H. (2004). Handbook of Explosion Prevention and Protection (p. 5). Weinheim: Wiley-VCH.

Indra, E., Sinha, N., Ghose, M. K., Singh, G., Srivastava, S., Sinha, I., (2004). Classification of air pollution dispersion models: a critical review. Proceedings of the National Seminar on Environmental Engineering with special emphasis on Mining Environment. pp. 19-20.

Jenkins, H. D. B. (2008). Chemical Thermodynamics at a Glance. Oxford, England: Blackwell.

John Duffy Energy Services. (2006). Material Safety Data Sheet (MSDS) - Kerosene 1-K Dyed. Retrieved from http://duffyenergy.com/dev-site-duffyenergy-2015/wp-content/uploads/2015/07/Kerosene-MSDS.pdf

Lim, S. S., Vos, T., Flaxman, A. D., Danaei, G., Shibuya, K., Adair-Rohani, H., & Aryee, M. (2012). A comparative risk assessment of burden of disease and injury attributable to 67 risk factors and risk factor clusters in 21 regions, 1990–2010: a systematic analysis for the Global Burden of Disease Study 2010. The Lancet, 380(9859), pp. 2224-2260.

Lin, J. C. (2012). Lagrangian Modeling of the Atmosphere: An Introduction. Washington, DC: Geopress

Lüttgens, G., Lüttgens S. and Schubert W. (2017). Static Electricity. Weinheim, Germany: Wiley-VCH

Mackay, D. and Matsugu, R. S. (1973), Evaporation rates of liquid hydrocarbon spills on land and water. Can. J. Chem. Eng., 51: 434-439.

Mackay, D., & Wesenbeeck, I. V. (2014). Correlation of Chemical Evaporation Rate with Vapor Pressure. Environmental Science & Technology, 48(17), 10259–10263.

Mannan, S. (2014). Lees' process safety essentials (p. 218). Amsterdam: Elsevier, Butterworth-Heinemann.

Markiewicz, M. T. (2006). Modeling of the air pollution dispersion. MANHAZ monograph, models and techniques for health and environmental hazard assessment and management. pp.303-348

Martin, D. O. (1976). Comment on the change of concentration standard deviations with distance. Journal of the Air Pollution Control Association, 26:2, 145-147.

Monteith, J. L. and Unsworth, M. H., (2013) Principles of Environmental Physics Plants, Animals, and the Atmosphere, Fourth Edition (4th ed., p. 135). San Diego: Elsevier.

Moosemiller, M. (2014). Guidelines for determining the probability of ignition of a released flammable mass (p. 9). Hoboken, NJ: Wiley.

Namdeo, A., Sohel, I., Cairns, J., Bell, M., Khare, M., Nagendra, S., (2012). Performance evaluation of air quality dispersion models in Delhi, India. Urban Environment: Proceedings of the 10th Urban Environment Symposium, pp. 121-130

Nesaratnam, S. and Taherzadeh, S. (2014). Air Quality Management. Chichester: John Wiley & Sons Ltd.

Nolan, D. (2014). Handbook of Fire and Explosion Protection Engineering Principles, 3rd Edition (3rd ed., p. 441). Eastbourne: Elsevier Science and Technology Books, Inc.

National Fire Protection Association (NFPA), (2003a). Code for Motor Fuel Dispensing Facilities and Repair Garages (2003 ed.).

National Fire Protection Association (NFPA), (2003b). Flammable and Combustible Liquids Code (2003 ed.).

Pasquill, F. "The Estimation of the Dispersion of Windborne Material", Meteorological Magazine, Vol. 90, pp.33 – 49, 1961.

Purser, D. A., Maynard, R. L., Wakefield, J.C. (2016). Toxicology, Survival and Health Hazards of Combustion Products. Cambridge, UK: Royal Society of Chemistry

Reijnhart, R., & Rose, R. (1982). Evaporation of crude oil at sea. Water Research, 16(8), 1319–1325.

Quinn, M. F., Marron, K., Patel, B., Abu-Tabanja, R., & Al-Bahrani, H. (1990). Modelling of the ageing of crude oils. Oil and Chemical Pollution, 7(2), 119–128.

Roth, D., Sharma, P., Haeber, T., Schiessl, R., Bockhorn, H., & Maas, U. (2014). Ignition by Mechanical Sparks: Ignition of Hydrogen/Air Mixtures by Submillimeter-Sized Hot Particles. Combustion Science and Technology, 186(10-11), 1606-1617.

Russell, A., Holmes, H., Friberg, M., Ivey, C., Hu, Y., Balachandran, S., Mulholland, J., Tolbert, P., Sarnat, J., Sarnat, S., Strickland, M., Chang, H. and Liu, Y., (2014). Use of Air Quality Modeling Results in Health Effects Research. Air Pollution Modeling and its Application XXIII, pp. 1-4

Schaschke, C. (2014). Dictionary of Chemical Engineering. Oxford, U.K.: Oxford University Press.

Singh, K. (2018). Air pollution modelling. International Journal of Advance Research, Ideas and Innovations in Technology, 4(3), pp. 951-959.

Speight, J. G. (2011). Handbook of Industrial Hydrocarbon Processes. Burlington: Gulf Professional Publishing.

Speight, J. G. (2014). The Chemistry and Technology of Petroleum. 5th ed. Boca Raton: CRC Press.

Speight, J. G. (2017). Rules of Thumb for Petroleum Engineers. Hoboken: John Wiley & Sons.

Speight, J. G. and El-Gendy, N. S. (2018). Introduction to Petroleum Biotechnology. Cambridge: Gulf Professional Publishing.

Spellman, F. R. and Stoudt, M. L. (2013). Environmental Science: Principles and Practices. Lanham: Scarecrow Press, Inc.

Spicer, T. and Havens, J. (1989). User's Guide for the DEGADIS 2.1 Dense Gas Dispersion Model. North Carolina: EPA.

Sriram, G., Mohan, N. K., & Gopalasamy, V. (2006). Sensitivity study of Gaussian dispersion models. Journal of Scientific & Industrial Research Vol.65, pp. 321-324.

Stiver, W. and Mackay, D. (1984). "Evaporation Rate of Spills of Hydrocarbons and Petroleum Mixtures". Environmental Science and Technology, Vol. 18, pp. 834-840.

Sutherland, A. R. & Hansen, V. F. & Bach, D. W. (1986). A quantitative method for estimating Pasquill stability class from windspeed and sensible heat flux density. Boundary-Layer Meteorology, 37, pp.357-369.

Thermo Fisher Scientific. (2018). Safety Data Sheet (SDS) – n-Dodecane. Retrieved from https://www.fishersci.com/msdsproxy%3FproductName%3DO2666500%26productDescription%3DN-DODECANE%2BP%2B500ML%26catNo%3DO2666-500%2B%26vendorId%3DVN00033897%26storeId%3D10652

Turner, D.B. (1994). Workbook of Atmospheric Dispersion Estimates, 2nd Ed., Boca Raton: Lewis Publishers.

Totten, G. E., Westbrook, S. R., Shah, R. J. (2003). Fuels and Lubricants Handbook - Technology, Properties, Performance, and Testing. West Conshohocken: ASTM International.

United States Air Force (USAF), (2013). Ground Servicing of Aircraft and Static Grounding/Bonding. Warner Robins: USAF.

United States Air Force (USAF), (2016). Concurrent Fuel Servicing of Commercial Contract Cargo and Passenger Aircraft. Warner Robins: USAF.

United States Air Force (USAF), (2018). Air Force Manual 91-203: Air Force Occupational Safety, Fire and Health Standards.

United States Department of Defense, (2015). MIL-DTL-83133E, Detail Specification: Turbine Fuel, Aviation, Kerosene Type, JP-8 (NATO F-34), NATO F-35, and JP-8+100 (NATO F-37).

Valdenebro, V., Sáez de Cámara, E., Gangoiti, G., Alonso, L., García, J.A., Ilardia, J.L., González, N. and Arraibi, E. (2014). The Use of a Mesoscale Modeling System Together with Surface and Upper Observational Data to Estimate Hourly Benzene Impacts in a Mountainous Coastal Area. Air Pollution Modeling and its Application XXIII, pp. 535-538.

Vallero, D. (2014). Fundamentals of Air Pollution. 5th ed., San Diego: Elsevier.

Vinnem, J. (2014). Offshore Risk Assessment vol 1 Principles, Modelling and Applications of QRA Studies. (3rd ed., p. 275). London, U.K.: Springer.

Walcek C. J. (2002). Lagrangian vs. eulerian dispersion modelling: effects of wind shear on pollution dispersion, 12th Joint Conference on the Applications of Air Pollution Meteorology with the Air and Waste Management Association, American Meteorological Society.

Wang, M. (2019). Understandable Electric Circuits - Key Concepts (2nd Edition). London, U.K.: Institution of Engineering and Technology.

Weber, E. (1982). Air Pollution Assessment Methodology and Modeling. New York: Springer Science+Business Media.

Woodward, J. L. (1998). Estimating the Flammable Mass of a Vapor Cloud (p. xvii). New York, N.Y.: Center for Chemical Process Safety of the American Institute of Chemical Engineers.

Yang, W. C., & Wang, H. (1977). Modeling of oil evaporation in aqueous environment. Water Research, 11(10), 879–887.

Yuan, Y., Yang, K., Du, C., Fu, X. (2017), Study on Schmidt Number of Pollutant Diffusion in Urban Street Atmosphere, Procedia Engineering, Volume 205, Pages 1711-1717.

Zannetti P. (1990) Lagrangian Dispersion Models. In: Air Pollution Modeling. Boston, MA: Springer.

Zapert, J. P., Londergan R. J. and Thistle, H. (1991). Evaluation of Dense Gas Simulation Models. North Carolina: EPA.